

## Annual Report 2005

Institute of Radiopharmacy



Forschungszentrum  
Rossendorf

Wissenschaftlich-Technische Berichte  
**FZR-449**  
2006

# **Annual Report 2005**

**Institute of Radiopharmacy**

**Editor: Prof. Dr. J. Steinbach**

**Editorial staff: Dr. S. Seifert**



**Forschungszentrum  
Rossendorf**

Cover Picture:

Transversal view of a micro PET image of the dopamine transporter ligand [ $^{18}\text{F}$ ]MCL-322 in a Wistar rat at 60 min p.i. (right), a micro MRT image of a rat brain in the same region (left), and image fusion (middle).

## FOREWORD

In 1992 the “Institut für Bioanorganische und Radiopharmazeutische Chemie” (Institute of Bioinorganic and Radiopharmaceutical Chemistry) was founded as one of the scientific units within the Forschungszentrum Rossendorf e. V. (Research Centre Rossendorf). Prof. Dr. Johannsen, who was the director until 2003, established the Institute and developed its scientific and organisational profile. From 2003 to 2005, during a challenging time of evaluation and major changes of the central administration, Dr. Spies and Prof. Dr. van den Hoff accepted the responsibility of leading the Institute through the transitional phase. Since October 1<sup>st</sup> 2005 the Institute has a new director, Prof. Dr. Jörg Steinbach.

The organisation of the Institute was adjusted to the Institute’s tasks. There are three departments working together:

- Department of Radiopharmaceutical Chemistry
- Department of Radiopharmaceutical Biology
- Department of Positron Emission Tomography

The first two departments are further structured according to their specialisation.

After years of successful work, on the 1<sup>st</sup> of January 2006, the name of the Institute was changed from “Institut für Bioanorganische und Radiopharmazeutische Chemie” to “Institut für Radiopharmazie” (Institute of Radiopharmacy). This is due to the changed characteristics of the scientific content. Whereas during the first years the chemical disciplines dominated the scientific approach, nowadays, biosciences have more influence on the scientific content. Taking this fact into account, the corresponding staffs of the Department of Radiopharmaceutical Biology was enlarged. Together with the Department of Radiopharmaceutical Chemistry, including the group for production of radiopharmaceuticals, and the medical and medical-physics oriented Department of Positron Emission Tomography (working in close connection with the Clinic of Nuclear Medicine of the Medical Faculty of the Technical University of Dresden) the Institute covers a broad spectrum of radiopharmaceutical disciplines. The adaptation of its name to suit the modern structure is the consequence.

The general scientific task remains similar: the development and application of radiotracers for visualisation and quantification of functional processes as well as the application of radionuclides for therapeutic purposes. The scientific activities will be further focused on radiopharmaceutical cancer research. Diagnostic as well as therapeutic questions will be investigated in a close collaboration with the Centre for Innovation Competence (OncoRay, radiotherapy). Overlapping investigations to metabolic research complete the general program.

The close coordination of the programmes of both, the Institute of Radiopharmacy, Research Centre Rossendorf and the Department of Radiopharmacy, Institute of Interdisciplinary Isotope Research, Leipzig within the “Radiopharmazieverbund Sachsen” (Saxonian Radiopharmaceutical Network) gives the chance to direct scientific questions to the most experienced site: the scientific activities in cancer research of the Rossendorf institute are complemented by the Leipzig institute, which focuses on radiopharmaceutical neuroscientific research.

On the basis of the tasks mentioned above and the new structure, the Institute of Radiopharmacy will continue its basic and application-oriented efforts for high-quality scientific research in the future. An important prerequisite is the close cooperation with various national and international institutions and companies. This is an already successfully ongoing process which has to be continued.

The high qualified and experienced, permanent and temporary staff of the Institute will guarantee for the success of further work.

The contributions of the Annual Report are already published in various scientific journals or deal with improvement of important techniques. This is different to the previous reports.

The members of the Institute wish to acknowledge the ongoing support of general funding by the Free State of Saxony and the Federal Government.



Prof. Dr. Jörg Steinbach



# Contents

<b>I. RESEARCH REPORTS.....</b>	<b>1</b>
<b>DIAGNOSTIC RADIOTRACERS IN TUMOUR AND METABOLISM RESEARCH.....</b>	<b>3</b>
<sup>11</sup> C-C Bond Formation by Palladium-Mediated Cross-Coupling of Alkenylzirconocenes with [ <sup>11</sup> C]Methyl Iodide .....	5
M. Berndt, F. Wüst	
Synthesis of [ <sup>11</sup> C]CH <sub>3</sub> OTf by Different Chemistry Routes, a Comparing Study .....	6
K. Rode, T. Kniess, F. Wüst	
Preparation of the Hypoxia-Tracer [ <sup>18</sup> F]FMISO for Medical Use.....	7
P. Mäding, F. Füchtner, J. Zessin, F. Wüst	
Towards Tc(III)- and Re(III)-Labelled Peptides with Tunable Lipophilicity.....	9
J.-U. Kuenstler, E. Gniazdowska, H. Stephan, H.-J. Pietzsch	
Neurotensin Receptor Subtypes: Molecular Characterisation in Adeno- and Squamous Cell Carcinoma .....	10
C. Haase, R. Bergmann, M. Baumann, J. Pietzsch	
<i>In Vitro</i> Neurotensin Receptor Protein Expression in Tumour Tissues and Cells.....	11
C. Haase, R. Bergmann, M. Baumann, J. Pietzsch	
Effects of Oligosaccharide Derivatives on the Metabolism of Tumour Cells .....	12
T. Kampfrath, B. Schwenzer, R. Bergmann, J. Oswald	
Cellular Uptake of Fluorine-18-Labelled Native and Hypochlorite-Modified Low Density Lipoproteins (LDL).....	13
S. Hoppmann, B. Steiniger, C. Haase, J. Pietzsch	
Catabolism of Hypochlorite-Modified Low Density Lipoproteins (LDL) <i>In Vivo</i> : Insights from Small Animal PET Studies .....	14
S. Hoppmann, B. Steiniger, C. Haase, J. Pietzsch	
Protein Oxidation in Human Disease: Prediabetes and Diabetes Mellitus Type 2 .....	15
J. Pietzsch, C. Haase	
Monitoring of Stem Cell Homing with Small Animal PET .....	17
J. Oswald, R. Bergmann	
Biochemical Characterisation of Fluorescein-Labelled Neurotensin Derivatives.....	18
R. Bergmann, V. Maes, Ch. Hultsch, S. Kohl, Th. Hanke, D. Tourwé	
Implementing a Small Animal Magnetic Resonance Imaging System.....	19
K. Strobel, R. Bergmann, J. van den Hoff	
Optimised List-Mode Acquisition and Data Processing Procedures for ACS2 Based PET Systems.....	20
J. Langner, P. Bühler, U. Just, C. Pöttsch, E. Will, J. van den Hoff	
User Guided Segmentation and Quantification of Three-Dimensional Structures in Oncological Whole Body PET - Continued .....	21
C. Pöttsch, F. Hofheinz, J. van den Hoff	
<b>RADIOMETAL THERAPEUTICS .....</b>	<b>23</b>
A Novel Rhenium Chelate System Derived from Dimercaptosuccinic Acid.....	25
T. Heinrich, W. Kraus, H.-J. Pietzsch, C. Smuda, H. Spies	
Optimised Procedure for Preparing <sup>188</sup> Re(V) Complexes under Mild Conditions .....	26
S. Seifert, H.-J. Pietzsch	
Hydrophilic Rhenium-188 Complexes for Attaching the Metal to Biomolecules	
6. Complex Design .....	28
E. Schiller, F. Tisato, H. Spies, H.-J. Pietzsch	
Hydrophilic Rhenium-188 Complexes for Attaching the Metal to Biomolecules	
7. Bioconjugation and Radiolabelling .....	29
E. Schiller, J.-U. Künstler, S. Seifert, H.-J. Pietzsch	
Formation of Stable Cu(II) Complexes with Hexadentate Bispidine Ligands .....	30
S. Juran, H. Stephan, J. Steinbach, G. Geipel, G. Bernhard	

Complexation of Cu(II) by Glycodendrimers .....	31
A. Röhrich, H. Stephan, J. Steinbach, G. Geipel, G. Bernhard, G. Bergamini, V. Balzani	
Molecular Structure of the Cluster Anion $[\text{TiW}_{11}\text{CoO}_{40}]^{8-}$ .....	32
H. Stephan, A. Röllich, Z. Matějka, G. Reck, W. Kraus	
Stability Investigation of Nanoparticles Formed by $[\text{Ti}_2\text{W}_{10}\text{PO}_{40}]^{7-}$ and Chitosan .....	33
T. Meißner, H. Stephan, W. Richter, H. Zänker, S. Weiß	
New Octahedral Rhenium Cluster Compounds Possessing 3,5-Dimethyl-pyrazole as Apical Ligands .....	34
K. A. Brylev, Y. V. Mironov, V. E. Fedorov, H. Spies, H.-J. Pietzsch, H. Stephan, W. Kraus	
<b>PET IN DRUG AND FOOD RESEARCH.....</b>	<b>35</b>
Special Issue: PET in Food Sciences .....	37
J. Pietzsch, J. van den Hoff	
Radiolabelled Flavonoids and Polyphenols	
IV. Biodistribution of an $^{18}\text{F}$ -Labelled Resveratrol Derivative .....	38
S. Gester, F. Wüst, B. Pawelke, R. Bergmann, J. Pietzsch	
<b>CYCLOTRON OPERATION .....</b>	<b>39</b>
Operation of the Rossendorf PET Cyclotron "CYCLONE 18/9" in 2005.....	41
St. Preusche, F. Wüst	
<b>II. PUBLICATIONS, LECTURES, PATENTS AND AWARDS OF.....</b>	<b>43</b>
<b>THE INSTITUTE AND THE PET-CENTRE ROSSENDORF</b>	
<b>III. COLLABORATIONS, FUNDED PROJECTS AND FINANCIAL SUPPORT .....</b>	<b>57</b>
<b>IV. SEMINARS.....</b>	<b>65</b>
<b>V. PERSONNEL .....</b>	<b>69</b>

# **I. RESEARCH REPORTS**





**DIAGNOSTIC RADIOTRACERS IN TUMOUR AND  
METABOLISM RESEARCH**



# <sup>11</sup>C-C Bond Formation by Palladium-Mediated Cross-Coupling of Alkenylzirconocenes with [<sup>11</sup>C]Methyl Iodide

M. Berndt, F. Wüst

The hydrozirconation of internal alkynes, followed by transmetalation with Pd(PPh<sub>3</sub>)<sub>4</sub> and subsequent cross-coupling with [<sup>11</sup>C]methyl iodide to give several <sup>11</sup>C-labelled α,α'-dimethyl substituted alkenes is described.

## Introduction

A synthetic strategy to form <sup>11</sup>C-labelled α,α'-dimethyl substituted alkenes includes formation of alkenylzirconocenes by the *syn*-insertion of a C-C triple bond into the Zr-H bond of Schwartz reagent [Cp<sub>2</sub>ZrHCl] followed by transition metal-mediated <sup>11</sup>C-C bond formation with [<sup>11</sup>C]methyl iodide (Fig. 1).

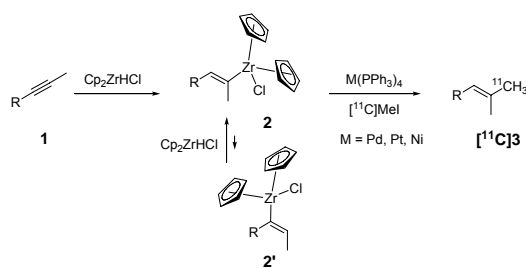


Fig. 1. Transmetalation of alkenylzirconocenes and subsequent cross-coupling with [<sup>11</sup>C]methyl iodide.

Addition of one equivalent Schwartz reagent onto unsymmetrically substituted internal alkynes may lead to a mixture of regioisomers **2** and **2'** enriched in the regioisomer where the zirconium-carbon bond is placed geminal to the sterically less demanding substituent [1]. However, further treatment with Schwartz reagent readily isomerises the mixture of regioisomers presumably *via* a dimetallated intermediate to favour the formation of the thermodynamically stable isomer **2**.

The reaction conditions were optimised by the conversion of prop-1-ynyl-benzene **1a** using several group 10 transition metal complexes [2]. Transition metal complexes Ni(PPh<sub>3</sub>)<sub>4</sub> or Pt(PPh<sub>3</sub>)<sub>4</sub> gave only 4 % and 11 % radiochemical yield, respectively, whereas sufficient radiochemical yields of up to 70 % could be obtained when Pd(PPh<sub>3</sub>)<sub>4</sub> was used.

## Results and Discussion

To elaborate the scope and limitations of the novel radiolabelling method, optimised reaction conditions were applied to the radiosynthesis of other <sup>11</sup>C-labelled alkenes bearing a prenyl group. The results are summarised in Table 1. In contrast to the hydrozirconation reaction employing model compound **1a**, a total amount of 2.5 equivalents of Schwartz reagent was used in the case of sterically less hindered internal alkynes **1b**, **1c**, **1d**, **1e** and **1g** to force the hydrozirconation reaction in favour to

thermodynamically controlled regioselectivity as described in Fig. 1.

Table 1. Radiochemical yield (RCY) determined by analytical radio-HPLC referring to as the percentage of the total amount of radioactivity in the reaction mixture.

R	Equiv. Cp <sub>2</sub> ZrClH	[ <sup>11</sup> C]CH <sub>3</sub> I [%]	RCY [%]
Ph ( <b>1a</b> )	1.2	30	70 ( <b>3a</b> )
Ph-O-CH <sub>2</sub> ( <b>1b</b> )	2.5	35	65 ( <b>3b</b> )
(CH <sub>3</sub> ) <sub>3</sub> C ( <b>1c</b> )	2.5	25	75 ( <b>3c</b> )
CH <sub>3</sub> CH <sub>2</sub> CH <sub>2</sub> ( <b>1d</b> )	2.5	50	50 ( <b>3d</b> )
TBDMSO-CH <sub>2</sub> ( <b>1e</b> )	2.5	30	70 ( <b>3e</b> )
OH-CH <sub>2</sub> ( <b>1f</b> )	5.0	38	62 ( <b>3f</b> )
(4-NO <sub>2</sub> -C <sub>6</sub> H <sub>4</sub> )-O-CH <sub>2</sub> ( <b>1g</b> )	2.5	95	5 ( <b>3g</b> )
Ph-CO <sub>2</sub> -CH <sub>2</sub> ( <b>1h</b> )	1.2	>95	- ( <b>3h</b> )

Subsequent transmetalation with Pd(PPh<sub>3</sub>)<sub>4</sub> and treatment with [<sup>11</sup>C]methyl iodide gave the desired cross-coupled products [<sup>11</sup>C]**3b**, [<sup>11</sup>C]**3c**, [<sup>11</sup>C]**3d** and [<sup>11</sup>C]**3e** in good radiochemical yields. The obtained low radiochemical yield (5 %) of 4-nitrophenyl compound [<sup>11</sup>C]**3g** is an example for the incompatibility of Schwartz reagent towards nitro groups. Radiosynthesis of ester [<sup>11</sup>C]**3h** completely failed due to undesired side reactions of Schwartz reagent with the ester group. In the case of butynol **1f** a larger excess of 5.0 equivalents of Schwartz reagent had to be used to compensate the reaction of Schwartz reagent with the free OH-group. In summary we have elaborated a novel <sup>11</sup>C-C bond forming reaction based upon the palladium-mediated cross-coupling between alkenylzirconocenes with [<sup>11</sup>C]methyl iodide. The excellent regioselectivity of the formed alkenyl-zirconocene complexes makes this approach a promising route for the convenient preparation of <sup>11</sup>C-labelled compounds containing a prenyl group. However, easily reducible functional groups such as nitro groups or esters are not compatible with the reaction conditions employing Schwartz reagent for the hydrozirconation reaction of internal alkynes.

Published in: Berndt, M., Wuest, F., J. Labelled Compd. Radiopharm. 49 (2006) 91-100.

## References

- [1] Wipf, P. *et al.*, Tetrahedron 52 (1996) 12853-12910.
- [2] Wüst, F. and Mäding, P., Annual Report 2004, FZR-424, p. 35.

# Synthesis of [<sup>11</sup>C]CH<sub>3</sub>OTf by Different Chemistry Routes, a Comparing Study

K. Rode, T. Kniess, F. Wüst

The synthesis of [<sup>11</sup>C]CH<sub>3</sub>OTf via the “wet chemistry route” (Nuclear Interface module) is compared with the synthesis of [<sup>11</sup>C]CH<sub>3</sub>OTf via gas phase iodination of [<sup>11</sup>C]CH<sub>4</sub> (GE TRACERlab FX<sub>c</sub> module). The obtained radiochemical yields and specific radioactivities are discussed. The N-methylation of a piperazine derivative with [<sup>11</sup>C]CH<sub>3</sub>OTf performed in the Nuclear Interface module resulted in radiochemical yields of 10 – 27 % and specific radioactivities of 60 - 100 GBq/μmol. The reaction in the GE TRACERlab FX<sub>c</sub> module gave radiochemical yields of 5 – 20 % and specific radioactivities of only 5 - 10 GBq/μmol.

## Introduction

[<sup>11</sup>C]CH<sub>3</sub>I and [<sup>11</sup>C]CH<sub>3</sub>OTf are important labeling precursors for the radiosynthesis of a broad variety of PET radiotracers. Using the “wet chemistry route”, cyclotron-produced [<sup>11</sup>C]CO<sub>2</sub> is reduced by means of 0.05 M LiAlH<sub>4</sub> in THF followed by iodination using concentrated HI at 120 °C [1]. [<sup>11</sup>C]CH<sub>3</sub>I is converted into [<sup>11</sup>C]CH<sub>3</sub>OTf passing over a cartridge containing silver triflate at 200 °C. [<sup>11</sup>C]CH<sub>3</sub>OTf is used for the N-methylation of a piperazine derivative. The N-methylated piperazine derivative was purified by semi-preparative HPLC and isolated via solid phase extraction on a RP18-cartridge.

The “gas phase method” to produce [<sup>11</sup>C]CH<sub>3</sub>I is based on the catalytic hydrogenation of [<sup>11</sup>C]CO<sub>2</sub> to [<sup>11</sup>C]CH<sub>4</sub> on a Ni-catalyst at 400 °C followed by iodination of [<sup>11</sup>C]CH<sub>4</sub> with iodine at 720 °C in a circulation process. [<sup>11</sup>C]CH<sub>3</sub>I is trapped on a Porapak Q trap at room temperature [2]. Subsequent release of trapped [<sup>11</sup>C]CH<sub>3</sub>I at 190 °C and passage over a heated AgOTf-cartridge in a stream of helium (6.0) gave [<sup>11</sup>C]CH<sub>3</sub>OTf.

## Results and Discussion

[<sup>11</sup>C]CO<sub>2</sub> was produced in an aluminium gas target via the <sup>14</sup>N[p,α]<sup>11</sup>C nuclear reaction using an IBA CYCLONE 18/9 cyclotron. A mixture of nitrogen (6.0) and 0.5 % oxygen (5.5) was used as the target gas. In a typical irradiation procedure (40 min, 25 μA) 70 GBq of [<sup>11</sup>C]CO<sub>2</sub> were produced at the end-of-bombardment (EOB).

Table 1 shows the summary of obtained radiochemical yields and specific radioactivities for the synthesis of an N-methylated piperazine derivative.

Table 1. Radiochemical yields (RCY) and specific radioactivities (AS) at end-of-synthesis (EOS)/C-11 synthesis module Nuclear Interface and GE TRACERlab FX<sub>c</sub> (Harshaw-Ni at 400 °C).

<sup>11</sup> C-synthesis module	RCY [%]	AS [GBq/μmol]
Nuclear Interface	10-27	60-100
GE TRACERlab FX <sub>c</sub>	5-20	5-10

Higher radiochemical yields and higher specific radioactivities were obtained by the “wet chemistry route”. Careful temperature-controlled trapping of [<sup>11</sup>C]CO<sub>2</sub> before LiAlH<sub>4</sub> reduction in the Nuclear Interface module proved to be advantageous to remove potential carbon contaminations in the target gas. Additionally a low volume (<0.2 ml) and low concentration (<10 μmol) of LiAlH<sub>4</sub>-solution should be used to obtain higher specific radioactivities [3].

For the [<sup>11</sup>C]CO<sub>2</sub>/[<sup>11</sup>C]CH<sub>4</sub> conversion in “gas phase method”, several Ni-catalysts and temperatures of the Ni-oven have been tested:

1. Harshaw-Ni: 330, 360 and 400 °C;
2. Shimalite®-Ni: 360, 400 and 430 °C;
3. Ni (Aldrich): 400 °C.

In general, using the GE TRACERlab FX<sub>c</sub> module, significant lower specific radioactivities were obtained. This is probably mainly caused by the reduction of target gas impurities by the Ni-catalysts to cold CH<sub>4</sub>. Although several Ni-catalysts were tested, maximum specific radioactivities of only 10 GBq/μmol could be obtained. Beside the proposed carbon contaminations originating from the target gas, the inorganic matrix of the highly reactive Ni-catalysts (Al<sub>2</sub>O<sub>3</sub>/SiO<sub>2</sub>) may also serve as a potential source for carbon contaminations resulting in low specific radioactivities.

## Conclusions

To obtain higher specific radioactivities with the GE TRACERlab FX<sub>c</sub> module the installation of a cooling trap is advantageous to freeze out the [<sup>11</sup>C]CO<sub>2</sub> before the reduction to [<sup>11</sup>C]CH<sub>4</sub>. Another possibility might be the application of pure Ni-catalyst without any carrier material.

Presentation on the 13. Workshop AG Radiochemie, Radiopharmazie, Seefeld/Austria, October, 2005.

## References

- [1] Långström, B. *et al.*, Int. J. Appl. Radiat. Isot. 27 (1976) 357-363.
- [2] Larsen, P. *et al.*, Appl. Radiat. Isot. 48 (1997) 153-157.
- [3] Matarrese, M. *et al.*, Nucl. Med. Biol. 30 (2003) 79-83.

# Preparation of the Hypoxia-Tracer [ $^{18}\text{F}$ ]FMISO for Medical Use

P. Mäding, F. Füchtner, J. Zessin, F. Wüst

The preparation of [ $^{18}\text{F}$ ]FMISO, a well known radiopharmaceutical for imaging hypoxia, was adapted to an automated module. The synthesis bases on the conversion of the precursor NITTP with a dried mixture of [ $^{18}\text{F}$ ]fluoride/ $\text{K}_2\text{CO}_3$ / $\text{K}222$  followed by a deprotection step. After HPLC purification, formulation and sterile filtration the uncorrected radiochemical yields of [ $^{18}\text{F}$ ]FMISO were in the range of 27 - 35 % (related to [ $^{18}\text{F}$ ]fluoride) within a synthesis time of 66 min.

## Introduction

Hypoxia in tumours is regarded as an important reason behind local failure of radiotherapy. Detection and quantification of oxygen levels in human tumours may have a significant influence on the outcome evaluation of patients treated with radiation and on the use of hypoxia-specific chemotherapeutic agents [1]. 2-Nitro-imidazole compounds are reduced and trapped in hypoxic cells. Therefore imaging techniques with radiolabelled 2-nitroimidazole derivatives have especially been used as a direct marker of oxygen tension in ischemic myocardium and tumours [2]. Among these,  $^{18}\text{F}$ -labelled fluoromisonidazole (1H-1-(3- $^{18}\text{F}$ fluoro-2-hydroxypropyl)-2-nitroimidazole, [ $^{18}\text{F}$ ]FMISO) is now the most widely used radiotracer in clinical PET imaging [3]. It is used as an *in vivo* marker of hypoxic cells in tumours and ischemic areas of the heart and the brain. Therefore we dealt with the preparation of [ $^{18}\text{F}$ ]FMISO via a one-pot, two-step synthesis procedure according to Fig. 1 using a commercial Tracerlab FX<sub>FN</sub> synthesis module from GE Medical Systems (see Fig. 2).

## Results and Discussion

Several procedures were described for synthesizing [ $^{18}\text{F}$ ]FMISO [4, 5, 6]. The synthesis was started from the precursor 1-(2'-nitro-1'-imidazolyl)-2-O-tetrahydro-pyranyl-3-O-toluene-sulphonyl-propanediol (NITTP) in the most cases. We have also used the conversion of the precursor NITTP with a dried mixture of [ $^{18}\text{F}$ ]fluoride/ $\text{K}_2\text{CO}_3$ / $\text{K}222$  in MeCN followed by hydrolysis of the tetrahydropyranyl protecting group using 1 M HCl. No significant influence on the radiochemical yield was found by use of 5 mg or 10 mg NITTP. Nonconverted [ $^{18}\text{F}$ ]fluoride was separated from the reaction mixture by means of an  $\text{Al}_2\text{O}_3$  cartridge before HPLC purification of the [ $^{18}\text{F}$ ]FMISO with a Nucleosil 100-7 C18 column (EP250/16; Macherey-Nagel). The eluent was isotonic NaCl : EtOH =

95 : 5, which was buffered with phosphate buffer to pH 7. Under these conditions the chemical purity was more reproducible. We have also tested a purification method with a combination of 3 cartridges (SCX, RP18 and Alumina N) instead of HPLC according to [6]. But this method was not qualified to obtain a pure radiotracer (only 80 % radiochemical purity and 3.3 % chemical purity). The separated HPLC fraction of [ $^{18}\text{F}$ ]FMISO was diluted with isotonic saline followed by sterile filtration. In this way a sterile and pyrogen free, injectable solution was obtained. The uncorrected radiochemical yield of [ $^{18}\text{F}$ ]FMISO was in the range of 27 - 35 % (related to [ $^{18}\text{F}$ ]fluoride; n = 13) within a synthesis time of 66 min. Thus, in a typical experiment 11 GBq [ $^{18}\text{F}$ ]fluoride could be converted into 3.4 GBq [ $^{18}\text{F}$ ]FMISO. For clinical use, quality specifications were defined in compliance with established pharmaceutical rules. Specifications and results of three validation runs are summarised in Table 1.

## Conclusions

A procedure for [ $^{18}\text{F}$ ]FMISO production was developed based on a module for nucleophilic substitution (GE Medical Systems). In this way [ $^{18}\text{F}$ ]FMISO could be obtained in reproducible yield and purity, which allows the clinical use.

## References

- [1] Gronroos, T. *et al.*, J. Nucl. Med. 42 (2001) 1397-1404.
- [2] Britz-Cunningham, S. H. *et al.*, J. Nucl. Med. 44 (2003) 1945-1961.
- [3] Couturier, O. *et al.*, Eur. J. Nucl. Med. Mol. Imaging 31 (2004) 1182-1206.
- [4] Lim, J. L. *et al.*, Appl. Radiat. Isot. 44 (1993) 1085-1191.
- [5] Kämäräinen, E.-L. *et al.*, J. Labelled Compd. Radiopharm. 47 (2004) 37-45.
- [6] Tang, G. *et al.*, Nucl. Med. Biol. 32 (2005) 553-558.

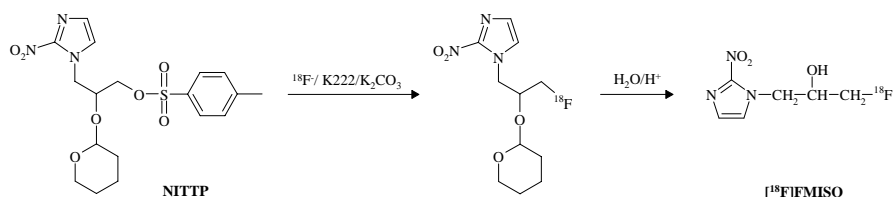


Fig. 1. Synthesis of [ $^{18}\text{F}$ ]FMISO

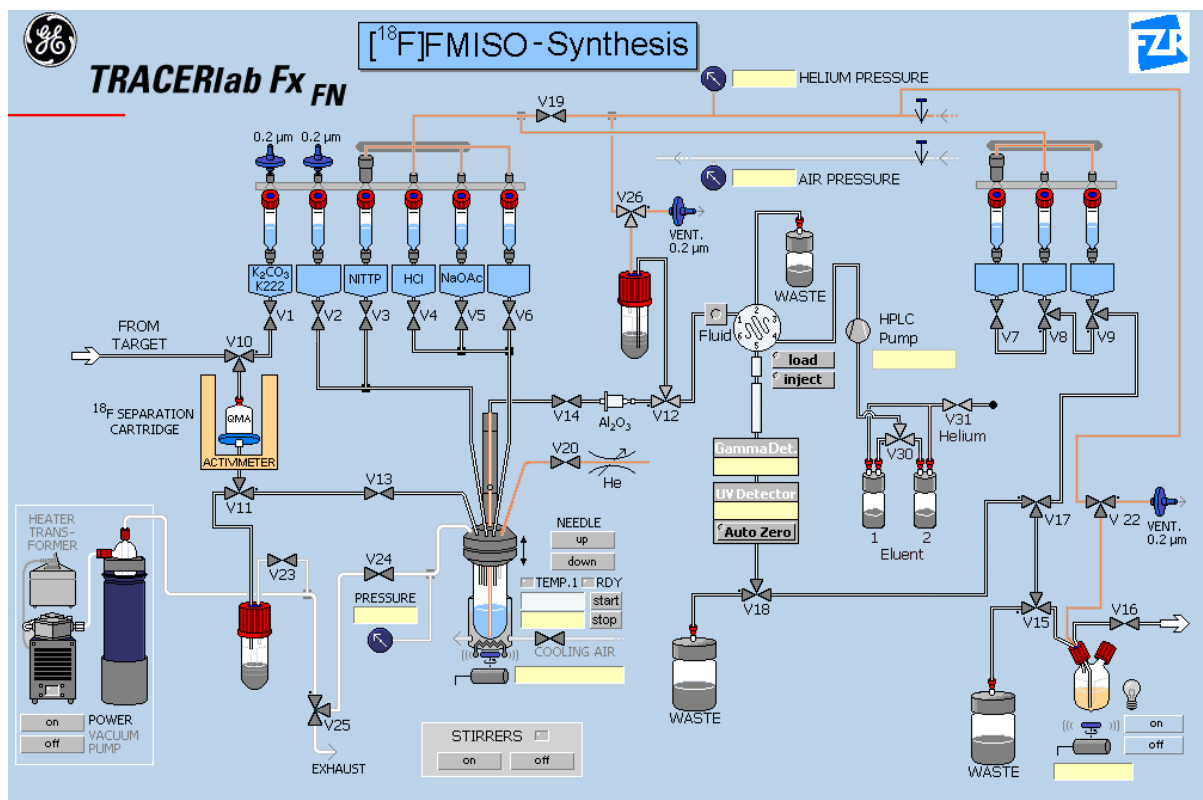


Fig. 2. Scheme of the module for the preparation of [<sup>18</sup>F]FMISO.

Table 1. Quality control of [<sup>18</sup>F]FMISO – specifications and results

Parameter/method	Specification	Result (n = 3)
Appearance (visual)	Clear, colourless	Clear, colourless
Identity (HPLC)	$\Delta t_R \leq 0,5$ min	$0.022 \pm 0,015$ min
Identity (Gamm spectroscopy)	$511 \pm 25$ keV	$501 \pm 3$ keV
Radiochemical purity (HPLC)	$\geq 95$ % [ <sup>18</sup> F]FMISO	$99.9$ % [ <sup>18</sup> F]FMISO
Chemical purity (HPLC)	$\geq 90$ % FMISO	$93.3 \pm 2$ % FMISO
	+ DH MISO	$3.4 \pm 0.4$ % DH-MISO
	$\leq 10$ $\mu$ g FMISO/batch	$4.6 \pm 0.26$ $\mu$ g FMISO
	$\leq 1$ $\mu$ g DH-MISO/batch	$0.17 \pm 0.01$ $\mu$ g DH-MISO
Residual solvents (GC/MS)	$\leq 1000$ $\mu$ g/ml acetone	$1$ $\mu$ g/ml acetone
	$\leq 410$ $\mu$ g/ml acetonitrile	$1$ $\mu$ g/ml acetonitrile
Radionuclidic purity (half-life)	$1.75 - 1.92$ h	$1.83 \pm 0.006$ h
pH	$5.0 - 8.5$	$7.0 \pm 0.06$
Bacterial endotoxines (LAL)	$\leq 10$ I.U./ml	$< 0.01$ I.U./ml
Sterility	sterile	sterile
Specific activity	$\geq 37$ GBq/ $\mu$ mol	$128 \pm 11$ GBq/ $\mu$ mol

DH-MISO: 1-(2,3-Dihydroxypropyl)-2-nitroimidazole

# Towards Tc(III)- and Re(III)-Labelled Peptides with Tunable Lipophilicity

J.-U. Kuentler, E. Gniazdowska<sup>1</sup>, H. Stephan, H.-J. Pietzsch

<sup>1</sup>Institute of Nuclear Chemistry and Technology, Warsaw, Poland

In order to increase the hydrophilicity of labelled peptides using the "4+1" approach a new "4+1" complex bearing three carboxyl groups was synthesised and applied for <sup>99m</sup>Tc-labelling of a model peptide.

## Introduction

To improve the biobehaviour of <sup>99m</sup>Tc-labelled peptides containing a "4+1" complex as in <sup>99m</sup>Tc(NS<sub>3</sub>)(CN-GGY) (Fig. 2) showing a high liver uptake [1], a new hydrophilic "4+1" complex bearing three carboxyl groups was introduced.

## Results and Discussion

The carboxyl-groups bearing ligand NS<sub>3</sub>(COOH)<sub>3</sub> (Fig. 1) was synthesised by conjugation (DCC) of the dendritically functionalised amine H<sub>2</sub>N-C(-CH<sub>2</sub>-O-CH<sub>2</sub>-CH<sub>2</sub>-COO-Me)<sub>3</sub> [2] to the S-benzyl protected NS<sub>3</sub>COOH [1] followed by deprotection.

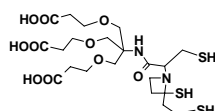
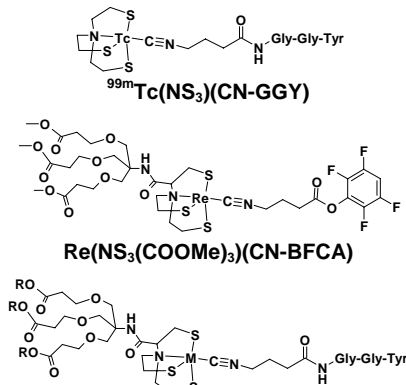


Fig. 1. NS<sub>3</sub>(COOH)<sub>3</sub>.

The isocyanide group was coupled to the model peptide Gly-Gly-Tyr *via* an aliphatic linker (CN-BFCA). For <sup>99m</sup>Tc-labelling a two-step procedure [1] was applied using <sup>99m</sup>Tc-EDTA/mannitol (400 MBq) which was reacted with 20 μg isocyanide-modified peptide and 300 μg NS<sub>3</sub>(COOH)<sub>3</sub>. <sup>99m</sup>Tc-labelling resulted in a radiochemical yield of app. 25 % (HPLC), Fig. 3. The yield can be increased by using a higher peptide amount.

To verify the identity of the <sup>99m</sup>Tc-labelled peptide the analogous "4+1" Re compound Re(NS<sub>3</sub>(COOH)<sub>3</sub>)(CN-GGY) was synthesised (Fig. 2).



<sup>99m</sup>Tc(NS<sub>3</sub>(COOH)<sub>3</sub>)(CN-GGY), M = <sup>99m</sup>Tc, R = H  
 Re(NS<sub>3</sub>(COOH)<sub>3</sub>)(CN-GGY), M = Re, R = H  
 Re(NS<sub>3</sub>(COOMe)<sub>3</sub>)(CN-GGY), M = Re, R = Me

Fig. 2. Prepared "4+1" compounds.

For a convenient synthesis of peptides containing the new hydrophilic Re "4+1" complex, the active ester Re(NS<sub>3</sub>(COO-Me)<sub>3</sub>)(CN-BFCA) as shown in Fig. 2 was prepared starting from NS<sub>3</sub>(COOH)<sub>3</sub>, [Re(tu)<sub>6</sub>]Cl<sub>3</sub> and PMe<sub>2</sub>Ph followed by ligand exchange with CN-BFCA. Reaction of Re(NS<sub>3</sub>(COOMe)<sub>3</sub>)(CN-BFCA) with the peptide and hydrolysis of the methyl ester gave the desired peptide derivative.

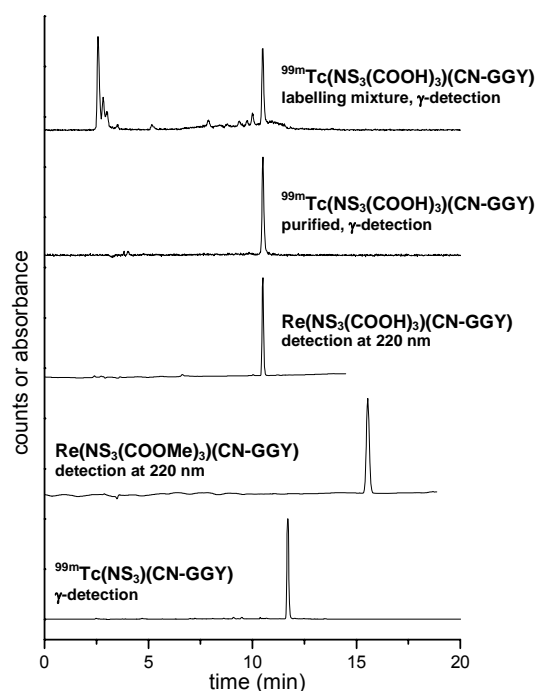


Fig. 3. Chromatograms of prepared compounds (HPLC, Jupiter proteo, eluent: A: MeCN, 0.1 % TFA; B: H<sub>2</sub>O, 0.1 % TFA; gradient elution: 20 to 80 % A in 20 min).

The increased hydrophilicity of the new "4+1" complex was shown by HPLC investigations (Fig. 3) and determination of the partition coefficient (Log D, octanol/PBS, pH 7.4).

<sup>99m</sup>Tc(NS<sub>3</sub>(COOH)<sub>3</sub>)(CN-GGY) showed a log D value of -2.6 ± 0.3 (n = 3) compared with the log D value of -1.5 ± 0.2, <sup>99m</sup>Tc(NS<sub>3</sub>)(CN-GGY).

As a next step peptides bearing the new "4+1" complex have to be evaluated in animal experiments.

## References

- [1] Seifert, S. *et al.*, Bioconjugate Chem. 15 (2004) 856-863.
- [2] Newkome, G. R. *et al.*, Synlett 1 (1992) 53-54.



# Neurotensin Receptor Subtypes: Molecular Characterisation in Adeno- and Squamous Cell Carcinoma

C. Haase, R. Bergmann, M. Baumann<sup>1</sup>, J. Pietzsch

<sup>1</sup>Clinic for Radiotherapy and Radiation Oncology, Medical Faculty Carl Gustav Carus, Dresden University of Technology

During the past twenty years peptides and peptide receptors have become an increasing interest in cancerogenic processes. Due to the large enrichment of these receptors in many primary human cancers they can be used for targeting with radiolabelled peptides for early diagnosis.

## Introduction

Neurotensin receptors (NTR) belong to the peptide receptors with great potential in the field of molecular targeting since they are known to be overexpressed in various tumour cell lines including small cell lung carcinoma, neuroblastoma, pancreatic or colon cancer. Three NT receptors (NTR1, NTR2 and NTR3) have been identified to date. NTR1 and NTR2 belong to the family of G protein-coupled receptors with seven transmembrane domains, whereas NTR3 is a single transmembrane domain protein that belongs to a recently identified family of sorting proteins. In order to verify the molecular characteristics of the NTR subtypes we studied mRNA expression in two different tumour cell lines and corresponding xenografts [1]. For preparation of total RNA from HT-29 (colorectal adenocarcinoma), FaDu (squamous cell carcinoma) cells and the corresponding xenografts a RNA isolation kit was used. The purity and integrity of RNA were analysed by measuring the absorbance ratio at  $A_{260}/A_{280}$  as well as by electrophoresis on a 1 % agarose gel. RT-PCR was performed with mRNA as template and 5' and 3' PCR specific primers for the human NTR subtype sequences. Products were analysed on a 1.5% agarose gel. The expression intensity was normalised to house-keeping gene (18S rRNA) expression.

## Results and Discussion

NTR1, NTR2 and NTR3 mRNA was present in all cells and corresponding xenografts. Tumour cells always express higher levels of NTR3 mRNA compared to NTR1 and NTR2 (Fig. 1). NTR3 expression in HT-29 cells was about 3.5-fold higher to NTR1 and 2.5-fold higher to NTR2. Similar results were observed in FaDu cells with about fourfold higher expression to NTR1 and twofold higher expression to NTR2. Moreover FaDu cells overall revealed a higher receptor expression than HT-29 (Fig. 1). NTR distribution studies in the corresponding xenografts also revealed a strong expression of NTR3 similar to those in tumour cell lines. A minor decrease of NTR3 has been detected in xenografts compared to cultures cells (Fig. 2). NTR mRNA expression levels can be ordered

as follows: NTR3>>NTR2>NTR1 for cultured tumour cells and NTR3>NTR1>NTR2 for the corresponding xenografts.

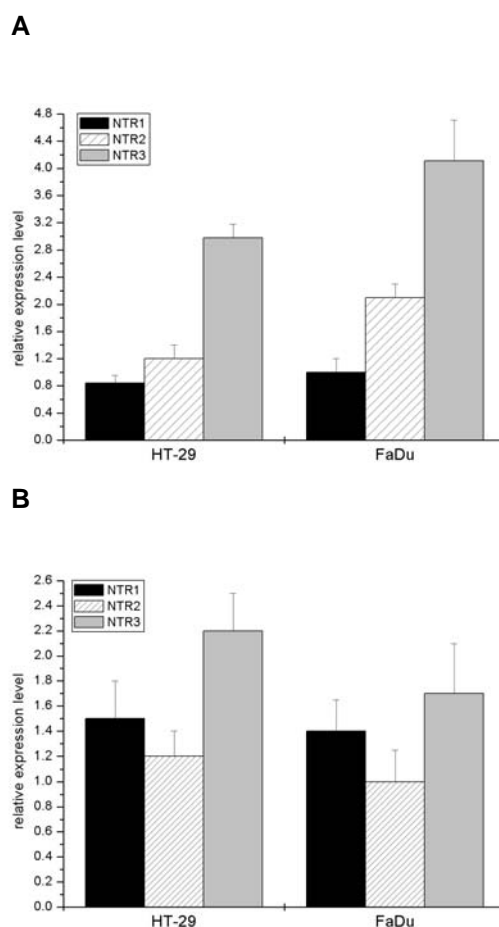


Fig. 1. Quantitative PCR analysis of NTR expression in (A) HT-29 and FaDu cells and (B) corresponding xenografts. NTR expression was normalised to house-keeping gene 18S rRNA expression. Data are mean  $\pm$  SD (n = 3).

Our results based on the molecular characterisation give raise to the assumption that NTR subtypes are good targets for advanced cancer diagnosis, e.g., by using positron emission tomography, because of the high mRNA expression in tumour cells and xenografts [2].

## References

- [1] Reubi, J. C. *et al.*, J. Nucl. Med. 46 (2005) 67S-75S.
- [2] Haase, C. *et al.*, submitted to Cancer Lett.

# In Vitro Neurotensin Receptor Protein Expression in Tumour Tissues and Cells

C. Haase, R. Bergmann, M. Baumann<sup>1</sup>, J. Pietzsch

<sup>1</sup>Clinic for Radiotherapy and Radiation Oncology, Medical Faculty Carl Gustav Carus, Dresden University of Technology

Receptor expression studies by real-time PCR (RT-PCR) indicates that mRNA can be quantified precisely. It should be remembered that RT-PCR identifies extremely low message levels that may not translate into the expression of functional levels of receptors. Understanding the properties of receptor protein will be a helpful tool to identify and define radiolabelled ligands for molecular imaging.

## Introduction

Because it is the receptor protein that is targeted *in vivo*, it should also be the protein that is investigated *in vitro*. In human tumours the mRNA and the protein levels for selected peptide receptors may differ, therefore, it is important to gain information about receptor protein expression. Different methods, e.g., receptor autoradiography and immunohistochemistry, provide such basic information on receptor protein.

In order to verify the receptor protein expression of the human neurotensin receptor (NTR) subtypes we used two different tumour cell lines HT-29 (colorectal adenocarcinoma) and FaDu (squamous cell carcinoma) and the corresponding xenografts. For Western blot and 2D-gel electrophoresis membrane proteins were extracted by a detergent-based protein purification method. Immunoblot analysis was done with polyclonal NTR1, NTR2 and NTR3 specific antibodies and visualised by chemoluminescence using a peroxidase conjugated secondary antibody. Immunohistochemistry was further performed on frozen HT-29 and FaDu tumour tissue slices using the same antibodies as described above.

FAST-3,3'-diaminobenzidine tablets were used as a precipitating substrate for the detection of peroxidase activity.

## Results and Discussion

In contrast to mRNA analysis, the corresponding xenografts for FaDu (Fig. 1A) and HT-29 (Fig. 1E) were strongly immunopositive for NTR1. NTR2 (Fig. 1B+F) expression showed a weaker reaction compared with NTR1. The weakest immunopositive signal was detected for NTR3 expression in FaDu (Fig. 1C) and HT-29 (Fig. 1G) xenografts.

Western blotting analysis of purified membrane proteins from HT-29 and FaDu cells showed similar results compared to xenografts. HT-29 and FaDu cells were strongly immunopositive for NTR1 compared to NTR2 (~50kDa) (Fig. 2). Western blotting experiments with NTR3 revealed no detectable signal in both corresponding xenografts. The overall expression of NTR1 protein in FaDu xenografts and cells

compared to HT-29, respectively, were always higher.

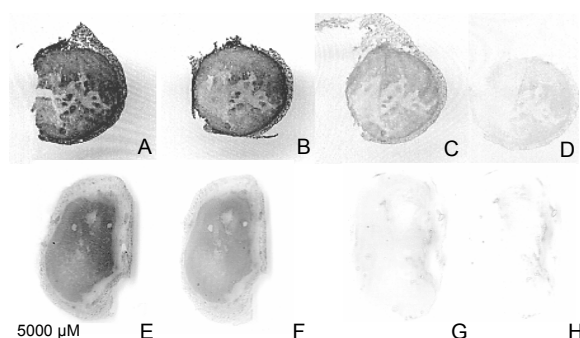


Fig. 1. Immunohistochemistry for NTR in FaDu (A-D) and HT-29 (E-H) xenografts for NTR1 (A+E), NTR2 (B+F) and NTR3 (C+G), controls (D+H).

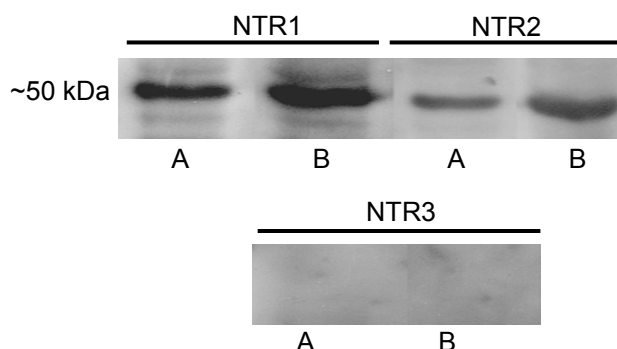


Fig. 2. Immunoblot of 100 ng purified membrane protein from HT-29 (A) and FaDu (B) cells with NTR1, 2 and 3 antibodies.

In conclusion, our results give raise to the assumption that NTR1 is a good target for advanced cancer diagnosis, e.g., by using positron emission tomography, because of the high protein expression in tumour cells and xenografts [2].

## References

- [1] Haase, C. *et al.*, *this report*, p. 10.
- [2] Haase, C. *et al.*, *submitted to Cancer Lett.*

# Effects of Oligosaccharide Derivatives on the Metabolism of Tumour Cells

T. Kampfrath<sup>1</sup>, B. Schwenzer<sup>1</sup>, R. Bergmann, J. Oswald  
<sup>1</sup>Institute of Biochemistry, Dresden University of Technology

## Introduction

This study investigates the effect of oligosaccharide derivatives on proliferation, metabolic activity, and apoptosis of cultivated tumour cells. The effect of a complex oligosaccharide derivative of marine origin with anti-tumour activity has been compared with a defined trimeric oligosaccharide based on chitosan.

## Methods

The human bladder carcinoma cell line EJ-28 was used as tumour model and compared to the human fibroblast cell line NHDF 6369. For quantification of the glucose metabolism [<sup>18</sup>F]FDG-uptake was measured. The initial activity was 60 MBq in 10 ml culture medium. The cells were incubated for one hour. The incorporated activity was measured with a gamma counter. Further we studied the programmed cell death with flow cytometry. Early phase of apoptosis was detected by annexin staining and late phase by propidium iodide staining. The protein kinase inhibitor staurosporine was used as control substance in all experiments.

## Results

EJ-28 cells treated for 24 hours with oligosaccharide derivatives and chitosan trimers showed a decreased [<sup>18</sup>F]FDG-uptake of about 50 % in comparison to the untreated reference. On the other hand, NHDF 6369 incubated with these agents, showed an increased [<sup>18</sup>F]FDG-uptake up to 150 %. The protein kinase inhibitor staurosporine decreased the [<sup>18</sup>F]FDG-uptake to 10 % in both cell lines. Furthermore, incubation for 24 hours increased the rate of apoptosis. Oligosaccharide derivatives and chitosan trimer were able to raise the rate of apoptosis in EJ-28 from 7 % (6 h incubation) to 60 % (24 h incubation). In NHDF 6369 cells the substances induced an increase of apoptosis rates from 15 % (6 h) to 40 % (24 h). Staurosporine increased the apoptosis rates from 20 % (6 h) to 65 % in EJ-28 and 35 % in NHDF 6369 (24 h) in both cell lines, respectively.

## Conclusions

Our data showed reduced metabolic activity and increased apoptosis rates of cultivated tumour cells treated with oligosaccharide derivatives and chitosan derived trimers. The effects of chitosan trimers were comparable to the effects of the oligosaccharide derivatives of the marine nature material.

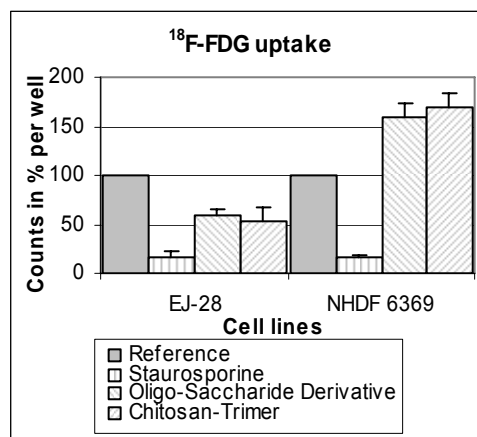


Fig. 1. [<sup>18</sup>F]FDG-uptake after 24 hours incubation; comparison between tumour and non-tumour cells.

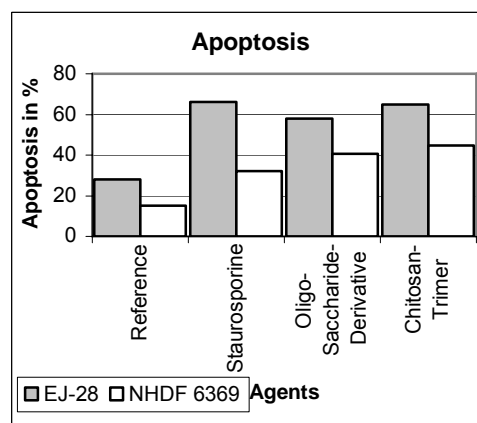


Fig. 2. Apoptosis rate after 24 hours incubation; comparison between tumour and non-tumour cells.

# Cellular Uptake of Fluorine-18-Labelled Native and Hypochlorite-Modified Low Density Lipoproteins (LDL)

S. Hoppmann, B. Steiniger, C. Haase, J. Pietzsch

## Introduction

Oxidation of LDL apolipoprotein (apo) B-100 by myeloperoxidase-generated hypochlorite (HOCl) is regarded as a crucial event in atherogenesis. Recently, HOCl-modified LDL (OCI-LDL) has been shown to be present in human atherosclerotic lesions [1]. In this report we present an improved methodology for radiolabelling of both native LDL (nLDL) and OCI-LDL with the positron-emitter fluorine-18 ( $^{18}\text{F}$ ) by the amino group-reactive radiolabelling agent *N*-succinimidyl-4- $^{18}\text{F}$ fluorobenzoate ( $^{18}\text{F}$ -SFB) and the use of  $^{18}\text{F}$ -fluorobenzoated LDL ( $^{18}\text{F}$ FB-LDL) for uptake studies in various human cells (Fig. 1) [2]. The aim of cellular uptake studies was to scrutinise that typical biological properties of  $^{18}\text{F}$ FB-LDL have been preserved. Furthermore, possible differences in cellular uptake of  $^{18}\text{F}$ FB-nLDL and  $^{18}\text{F}$ FB-OCI-LDL should be examined.

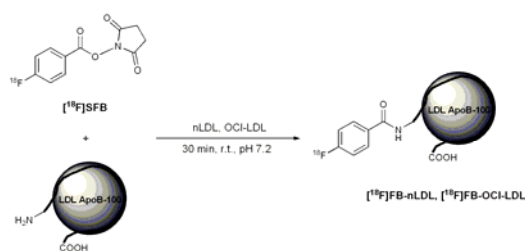


Fig. 1. Proposed reaction scheme for  $^{18}\text{F}$ -radiolabelling of LDL with  $^{18}\text{F}$ -SFB at pH 7.2. As recently proposed, at pH 7.2  $^{18}\text{F}$ -SFB reacts mainly with the chemically accessible, deprotonated *N*-terminal glutamate side chain residue of apoB-100 and only to a minor extent with the lysine side chain residues that are majorly protonated at pH 7.2 [2]. Typically, LDL radiolabelling with  $^{18}\text{F}$ -SFB resulted in radiochemical yields of  $30 \pm 10\%$  (nLDL; corrected for decay) and  $10 \pm 5\%$  (OCI-LDL), respectively, with specific radioactivity of 50 - 400 GBq/ $\mu\text{mol}$ .

## Results and Discussion

Cellular uptake studies (Fig. 2 and 3) demonstrated an enhanced uptake of OCI-LDL in human monocytic cell line THP-1 (activated by phorbol esters), representing a typical scavenger receptor bearing cell type, when compared with nLDL. THP-1 cells treated with fucoidan, a specific inhibitor of scavenger receptors class A, show a lower uptake of OCI-LDL than untreated THP-1 cells. These results indicate that  $^{18}\text{F}$ FB-OCI-LDL majorly were taken up *via* class A scavenger receptors. The uptake in human hepatocellular liver carcinoma cells (HepG2), representing a typical LDL receptor bearing cell, is high for  $^{18}\text{F}$ FB-nLDL and significantly lower for  $^{18}\text{F}$ FB-OCI-LDL.

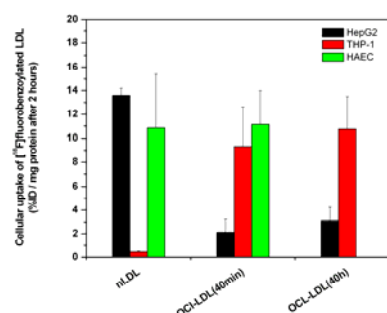


Fig. 2. Cellular uptake of  $^{18}\text{F}$ FB-nLDL,  $^{18}\text{F}$ FB-OCI-LDL(40 min) and  $^{18}\text{F}$ FB-OCI-LDL(40 h) in HepG2, THP-1 and HAEC (mean  $\pm$  SEM).

In contrast, human aortic endothelial cells (HAEC) take up  $^{18}\text{F}$ FB-nLDL and  $^{18}\text{F}$ FB-OCI-LDL to the same degree because they have both LDL-receptors and scavenger receptors [3].

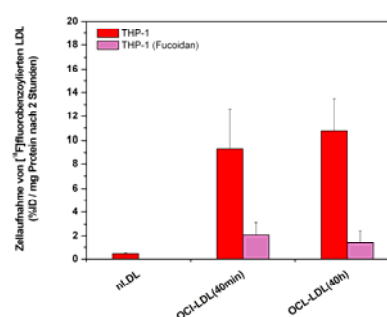


Fig. 3. Cellular uptake of  $^{18}\text{F}$ FB-nLDL,  $^{18}\text{F}$ FB-OCI-LDL (40 min) and  $^{18}\text{F}$ FB-OCI-LDL (40 h) in THP-1 cells with and without inhibitor (64 nM fucoidan; mean  $\pm$  SEM).

The cellular uptake of native and modified LDL *in vitro* correlated well with the presence of LDL receptors and scavenger receptors in different cell types.  $^{18}\text{F}$ -SFB labelling of LDL and the use of cellular uptake studies provide a valuable prerequisite for examinations of the metabolic fate of native and oxidised LDL in animal models *in vivo*.

This work is part of the diploma thesis of S.H. (University of Wuerzburg, Germany).

## References

- [1] Pietzsch, J. *et al.*, J. Clin. Pathol. 56 (2003) 622-623.
- [2] Pietzsch, J. *et al.*, Nucl. Med. Biol. 31 (2004) 1043-1050.
- [3] Hoppmann, S. *et al.*, Recent Res. Develop. Pathol. Biochem., *in press*.

# Catabolism of Hypochlorite-Modified Low Density Lipoproteins (LDL) *In Vivo*: Insights from Small Animal PET Studies

S. Hoppmann, B. Steiniger, C. Haase, J. Pietzsch

## Introduction

Oxidative modification of LDL apolipoprotein (apo) B-100 by myeloperoxidase-generated hypochlorite (HOCL) is regarded as a crucial event in atherogenesis. In this report we present the use of [<sup>18</sup>F]-fluorobenzoylated LDL particles ([<sup>18</sup>F]FB-LDL) in dynamic small animal PET studies in rats.

## Results and Discussion

The method was initially evaluated with respect to the uptake of [<sup>18</sup>F]-fluorobenzoylated native ([<sup>18</sup>F]FB-nLDL) and oxidised LDL ([<sup>18</sup>F]FB-OCI-LDL) in various human cells [1, 2]. As a result, radiolabelling of native and modified LDL using [<sup>18</sup>F]-SFB caused no alteration of their biological activity and functionality *in vitro*. Biodistribution studies in rats revealed high *in vivo* stability for the [<sup>18</sup>F]FB-LDL (data not shown in detail). The metabolic fate of ([<sup>18</sup>F]FB-nLDL and ([<sup>18</sup>F]FB-OCI-LDL *in vivo* was delineated by dynamic PET studies (Fig. 1).

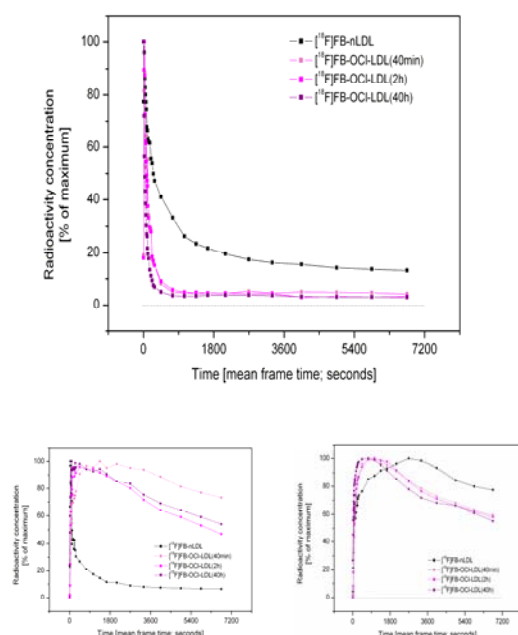


Fig. 1. Representative time-activity-curves showing *in vivo* kinetics of <sup>18</sup>F-radioactivity concentration after *i.v.* injection of either [<sup>18</sup>F]FB-nLDL or various species of [<sup>18</sup>F]FB-OCI-LDL in rats (blood, top; spleen, bottom left; liver, bottom right) as calculated from region-of-interest (ROI) analysis of dynamic small animal PET scans.

The *in vivo* distribution and kinetics of both native and modified LDL particles in the rat correlated well with the anatomical localization of LDL receptors and scavenger receptors

(Fig. 2). As an important result, dynamic PET studies in rats revealed a strongly enhanced catabolism of [<sup>18</sup>F]FB-OCI-LDL when compared with [<sup>18</sup>F]FB-nLDL. In this line, the high accumulation of [<sup>18</sup>F]FB-OCI-LDL in liver and spleen is supposed to be attributed to the scavenger receptor activity of endothelial cells and resident macrophages in these organs, e.g., hepatic Kupffer cells and splenic marginal zone macrophages. In contrast, the major binding sites of [<sup>18</sup>F]FB-nLDL particles are LDL receptor carrying hepatocytes, adrenal cells as well as glomerular and mesangial epithelial cells.

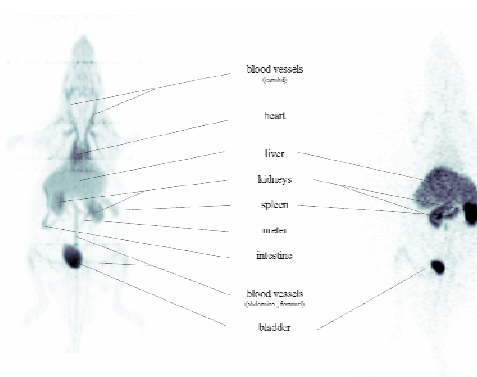


Fig. 2. Representative whole body PET scans showing <sup>18</sup>F-radioactivity distribution (120 min *p.i.*) after *i.v.* injection of either [<sup>18</sup>F]FB-nLDL (*left*) and [<sup>18</sup>F]FB-OCI-LDL (40 min) (*right*) in rats.

The results of the present *in vivo* examinations show that circulating OCI-LDL were cleared very effectively and fast by the reticuloendothelial system (RES). These investigations are of value for further evaluation of circulating oxidatively modified LDL as a potential indicator for oxidative stress and atherosclerotic risk [2]. [<sup>18</sup>F]SFB-labelling of LDL and the use of small animal PET provide a valuable tool to discriminate the kinetics and the metabolic fate of both native and oxidised LDL in animal models *in vivo*.

The authors are grateful to Mareike Barth and Regina Herrlich for their expert technical assistance. This work is part of the diploma thesis of S. H. (University of Wuerzburg, Germany).

## References

- [1] Hoppmann, S. *et al.*, *this report*, p. 13.
- [2] Hoppmann, S. *et al.*, *Recent Res. Develop. Pathol. Biochem.*, *in press*.

## Protein Oxidation in Human Disease: Prediabetes and Diabetes Mellitus Type 2

J. Pietzsch, C. Haase

*Hyperglycemia increases the formation of both oxidised low density lipoproteins (oxLDL) and glycated/glycoxidised LDL (glycLDL) which are important modulators of atherosclerosis and cardiovascular death. Recent advances in our understanding of oxidative and glycative stress under hyperglycemic conditions in vitro and in vivo have included: identification by mass spectrometry of the chemical nature of specific oxidative and glycative modifications in LDL, identification of oxLDL/glycLDL in disease-related tissue compartments and establishing the role of specific receptors that recognize oxLDL/glycLDL. This minireview summarises some recent results providing further evidence that both oxidation and glycation of human LDL play a pivotal role in the pathogenesis of atherosclerosis in prediabetes and diabetes mellitus Type 2.*

Patients with overt diabetes mellitus Type 2 and subjects with prediabetes, e.g., impaired glucose tolerance, are at very high cardiovascular risk. In atherogenesis oxidatively modified LDL (oxLDL) play a crucial role. LDL oxidation is a major event occurring within the vascular wall, which transforms LDL into cytotoxic agents able to promote complex sequences of proatherogenic events that participate to endothelial dysfunction, smooth muscle cell migration and proliferation, chemoattraction of inflammatory mononuclear cells, and apoptosis of vascular cells. The biological properties of oxLDL depend on the presence of oxidatively modified lipids and apolipoproteins, and on their uptake by cells through specific receptors. The excessive uptake of oxLDL via scavenger receptors in macrophages, vascular smooth muscle cells, and endothelial cells in an unregulated fashion leads to foam cell formation. The presence of foam cells in the vascular wall is considered to be the first morphological substrate of atherosclerosis. In contrast, native LDL (nLDL) will not promote the formation of foam cells under most circumstances, as uptake of nLDL by the LDL receptor pathway results in down-regulation of endogenous cholesterol synthesis and LDL receptor expression. Growing evidence indicates that oxidative modification of LDL is strongly increased both in subjects with prediabetes and in patients with overt diabetes mellitus Type 2, thereby implicating hyperglycemia as a causative factor [1, 2]. However, the mechanisms underlying the relation between hyperglycemia and increased LDL oxidation are not fully understood. LDL particles can undergo several oxidative modification reactions all of which are facilitated under conditions of high glucose-induced oxidative stress. On the one hand, the lipid constituents of the LDL particle are oxidised by reactive oxygen species. On the other hand, the major structural protein of LDL, apolipoprotein (apo) B-100, can also be oxidatively modified either by covalent binding to lipid peroxidation products or by direct oxidation of its amino acid side chain residues [3]. Glucose itself can directly modify apoB-100 amino acid residues in a process called glycation or glycoxidation [4].

However, the nature of specific modifications of protein amino acid residues altering their cellular functions still remains a subject of debate. Exemplarily, evidence for the important role of transition-metal catalysed processes in diabetes-associated lipoprotein oxidation is emerging [5]. However, no consensus has been achieved on whether these processes involving both copper and iron interact with the glycation/glycoxidation mechanism, or are independent. One recent study found the lack of any further stimulation of  $\text{Cu}^{2+}$ -induced lipid peroxidation or protein oxidation by glucose [4]. Others described increase of both  $\text{Cu}^{2+}$ -mediated LDL oxidation and the chemotactic activity of oxidised LDL towards pro-inflammatory cells by glucose in a concentration-dependent manner [6]. The incubation with glucose alone, under the conditions of very minor oxidation, also increased the chemotactic properties of LDL particles. In another study [7], glucose induced formation of conjugated dienes and thiobarbituric acid reacting substances and increased LDL electrophoretic mobility, also in a concentration-dependent manner. Some of these effects of glucose have been observed in the model of iron-mediated LDL oxidation [8]. Whereas the *in vivo* availability of free copper or iron ions is under tight control under normal physiological conditions, these transition metal imbalances are well documented in diabetes mellitus. For this reason, oxidation systems containing complexed, porphyrin-bound redox active iron are considered experimental models of high pathophysiological relevance [9]. These systems involve binding of, e.g., hemein ( $\text{Fe}^{3+}$ -protoporphyrin IX), a blood product and a physiological source of iron, to discrete binding sites of LDL and apoB-100, respectively, thus forming centers for redox cycling and repeated radical production and subsequent oxidation of LDL [9]. For apoB-100 these modifications finally result in the formation of new epitopes, e.g., by formation of apoB-100 crosslinks and loss of free amino groups. Recently, *in vitro* studies revealed that hemein induces oxidation of both proline and arginine residues of apoB-100 with the formation of  $\gamma$ -glutamyl semialde-

hyde ( $\gamma$ GSA) which can be easily reduced to the stable product 5-hydroxy-2-aminovaleric acid (HAVA) [9, 10]. Very recently, assessment of HAVA by a sensitive GC-MS approach also was employed to test the hypothesis that redox-active glucose further stimulates transition metal-induced LDL apoB-100 oxidation [11]. We performed *in vitro* studies to *i*) identify potential mechanisms of HAVA formation in LDL apoB-100, using various well-characterised oxidation systems, and *ii*) to explore the effects of increasing concentrations of glucose on hemin-induced  $\gamma$ GSA formation. These studies showed that glucose markedly enhanced the hemin-mediated oxidation process in a concentration-dependent manner. This effect is probably mediated *via* acceleration of the redox cycling of coordinatively bound  $\text{Fe}^{3+}$  due to enhanced reduction of iron by glucose. The stimulating effect of physiological and pathophysiological concentrations of glucose on the hemin-catalysed LDL apoB-100 oxidation appeared superoxide-dependent, and was completely inhibited by manganese superoxide dismutase. Thus, glucose mediates reduction of complex-bound iron *via* superoxide-dependent mechanism. In contrast, in the absence of glucose the hemin-catalysed LDL apoB-100 oxidation was not affected by the manganese superoxide dismutase, thus pointing to the fact that the redox cycling of coordinatively bound ferric iron is superoxide-independent [11]. We have also assessed LDL apoB-100 HAVA concentrations *in vivo*, in subjects with normal and impaired glucose tolerance as well as with clinically manifest diabetes mellitus. These studies revealed markedly elevated LDL apoB-100 HAVA levels in patients with prediabetes and overt diabetes mellitus Type 2 compared to healthy normolipidemic and normoglycemic individuals [11]. The LDL HAVA levels in patients with diabetes mellitus in this present study appeared remarkably similar to those in circulating LDL of hypercholesterolemic subjects with a high risk for atherosclerosis [12]. Recently,  $\gamma$ GSA formation has also been demonstrated in LDL apoB-100 in atherosclerotic lesions [13], thus providing additional information implicating oxidative modification of LDL apoB-100 proline and arginine residues in the development of atherosclerosis. In conclusion, our *in vitro* studies provide evidence of superoxide-mediated glucose enhancement of the hemin-induced LDL apoB-100 oxidation [11]. The latter is consistent with the *in vivo* evidence of enhanced iron-mediated LDL oxidation in the diabetic and prediabetic state. Our findings suggest that elevated plasma glucose concentrations provide a major contribution to increased formation of circulating modified LDL particles in subjects with prediabetes and overt

diabetes mellitus Type 2. Glucose-enhanced LDL apoB-100 oxidation may represent one mechanism of increased atherosclerosis in these subjects. However, further studies are needed to understand both the nature of the original oxidative insult and the specific consequences of formation of  $\gamma$ GSA or other specific oxidation products for the metabolic fate of apoB-100-containing lipoproteins *in vivo*. Moreover, the role of circulating modified LDL species in disease is of particular interest. In this line, the development of novel methodologies for radiolabelling of nLDL and various species of modified LDL, including oxLDL and glycLDL, with  $^{18}\text{F}$  or other positron emitting nuclides and the use of small animal PET to investigate the metabolism of these several lipoprotein species *in vivo* is currently in progress [3, 14-16].

The authors wish to thank Mareike Barth, Susan Hoppmann, Regina Herrlich, Ralf Bergmann, PhD, for their expert technical assistance. We thank Bjoern Steiniger, MSc, and Mathias Berndt, PhD, for radiochemical syntheses. We are also very grateful to Sigrid Nitzsche, Steffi Kopprasch, PhD, and Ulrich Julius, MD, from the Medical Clinic and Outpatient Department III, University Hospital Dresden, for their expert advice and many stimulating discussions.

## References

- [1] Kopprasch, S. *et al.*, Diabetes 51 (2002) 3102-3106.
- [2] Kopprasch, S. *et al.*, Trends Cell Mol. Biol. 1 (2005) 1-14.
- [3] Pietzsch, J. *et al.*, Recent Res. Devel. Mol. Cell. Biochem. 2 (2005) 153-177 (*and references therein*).
- [4] Knott, H. M. *et al.*, Eur. J. Biochem. 270 (2003) 3572-3582.
- [5] Stadtman, E. R. and Levine, R. L. Amino Acids 25 (2003) 207-218.
- [6] Millican, S. *et al.*, Free Radic. Res. 28 (1998) 533-542.
- [7] Otero, P. *et al.*, Free Radic. Biol. Med. 33 (2002) 1133-1140.
- [8] Mowri, H. O. *et al.*, Free Radic. Biol. Med. 29 (2000) 814-824.
- [9] Pietzsch, J., Biochem. Biophys. Res. Commun. 270 (2000) 852-857.
- [10] Pietzsch, J. and Julius, J., FEBS Lett. 491 (2001) 123-126.
- [11] Julius, U. and Pietzsch, J., Antiox. Redox. Signal. 7 (2005) 1507-1512.
- [12] Pietzsch, J. *et al.*, Arterioscler. Thromb. Vasc. Biol. 20 (2000) E63-E67.
- [13] Pietzsch, J. and Bergmann, R., J. Clin. Pathol. 56 (2003) 622-623.
- [14] Pietzsch, J. *et al.*, Amino Acids 29 (2005) 389-404.
- [15] Pietzsch, J. *et al.*, Amino Acids 29 (2005) 18-19 (Abstract).
- [16] Pietzsch, J. *et al.*, Diabetologia 48 (2005) 416 (Abstract).



# Monitoring of Stem Cell Homing with Small Animal PET

J. Oswald, R. Bergmann

*Stem cells and progenitor cells are widely used in therapeutic approaches, e.g., for the reconstitution of the hematopoietic system during the therapy of leukemia. We show here the feasibility of tracking labelled hematopoietic stem cells with small animal PET.*

## Introduction

Bone marrow derived hematopoietic stem cells are widely used for the therapy of various malignancies like leukemia or other neoplasia. Following myeloablative chemotherapy, which eliminates both tumour cells and bone marrow cells of the patient, donor hematopoietic cells can be transplanted, which then migrate from the peripheral blood to the bone marrow. This process is generally termed “homing”, because the transplanted donor cells migrate autonomously to their native environment, i.e. the bone marrow of the host [1]. In our approach we wanted to monitor the early steps of blood stem cell homing utilising positron emission tomography (PET). We therefore labelled human hematopoietic stem cells with the glucose analogue [ $^{18}\text{F}$ ]fluorodesoxyglucose ([ $^{18}\text{F}$ ]FDG) and transplanted them in NMRI nude mice, which comprises a valuable mouse model for xenotransplantations, i.e. the transfer of human or other non-murine cells in mice. The biodistribution of the labelled cells was then monitored with a small animal PET.

## Results and Discussion

Human hematopoietic stem cells (a kind gift of Prof. Denis Corbeil, Biotechnologisches Zentrum der TU Dresden) were isolated using immunomagnetic beads.  $1 \times 10^6$  were then radiolabelled with 20 MBq [ $^{18}\text{F}$ ]FDG for one hour in glucose-free medium. Approximately 20 KBq per cell preparation could be applied to the anaesthetised mice. Using the microPET<sup>®</sup> P4 the biodistribution of the cells was observed for four hours. The time activity curves in the interested organs were derived from 3D regions of interest by the program ROIFinder and analysed using the program system R. Data analysis revealed that the majority of cells first migrated into the lungs where they were captured in the small vessels. Subsequently, cells also migrated to liver, spleen and kidney. Our data showed the feasibility of stem cell tracking utilising small animal PET. The PET tracer [ $^{18}\text{F}$ ]FDG might not be the optimal label, because the efficiency of the metabolic labelling with [ $^{18}\text{F}$ ]FDG was very low.

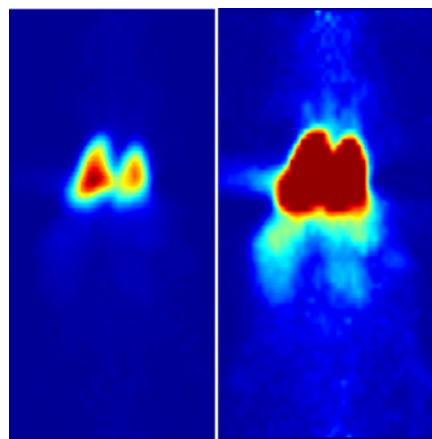


Fig. 1. Biodistribution of [ $^{18}\text{F}$ ]FDG labelled hematopoietic stem cells after 4 hours (left figure: colors normalised to the maximum; right figure: color scale expanded to visualise also the low activity areas).

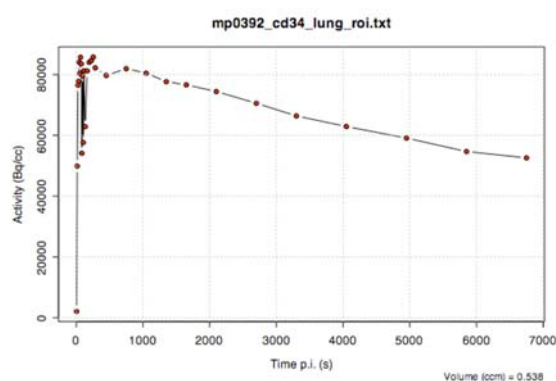


Fig. 2. Kinetics of the labelled cells in the lung.

Future experiments with either different methods like the direct labelling of cells with [ $^{18}\text{F}$ ]SFB or other radionuclides with longer half-lives might improve the labelling efficiency which then will allow an extended monitoring of stem cell homing.

## References

- [1] Lapidot, T. *et al.*, Blood 106 (2005) 1901-1910.



# Biochemical Characterisation of Fluorescein-Labelled Neurotensin Derivatives

R. Bergmann, V. Maes<sup>1</sup>, Ch. Hultsch, S. Kohl, Th. Hanke<sup>2</sup>, D. Tourwé<sup>1</sup>

<sup>1</sup>Organic Chemistry Department, Vrije Universiteit Brussel, Belgium, <sup>2</sup>Institut für Materialforschung, TU Dresden

Neurotensin(8-13) analogues containing a glycine or 5-aminovaleroyl spacer were labelled with fluorescein through formation of a N-terminal thiourea function. The receptor binding was measured in HT-29 cell cultures and showed a substantial decrease in affinity, especially for the metabolically stabilised [MeArg9, Tle11] analogue. Using fluorescence microscopy, the internalisation of the fluorescent neurotensin analogues into HT-29 cells was observed.

## Introduction

In recent years it has become evident that neuropeptide receptors allow the successful *in vivo* targeting of many tumours. A major limitation of the use of neuropeptides as targeting molecules is their rapid degradation by plasma and tissue proteases. As an extension of our studies on radiolabelled neurotensins for tumour diagnosis and therapy, we here present our results on the characterisation of fluorescein-labelled neurotensin analogues, and their uptake in HT-29 tumour cells.

## Results and Discussion

### Design and synthesis of peptides

An influence of the fluorescein group that is linked through a thiourea function to the peptide cannot be excluded. Therefore, a Gly spacer and a longer 5-aminovaleroyl (Ava) spacer were inserted. The FITC group was introduced by reaction with fluorescein isothiocyanate.

Table 1. Peptide structure of FITC-neurotensin analogues.

NT	Neurotensin
NT(8-13)	Arg-Arg-Pro-Tyr-Ile-Leu-OH
1	FITC-Gly-Arg-Arg-Pro-Tyr-Ile-Leu-OH
2	FITC-Ava-Arg-Arg-Pro-Tyr-Ile-Leu-OH
3	FITC-Ava-Arg-MeArg-Pro-Tyr-Tle-Leu-OH

### Receptor affinity

The affinity of the peptides for the NTR-1 was determined in HT-29 cells.

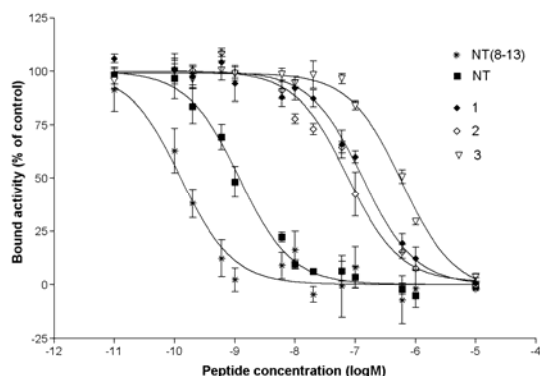


Fig. 1. Inhibition of [<sup>3</sup>H]neurotensin binding to HT-29 cell membranes.

### Fluorescence microscopy

HT-29 cells were incubated with the neurotensin analogues and after removal of the incubation liquid the cells were examined using a wide-field fluorescence microscope. After binding to the neurotensin receptor, the receptor-ligand complex is internalised.

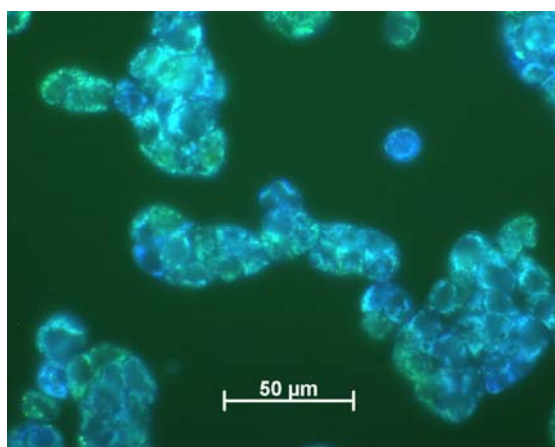


Fig. 2. The image represents a superposition of the blue and green channel images. In this figure the FITC-labelled ligand 2 appears in a light greenish colour.

The introduction of a fluorescein group at the N-terminus of NT(8-13) reduces the receptor affinity. The modifications of the peptide sequence in order to limit the metabolic breakdown further reduce the receptor affinity, in contrast to what has been observed for the corresponding <sup>99m</sup>Tc-labelled analogues. Nevertheless, for the most potent analogue 1 the internalisation into HT-29 cells can be visualised using confocal microscopy. The application of a fluorescently labelled NT analogue will require that more potent analogues will be developed.

Accepted in Journal of Peptide Science.

## References

- [1] Reubi, J. C. *et al.*, J. Nucl. Med. 46 (2005) 67S-75S.
- [2] Bergmann, R. *et al.*, Nucl. Med. Biol. 29 (2002) 61-72.
- [3] Bläuenstein, P. *et al.*, Cancer Biother. Radiopharm. 19 (2004) 181-188.

# Implementing a Small Animal Magnetic Resonance Imaging System

K. Strobel, R. Bergmann, J. van den Hoff

*The implementation of Magnetic Resonance Imaging and Magnetic Resonance Spectroscopy for small animals at the PET-centre is described.*

## Introduction

Since January 2005 a small animal Magnetic Resonance Imaging system with magnetic field strengths of 7 T (BioSpec™ 70/30, Bruker Biospin MRI GmbH, Ettlingen, Germany) operates at the PET-centre. The information obtained by Magnetic Resonance Imaging (MRI) and Spectroscopy (MRS) are complementary to that obtained by Positron Emission Tomography (PET). The combination of the anatomical and morphological information of MRI and the functional information of the PET data allows a better understanding of tumour biology and metabolism.

## Results and Discussion

In the framework of the implementation of the MRI system, own measurement protocols were created (e.g. t1-weighted, t2-weighted), to get optimal contrast in various organs and/or tissues (e.g. tumours, vascular system).

Furthermore, a file conversion tool was developed and implemented to convert two and three dimensional data from the MRI file format to a file format which is compatible to the PET file format (here: ECAT7). This was done to allow the fusion of anatomical and morphological MRI data and the functional PET data with existing software (Fig. 1).

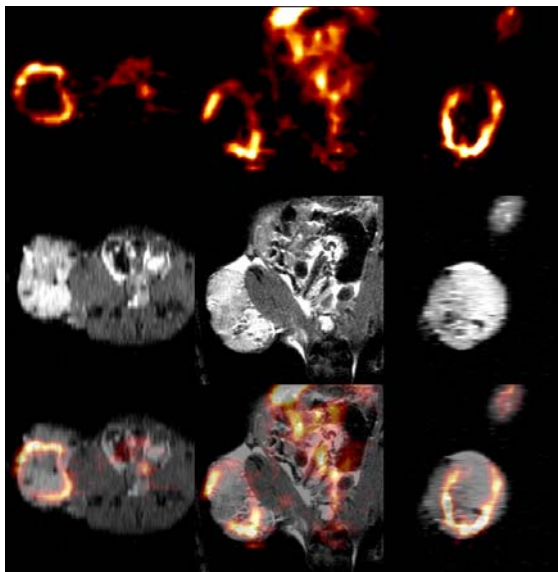


Fig. 1. The image fusion (lower row) of PET (upper row) and MRI (middle row) of a tumour xenograft on the leg of a nude mouse is shown.

The image fusion of MRI and PET allows the identification of the anatomical regions of increased tracer uptake. The image fusion of the PET and MRI was performed using the Multi Purpose Imaging Tool (MPI Tool, ATV GmbH, Germany).

Moreover, measurement protocols for localised spectroscopy (e.g. PRESS) in very small volumes (~ 2 x 2 x 2 mm) were tested and improved for proton (1H) MRS. First spectra were derived from human xenograft tumours transplanted in nude mice (Fig. 2).

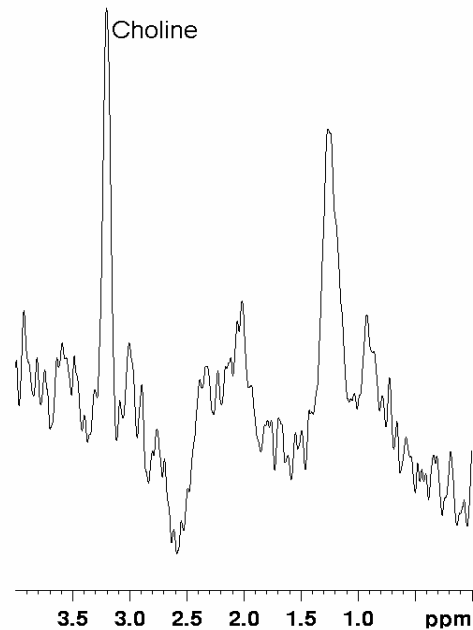


Fig. 2. PRESS proton spectra (TR = 1.2 s, TE = 20 ms, 1200 Averages) on a 1.5 x 1.5 x 1.5 mm voxel of a tumour xenograft on the leg of a nude mouse.

The choline peak at 3.2 ppm is typical for growing tumour cells. This information together with the information acquired from the radio tracer PET data yield a more complete picture of the tumour metabolism.

## Conclusions

MRI and MRS provide valuable information, complementary to that obtained with PET, thus allowing a better assessment of tumour biology, structure and metabolism.

# Optimised List-Mode Acquisition and Data Processing Procedures for ACS2 Based PET Systems

J. Langner, P. Bühler, U. Just, C. Pötzsch, E. Will, J. van den Hoff

## Introduction

Modern positron emission tomography (PET) scanners usually acquire data in so-called *histogram-mode*, where all coincidences are sorted online into three-dimensional histograms. This saves storage space and minimises the required bandwidth, but it also represents a loss of information. Therefore, PET scanners like the ECAT Exact HR+ allow for the acquisition of data in a separate mode, called *list-mode*. Based on this data, methods aiming at the modification of the coincidence events information can be applied prior to the image reconstruction, e.g. for correction of patient motion [1]. However, several aspects hinder the routine use of *list-mode*. For example, the limited network capabilities of the underlying acquisition control system (ACS2) lead to long time delays of up to several hours. As a result, the image data is often available only the next day, thus representing an unacceptable delay for clinical PET. To overcome these obstacles, we have developed custom hardware and software. These methods do not only allow for the integration of *list-mode* in routine operation, they also improve the overall runtime stability of ACS2-based PET systems, making them also attractive for *histogram-mode* acquisitions.

The ACS2 usually stores the acquisition data on an internal SCSI-2 hard disk. Although this bus type supports a maximum theoretical throughput of 10 MB/s, the ACS2 does not allow for the transfer of data to other systems with rates higher than  $\approx 0.5$  MB/s. We replaced the internal hard disk of the ACS2 with a dual-channel *Ultra160-SCSI* RAID. To arrange for a parallel access from another machine, we connected the second channel of the RAID device to a Linux system (Fig. 1).

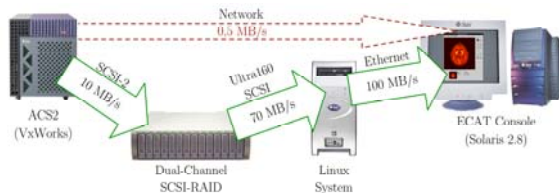


Fig. 1. Using a dual-channel Ultra160-SCSI RAID storage device, it is possible to access the stored acquisition data from another system in parallel with a maximum throughput of  $\approx 70$  MB/s.

Furthermore, to be able to access the data from the Linux system, we reverse-engineered the structure of the used file system and developed an own implementation. Although this

solution accesses data considerably faster, the PET system still has to be explicitly switched into another acquisition mode prior to each *list-mode* acquisition. To improve this situation, we verified the routing of the raw coincidence data on the ACS2 by sampling it from externally accessible data cables using a digital oscilloscope. In order to permanently sample the data we have developed a separate hardware adapter card. It uses optoelectronic couplers and allows, together with two PCI-based digital data acquisition cards (DAQ), to retrieve all coincidence data in real-time (Fig. 2).

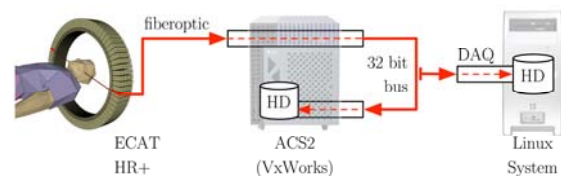


Fig. 2. Two digital acquisition cards (DAQ) are used in a Linux system to acquire the raw data in parallel and to save it to a separate hard disk (HD) device.

## Results and Discussion

Our hardware based acquisition methods overcome certain long-term hardware limitations of the ACS2 of the ECAT Exact HR+ PET Scanner series. After implementation, we were able to observe a high speed-up. The methods allow to transfer stored data from the ACS2 to another system with a max. throughput of  $\approx 70$  MB/s, a  $140\times$  speed-up in comparison to the ACS2's original capabilities. For *list-mode* acquisitions, such a speed improvement means that a typical data transfer requires only  $\approx 1$  min in contrast to the previously  $\approx 2.5$  h for an amount of  $\approx 4$  GB of data (one hour  $^{18}\text{F-FDG}$  @  $\approx 330$  MBq). In addition, the immediate transfer of the acquired data also improves the general runtime stability of the ACS2, and thus is also attractive for conventional *histogram-mode* acquisitions. Moreover, by using our DAQ-based acquisition solution, the ECAT Exact HR+ can be operated in conventional *histogram-mode*, while a concurrently running Linux system reads out the raw *list-mode* stream in real-time. This, in combination with our software solutions, permits to integrate *list-mode* in clinical PET investigations.

Published in: Langner, J. *et al.*, *Z. Med. Phys.* 16 (2006) 77-84.

## References

- [1] Langner, J. *et al.*, *Annual Report 2004*, FZR-424, p. 12.

# User Guided Segmentation and Quantification of Three-Dimensional Structures in Oncological Whole Body PET - Continued

C. Pöttsch, F. Hofheinz, J. van den Hoff

## Introduction

In the last report [1] we described a tool for analysis and quantification of volumes of interest (VOI) in three-dimensional tomographic datasets which are obtained by positron emission tomography (PET). This tool has several advantages compared to other programs on the market, like a comfortable viewer with three different views, threshold based three dimensional VOI evaluations, export filters for the statistic values and the availability for different operation systems (Windows, MacOS X and Unix/Linux).

Because of technical improvements in the area of PET and PET/CT, and the upcoming usage of PET datasets in treatment planning some additional features were implemented this year. One aim was the handling of several studies at once to allow simultaneous delineation of VOIs at identical locations in different studies. Moreover, user-independent segmentation was a field of our research.

## Results and Discussion

To achieve the aforementioned, a multi study display was introduced (see Fig. 1).

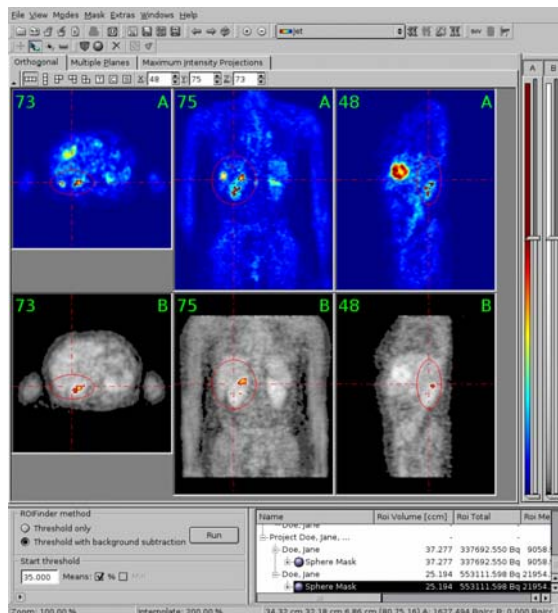


Fig. 1. Parallel display of a follow up study.

This parallel display allows the user to view and process 2 or more studies at the same time. All operations like mask creation or VOI evaluation which are performed on one of the

images are done in parallel on the others. Different PET scans usually imply different positioning of the patient. To achieve an optimal alignment of the images the corresponding volume data are coregistered, where the alignment is measured by the mutual information of the data. Consequently, the user can work on PET and CT studies at the same time to combine the information provided by the different modalities like the morphology in CT and the metabolism in PET. Additionally this allows the comparison of VOIs in two PET studies at different times to assess treatment success or failure.

To use other modalities the import filters were rewritten. Currently, images of the Concorde microPET and Siemens ECAT7 are supported. To be more manufacturer independent the DICOM protocol can be used to import files from hard disk and over network.

The automatic threshold based segmentation uses a new target/background algorithm and a contrast-based threshold [2] to identify the VOIs independently of the user. This ensures minimal Inter-Observer variability and generally leads to stable and reproducible results.

For a better integration in routine work and the intended commercialisation of the program in cooperation with ABX Radeberg (Advanced Biochemical Compounds, Radeberg) a comprehensive online help, a licensing system and installers for various operation systems have been implemented.

Future developments will aim at improving export and import of the resulting data (masks, VOIs,...) which gives the user the ability to save time by defining templates or reload previously analysed studies. Further improvement of the segmentation algorithm should further stabilise the results in most circumstances.

## References

- [1] Pöttsch, C. *et al.*, *Annual Report 2004*, FZR-424, p. 10.
- [2] Pöttsch, C. *et al.*, *Nucl. Med.* 44 (2005) A16.



# **RADIOMETAL THERAPEUTICS**





# A Novel Rhenium Chelate System Derived from Dimercaptosuccinic Acid

T. Heinrich, W. Kraus<sup>1</sup>, H.-J. Pietzsch, C. Smuda, H. Spies

<sup>1</sup>Bundesanstalt für Materialforschung und -prüfung, Berlin

A novel type of tetradentate ligand derived from DMSA has been synthesised. The tetrathiolato S<sub>4</sub> ligand forms anionic five-coordinated oxorhenium(V) complexes with square-pyramidal coordination geometry. The orientation of the metal oxo group is *exo* in relation to the carbamido groups of the ligand.

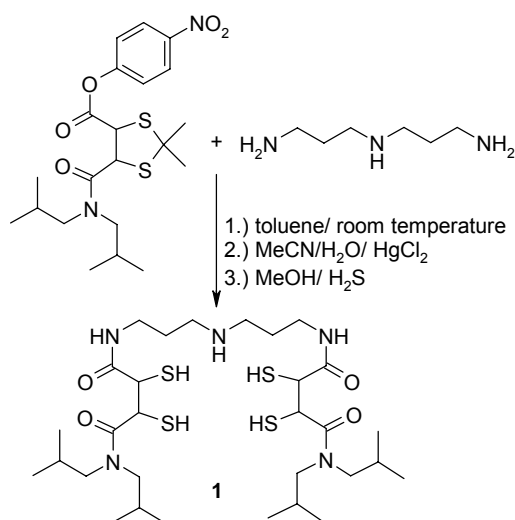
## Introduction

This work is part of our efforts to develop chelating agents for stable binding and easy conjugation of rhenium-188 to targeting molecules. Keeping in mind the high *in vivo* stability of [<sup>188</sup>Re<sup>V</sup>O(DMSA)<sub>2</sub>] [1] we want to exploit this coordination system for the synthesis of novel, even higher stable <sup>188</sup>Re<sup>V</sup>O–S<sub>4</sub>-chelates.

## Results and Discussion

A new type of tetradentate ligand has been synthesised starting with *meso*-DMSA by bridging two molecules of *N,N'*-diisobutyl-2,3-dimercaptosuccinamide with *N*-(3-aminopropyl)-propane-1,3-diamine.

Scheme 1. Synthesis of S<sub>4</sub> diamide ligand **1**.



The resulting stereoisomeric tetrathiolato S<sub>4</sub>-ligand **1** of the composition (i-Bu)<sub>2</sub>N(O)C–C(SH)–C(SH)–C(O)NH–(CH<sub>2</sub>)<sub>3</sub>–NH–(CH<sub>2</sub>)<sub>3</sub>–NHC(O)–C(SH)–C(SH)–C(O)N(i-Bu)<sub>2</sub> forms anionic five-coordinated oxorhenium(V) complexes **2** and **3** by ligand exchange reaction of NBu<sub>4</sub>[ReOCl<sub>4</sub>] in methanol. The mixture of isomers as indicated by HPLC was separated by chromatographic methods.

X-ray crystal structure determination of both stereoisomeric forms reveals the square-pyramidal coordination geometry of the Re<sup>V</sup>OS<sub>4</sub> core. The equatorial plane is formed by four thiolate sulfur atoms, whereas the oxygen occupies the apical position. The orientation of the metal-oxo core is *exo* in relation to the

carbamido groups in both isomers. Both complexes are stereoisomeric regarding the junction of the triamine chain. Compound **2** is the *exo-trans* and compound **3** is the *exo-cis* isomer.

In the absence of base, the oxorhenium(V) compounds were isolated as “betaine”, with the protonated nitrogen of the bridge serving as internal “counter ion” [2].

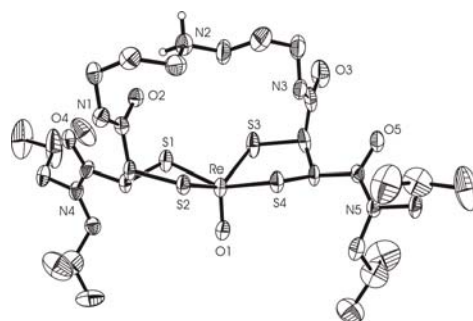


Fig. 1. ORTEP diagram of **2**. Atoms are drawn at 50 % probability.

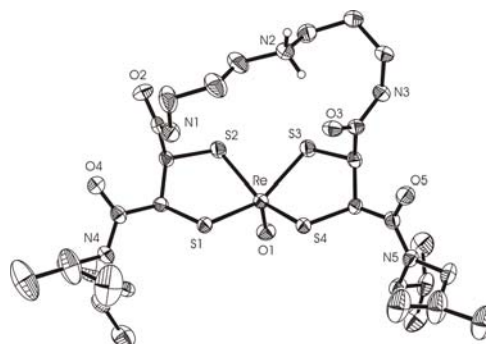


Fig. 2. ORTEP diagram of **3**. Atoms are drawn at 50 % probability.

Published in [2]: Heinrich T. K. *et al.*, *Inorg. Chem.* 44 (2005) 9930-9937.

## References

[1] Blower P. J. *et al.*, *Eur. J. Nucl. Med.* 25 (1998) 613-621.



# Optimised Procedure for Preparing $^{188}\text{Re(V)}$ Complexes under Mild Conditions

S. Seifert, H.-J. Pietzsch

*An easy and gentle method for the preparation of  $^{188}\text{Re(V)}$  complexes with bidentate and tetradentate ligands is described starting from the precursor complex  $^{188}\text{Re(III)-EDTA}$ .*

## Introduction

Complexes of  $^{188}\text{Re(V)}$  are commonly synthesised by a one-step route using huge amounts of auxiliary ligands (oxalic acid, cyclodextrines, citric acid, tartaric acid, ethylene diamine tetraacetic acid), reducing agents and in most cases also high temperatures. Another way to prepare the desired  $^{188}\text{Re(V)}$  complexes is a two-step procedure, in which, for example, a glucoheptonate, gluconate or citrate complex is first formed, and then in a second step undergoes a ligand exchange reaction with the appropriate ligand. Moreover, we found that  $^{188}\text{Re(III)-EDTA}$  also represents a suitable precursor for the preparation of  $^{188}\text{Re(V)}$  oxo and dioxo complexes.  $^{188}\text{Re(III)-EDTA}$  can be prepared in acidic solution at room temperature and in volumes of 1 - 10 ml [1]. The complex is stable to only a limited extent and is easily re-oxidised to perrhenate in neutral solutions. Considering this distinctive re-oxidation behaviour of  $^{188}\text{Re(III)-EDTA}$  it should be possible to prepare  $^{188}\text{Re}$  complexes of higher oxidation states by a combined ligand exchange/re-oxidation reaction with suitable ligands. This work presents a simple method for the preparation of oxorhenium(V) complexes as  $[\text{ReO}(\text{ECD})]$ ,  $[\text{ReO}(\text{DMSA})_2]$ , or  $[\text{ReO}(\text{MAG}_3)]^-$  ( $\text{ECD} = L,L$ -ethylene dicysteine diethyl ester,  $\text{DMSA} =$  dimercapto succinic acid,  $\text{MAG}_3 =$  mercaptoacetyl triglycine) and dioxorhenium(V) complexes as  $[\text{ReO}_2(\text{en})_2]^+$ ,  $[\text{ReO}_2(\text{tau})]^+$  or  $[\text{ReO}_2(\text{cyclam})]^+$  ( $\text{en} =$  ethylene diamine,  $\text{tau} = 1,4,8,11$ -tetraazaundecane,  $\text{cyclam} = 1,4,8,11$ -tetraazacyclotetradecane) using the precursor complex  $^{188}\text{Re(III)-EDTA}$ .

## Radiolabelling

$^{188}\text{Re(III)-EDTA}$  was prepared by adding 3 – 5 ml perrhenate eluate from a  $^{188}\text{W}/^{188}\text{Re}$  generator together with 0.05 ml 1 M HCl to a kit vial containing 5 mg EDTA, 5 mg mannitol and 1.0 mg  $\text{SnCl}_2$  in freeze-dried form under nitrogen. After 20 - 30 min at room temperature the complex formation was finished; yield: > 95 % (TLC). Alternatively, the same complex was prepared using BER (BER = borohydride exchange resin) instead of  $\text{SnCl}_2$  as the reducing agent [2]. For this purpose a mixture of 5 mg EDTA and 5 mg mannitol dissolved in 0.5 ml saline, and 2 ml perrhenate eluate containing 5  $\mu\text{l}$  of 85 %  $\text{H}_3\text{PO}_4$ , was added to a vial containing 10 mg BER under nitrogen. After 25 min

reaction time at room temperature 90 - 95 % of the desired complex was formed.

For preparation of the  $^{188}\text{Re(V)}$  complexes 0.1 – 10 mg of the appropriate ligand dissolved in 1.0 ml of 0.1 M phosphate buffer solution of pH 7.4 or 9 – 10 was added under nitrogen flushing to 1.0 ml of the acidic precursor solution and the final solution was allowed to stand for 10 – 20 minutes at room temperature. In most cases an ultrasonic bath was used for incubations.

## Results and Discussion

We found that  $[\text{Re}]$ perrhenate is easily reduced to a  $^{188}\text{Re(III)}$ -complex without heating and with only 1 mg of stannous chloride in an acidic solution of EDTA, also in volumes of 10 ml. To avoid the undesired formation of stannous hydroxides,  $\text{SnCl}_2$  may be substituted by BER. Using optimised conditions the resulting  $^{188}\text{Re(III)-EDTA}$  solution exhibits the same radiochemical purity, about 95 %, as that determined for a  $\text{Sn(II)}$ -reduced solution. Moreover, the BER is easy to remove from the complex solution. The re-oxidation studies performed with bidentate and tetradentate ligands resulted in high yields of the desired  $^{188}\text{Re(V)}$ -oxocomplexes when the ligands DMSA or ECD were dissolved in 0.1 M phosphate buffer pH 7.4 and added, with the exclusion of air, to the acidic  $^{188}\text{Re(III)-EDTA}$  solution (Table 1). Thus, the ligand exchange reaction between  $^{188}\text{Re(III)-EDTA}$ , which was prepared under a nitrogen atmosphere in the kit vial, and the respective ligand occurs in neutral solution and only small amounts of perrhenate are formed. However, when the preparations were performed without the exclusion of air and after neutralisation of the  $^{188}\text{Re(III)-EDTA}$  solution, 20 – 30 % perrhenate was always detected in the final solution. Obviously, the neutralisation of the  $^{188}\text{Re(III)-EDTA}$  solution must be carried out in the presence of the appropriate ligand in order to prevent a fast re-oxidation of  $^{188}\text{Re(III)-EDTA}$  to perrhenate. The identity of the prepared  $^{188}\text{Re}$  complexes was confirmed by simultaneously prepared and well-characterised  $^{99\text{m}}\text{Tc}$  complexes and cold rhenium complexes.  $^{188}\text{Re(V)-DMSA}$  prepared from  $^{188}\text{Re(III)-EDTA}$  at room temperature was compared by HPLC with "kit-prepared"  $^{99\text{m}}\text{Tc(V)-DMSA}$  and the other preparations were identified in the same way (Fig. 1).

Table 1. Yields and reaction conditions for the preparation of  $^{188}\text{Re(V)}$  complexes from  $^{188}\text{Re-EDTA}$ 

Complex formed	Yield [%]	Optimum reaction conditions
$^{188}\text{ReO(ECD)}$	$95 \pm 2$	0.5 mg ligand, ultrasonic, 10 min, pH 7, $\text{N}_2$
$^{188}\text{ReO(DMSA)}_2^-$	$94 \pm 3$	0.5 mg ligand, ultrasonic, 10 min, pH 7, $\text{N}_2$
$^{188}\text{ReO(MAG}_3)_-$	$95 \pm 2$	0.5 mg ligand, ultrasonic, 10 min, pH 9
$^{188}\text{ReO}_2(\text{en})_2^+$	$93 \pm 2$	10 mg ligand, ultrasonic, 10 min, pH 10
$^{188}\text{ReO}_2(\text{tau})^+$	$94 \pm 2$	5 mg ligand, ultrasonic, 10 min, pH 10
$^{188}\text{ReO}_2(\text{cyclam})^+$	$50 \pm 5$	20 mg ligand, ultrasonic, 10 min, pH 10, $\text{N}_2$

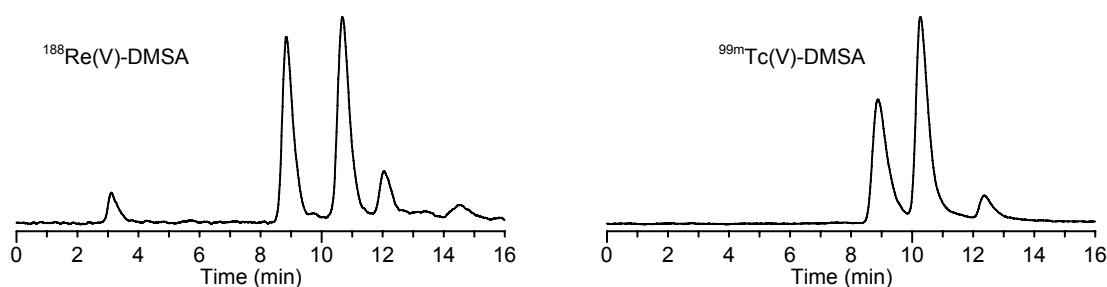


Fig. 1. Comparison of HPLC analyses of  $^{188}\text{Re(V)-DMSA}$  and a kit preparation of  $^{99\text{m}}\text{Tc(V)-DMSA}$ ; PRP-1 column; acetonitrile/0.1 % TFA (A)/water/0.1 % TFA (B); all three stereoisomers are well separated using a linear gradient 0 to 50 % A in 20 min ( $R_f$  values between 8 and 13 min).

The cationic dioxocomplexes with acyclic and cyclic polyamines were prepared according to the same procedure. The preparation of the complexes  $^{188}\text{ReO}_2(\text{en})_2^+$  and  $^{188}\text{ReO}_2(\text{tau})^+$  also succeeded in high yields of 90 – 95 % without addition of phosphate buffer solution at pH 9 - 10. It was observed, however, that the  $^{188}\text{Re(III)-EDTA}$  precursor complex only formed about 50 % of the cyclam complex, despite high ligand excess and different reaction conditions (room temperature or 50 - 100 °C, ultrasonic, pH 6 - 10). In contrast to the reactions with ECD, DMSA or the acyclic amines en and tau, which resulted in high yields of the desired ligand exchange product, 50 % or more of the starting activity was re-oxidised to perrhenate. This agrees with observations made by Prakash *et al.* [3], who found that only complexes with acyclic polyamine ligands are formed by direct reduction of perrhenate in aqueous solutions, while the synthesis of Re-188 complexes with cyclic polyamines like cyclam using the same procedure failed. Obviously, the formation of the  $^{188}\text{ReO}_2(\text{cyclam})^+$  complex needs longer time and higher activation energies than those needed for acyclic amine ligands. Thus, the re-oxidation to perrhenate is favoured against the ligand exchange reaction. The complexes were additionally characterised by paper electrophoresis and anion exchange separation using minicolumns filled with Dowex (1x8) ion exchange resin (Cl<sup>-</sup>-form). The cationic complexes were eluted with water from the anion exchange

column as radiochemically pure products, while the anionic impurities  $^{188}\text{Re(III)-EDTA}$  and  $^{188}\text{ReO}_4^-$  were retained at the column.

## Conclusions

Rhenium-188(V) oxo- and dioxocomplexes with bidentate or tetradentate ligands were prepared in high radiochemical yields (with exception of  $^{188}\text{ReO}_2(\text{cyclam})^+$ ) by a combined re-oxidation/ligand exchange reaction starting from  $^{188}\text{Re(III)-EDTA}$ . The formation of the precursor complex and the subsequent preparation of the desired Re(V)-complexes may be performed under mild conditions (room temperature, neutral or weak basic solutions, low amounts of reducing agent, ligands, and auxiliary ligands) and allows consequently the labelling of sensitive biomolecules coupled to such types of chelates.

Published in: Seifert, S. *et al.*, Appl. Radiat. Isot. 64 (2006) 223-227.

## References

- [1] Seifert, S. *et al.*, Bioconjugate Chem. 15 (2004) 856-863.
- [2] Park, S. H. *et al.*, J. Labelled Compd. Radiopharm. 47 (2004) 683-697.
- [3] Prakash, S. *et al.*, Nucl. Med. Biol. 23 (1996) 543-549.

# Hydrophilic Rhenium-188 Complexes for Attaching the Metal to Biomolecules

## 6. Complex Design

E. Schiller, F. Tisato<sup>1</sup>, H. Spies, H.-J. Pietzsch  
<sup>1</sup>ICIS-CNR, Padova, Italy

Rhenium-188 complexes with tetradentate/monodentate NS<sub>3</sub>/P ('4+1') coordination represent a flexible system which physico-chemical properties can easily be modified. As such modifications have a significant impact on the stability of the complexes, guidelines for a rational complex design are needed.

### Introduction

Application of rhenium-188 for therapeutical purposes in nuclear medicine requires appropriate systems for the stable complexation of the nuclide. The '4+1' approach appears to be among the promising tools to achieve this goal. Besides stability, high hydrophilicity of the rhenium-188 complexes plays an important role, aiming at fast renal excretion of radioactive metabolites. We synthesised hydrophilic ligands for the '4+1' approach and determined the *in vitro* stability of resulting rhenium-188 complex [1, 2]. These experiments showed a strong dependency of the *in vitro* stability on the nature of the ligands, especially on the monodentate phosphorous(III) ligand. Based on these findings our aim was to map out a strategy for a rational '4+1' complex design.

### Results and Discussion

*In vitro* stability studies showed that the bulkiness of phosphorus(III) ligand and the lipophilic character of the inner coordination sphere were the crucial factors to build up stable rhenium '4+1' complexes. Only complexes bearing a bulky phosphorous co-ligand (cone angle between 140 ° and 145 °) which is able to generate, along with the three thiolate sulfurs of the NS<sub>3</sub> ligand, a lipophilic area around the rhenium are of high *in vitro* stability. Presumably, this lipophilic area prevents the Re(III) center from the attack of hydrophilic water-derived (by radiolysis) species, such as H<sub>2</sub>O<sub>2</sub>, or water itself. Additionally, stability can be increased by introduction of electron-withdrawing phosphorous substituents, resulting in increased stability of rhenium towards oxidation.

Considering the results of the *in vitro* experiments, monodentate triphenylphosphine ligands seem to be well-suited to create an appropriate lipophilic area around the rhenium. An increase of overall hydrophilicity of the rhenium-188 complex can be achieved by preserving the lipophilic core in the inner coordination sphere and introduction of hydrophilic functional groups either at the monodentate ligand and/or at the NS<sub>3</sub> framework. For the latter approach the carboxyl group containing

tetradentate NS<sub>3</sub> ligand can be used as starting material.

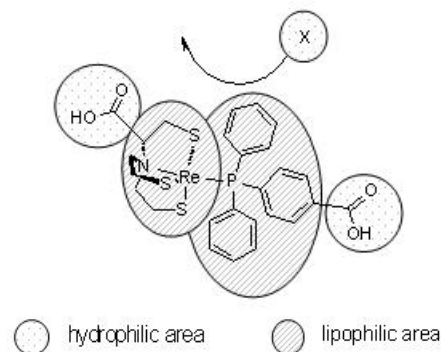


Fig. 1. Rational design of rhenium '4+1' complexes (X = H<sub>2</sub>O or water-derived species).

Fig. 1 summarises the arrangement of lipophilic and hydrophilic areas. The shown '4+1' structure is one possible implementation of the requirements discussed above. As can be seen in the picture, there are in principal two ways of bioconjugating and fine-tuning these rhenium-188 '4+1' complexes. First, the carboxyl group of the monodentate ligand can be used for attaching a target-seeking structure. In this case amines bound to the carboxyl group of the tetradentate ligand *via* amide bond serve as modulator of physico-chemical properties by what the biodistribution pattern and excretion can be influenced. The other way round, COOH of the NS<sub>3</sub> ligand can be used for bioconjugation and the carboxyl group of the triphenylphosphine derivative for fine-tuning the physico-chemical properties of the complex. The question which approach to use maybe depends on the carrier molecule which has to be labelled. Further investigations therefore are necessary.

Published in: Schiller, E. *et al.*, *Bioconjugate Chem.* 16 (2005) 634.

### References

- [1] Schiller, E. *et al.*, *Annual Report 2003*, FZR-394, p. 45.
- [2] Schiller, E. *et al.*, *Annual Report 2004*, FZR-424, p. 53.

# Hydrophilic Rhenium-188 Complexes for Attaching the Metal to Biomolecules

## 7. Bioconjugation and Radiolabelling

E. Schiller, J.-U. Künstler, S. Seifert, H.-J. Pietzsch

*Aiming at rhenium-188 labelling of target-seeking biomolecules via the so-called '4+1' concept, a water-soluble triphenylphosphine derivative was developed as a synthon for the conjugation of carrier molecules, such as peptides and proteins. Exemplary coupling reactions were performed with H-Arg-Tyr-OH and human serum albumin. Efforts have been made to label these conjugates with rhenium-188 according to the '4+1' approach.*

### Introduction

In vitro stability studies of rhenium-188 complexes with '4+1' coordination have shown dependencies between sterical and electronic features of the complex and its *in vitro* stability. These findings led to a model enabling a rational design of rhenium-188 '4+1' complexes of high *in vitro* stability [1, 2].

Complexes consisting of a carboxyl group containing tetradentate NS<sub>3</sub> ligand and 4-diphenylphosphino benzoic acid as monodentate ligand fulfil requirements of the proposed model. Methods how to attach these complexes to target-seeking biological structures, in particular peptides and proteins, have to be found.

### Results and Discussion

The sulfosuccinimidyl activated ester of 4-diphenylphosphino benzoic acid **1** was synthesised (Fig. 1). This water-soluble reactive compound serves as synthon for the conjugation to amino groups of peptides and proteins. The dipeptide H-Arg-Tyr-OH and the protein human serum albumin were chosen as model compounds for bioconjugation and labelling experiments.

#### Labelling of H-Arg-Tyr-OH

The reaction of a 2-fold excess of **1** with H-Arg-Tyr-OH was completed after 2.5 h at pH 8.0. Yield: approx. 50 %. The conjugate **2** was labelled *via* the '4+1' approach using a labile <sup>188</sup>Re(III)-EDTA intermediate [3]. Radiochemical yield after 30 minutes at 50 °C: 75 %.

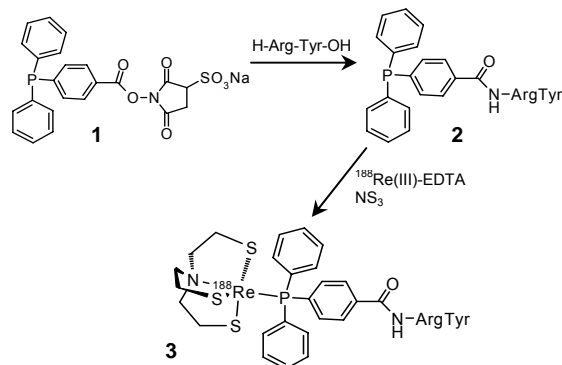


Fig. 1. Labelling of H-Arg-Tyr-OH.

The identity of **3** was proven by comparison of its retention time in HPLC with its non-radioactive analogue, synthesised in milligram amount and characterised by mass spectrometry.

#### Labelling of human serum albumin (HSA)

The activated ester **1** was reacted with HSA in aqueous solution at pH 8.0 at ratios of 10:1 and 20:1. The number of conjugated phosphine per HSA molecule was determined by MALDI-MS and was found to be 7 and 14, respectively, meaning a yield of 70 % for each coupling reaction.

Labelling experiments were done using the labile <sup>188</sup>Re(III)-EDTA intermediate. As reduction of perrhenate to this Re(III) species requires acidic conditions we had to neutralise this solution before adding the protein. Unfortunately, 25 – 45 % <sup>188</sup>ReO<sub>4</sub><sup>-</sup> are formed immediately after neutralisation. Another approach is the addition of acidic <sup>188</sup>Re(III)-EDTA solution to a phosphate buffered solution of HSA (3 mg of the 1:20 conjugate). After incubation for 30 minutes at 37 °C we found approx. 30 % of the radioactivity bound to the protein fraction and 30 % perrhenate.

### Summary

The activated ester **1** serves as suitable compound for <sup>188</sup>Re-labelling of peptides in aqueous solution. For labelling of proteins reaction conditions need to be further optimised. Crucial point is the concentration of phosphine for optimal complex formation and adjustment of the pH. The latter must be chosen so that on one hand the stability of the <sup>188</sup>Re(III)-EDTA intermediate is high enough for effective labelling and on the other hand the integrity of the protein is warranted.

### References

- [1] Schiller, E. *et al.*, *Bioconjugate Chem.* 16 (2005) 634.
- [2] Schiller, E. *et al.*, *this report*, p. 28.
- [3] Seifert, S. *et al.*, *Bioconjugate Chem.* 15 (2004) 856.

# Formation of Stable Cu(II) Complexes with Hexadentate Bispidine Ligands

S. Juran, H. Stephan, J. Steinbach, G. Geipel<sup>1</sup>, G. Bernhard<sup>1</sup>  
<sup>1</sup>Institut für Radiochemie

Time-resolved laser-induced fluorescence spectroscopy (TRLFS) has been used to determine the formation constants of bispidine ligands with copper(II). The formation of very stable 1:1 complexes has been proven.

## Introduction

Bispidines (bispidine = 3,7-diazabicyclo[3.3.1]nonane) show interesting complexation behaviour towards transition metals [1]. Considerably high complex stabilities towards Cu(II) have been found particularly in the case of pyridine-containing ligands [2]. The complex stability achieved for copper complexes with bispidines, lying in the same range as found for macrocyclic compounds, offers the possibility to apply such complexes for diagnostic and therapeutic radiopharmaceutical purposes (<sup>64/67</sup>Cu). Furthermore, the bispidine structure opens suitable chemical approaches to introduce biomolecules onto the skeleton. That is important in view of the targeting of such complexes.

Time-resolved laser-induced fluorescence spectroscopy (TRLFS) [3] has been applied to determine formal stability constants of the hexadentate bispidine ligands N<sub>2</sub>Py<sub>4</sub>, N<sub>2</sub>Py<sub>4</sub>-OH and the macrocyclic tetraamine cyclam for comparison (Fig. 1).

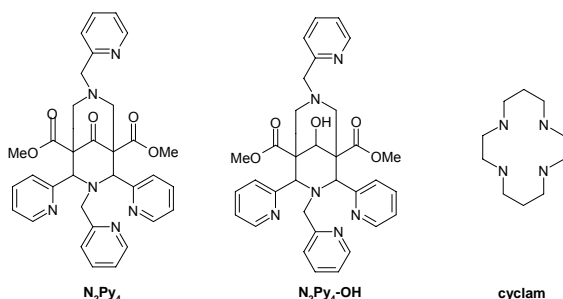


Fig. 1. Bispidine ligands N<sub>2</sub>Py<sub>4</sub> and N<sub>2</sub>Py<sub>4</sub>-OH, and the macrocyclic tetraamine cyclam.

## Results and Discussion

Cyclam was purchased from Aldrich. N<sub>2</sub>Py<sub>4</sub> was prepared according to the known procedure [2]. Reduction of N<sub>2</sub>Py<sub>4</sub> with NaBH<sub>4</sub> in dioxane gave the mono-ol N<sub>2</sub>Py<sub>4</sub>-OH. TRLFS experiments were performed as described recently [4]. The slope of the "Stern-Volmer-Plot" gives the formal stability constant [5]. Fig. 2 displays the fluorescence spectra of N<sub>2</sub>Py<sub>4</sub> in methanol and N<sub>2</sub>Py<sub>4</sub>-OH in water at different copper(II) concentrations. With adding copper(II) to the solution the fluorescence is almost completely quenched. This effect is characteristic for high stability constants. The for-

mation constant of a 1:1 complex of N<sub>2</sub>Py<sub>4</sub> with Cu(II) was found to be  $\log K_{11} = 5.94 \pm 0.09$  in methanol. The formation constant of N<sub>2</sub>Py<sub>4</sub>-Cu(II) is more than one order of magnitude higher compared to the Cu(II) cyclam complex ( $\log K_{11} = 4.61 \pm 0.21$  [6]). Even in water the bispidine ligand N<sub>2</sub>Py<sub>4</sub>-OH forms a very stable Cu(II) complex ( $\log K = 5.74 \pm 0.10$ ).

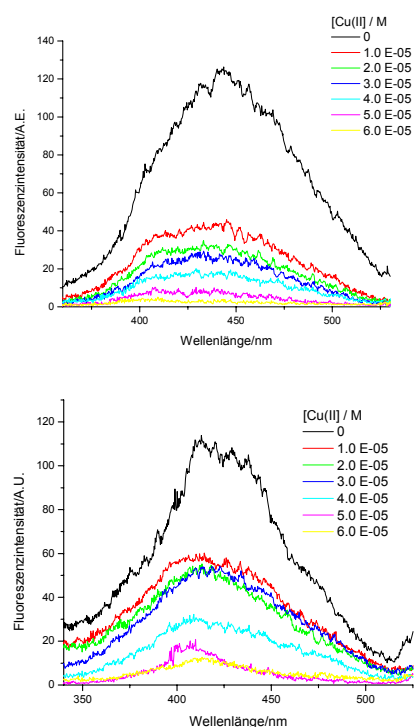


Fig. 2. Time resolved fluorescence spectra of bispidine ligands N<sub>2</sub>Py<sub>4</sub> (methanol, Cu(CF<sub>3</sub>SO<sub>3</sub>)<sub>2</sub>) and N<sub>2</sub>Py<sub>4</sub>-OH (H<sub>2</sub>O, Cu(NO<sub>3</sub>)<sub>2</sub>) in dependence on Cu(II) concentration.

## References

- [1] Comba, P. and Schiek, W. *Coord. Chem. Rev.* 238-239 (2003) 21-29.
- [2] Bleiholder, C. *et al.*, *Inorg. Chem.* 44 (2005) 8145-8155.
- [3] Geipel, G. *et al.*, *Wissenschaftlich-Technische Berichte, FZR-327* (2003) pp. 53-60.
- [4] Geipel, G. *et al.*, *Annual Report 2001, FZR-343*, p. 7.
- [5] Geipel, G. *et al.* *Spectrochim. Acta Part A* 60 (2004) 417-424.
- [6] Stephan, H. *et al.*, *Tetrahedron Lett.* 46 (2005) 3209-3212.

# Complexation of Cu(II) by Glycodendrimers

A. Röhrich, H. Stephan, J. Steinbach, G. Geipel<sup>1</sup>, G. Bernhard<sup>1</sup>, G. Bergamini<sup>2</sup>, V. Balzani<sup>2</sup>  
<sup>1</sup>Institut für Radiochemie, <sup>2</sup>University of Bologna, Italy

Kinetics and stability of Cu(II) complexation by glycodendrimers have been explored. Slow formation of stable 1:1 complexes was found.

## Introduction

Metalloradiopharmaceuticals of the metallic radionuclides <sup>64/67</sup>Cu, <sup>99m</sup>Tc, <sup>186/188</sup>Re and <sup>90</sup>Y are used for diagnostic and therapeutic purposes [1]. Cyclam and its derivatives form very stable complexes in particular with transition and rare earth metal ions as the radionuclides mentioned above [2]. In this nexus, we want to develop dendritic ligands having both enhanced complex stability and improved bio-availability. Thus, we built up two glycodendrimers possessing a cyclam core modified with thiourea-linked sugar residues at the periphery of the molecule (Fig. 1). D-Glucose and 2-acetamido-2-deoxy-D-glucose have been chosen as sugar moieties. The latter one is frequently a part of metabolites of aberrant glycosylation on cancer cells [3].

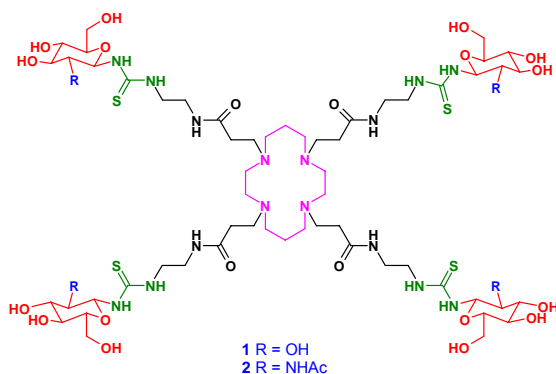


Fig. 1. Glycodendrimers 1 and 2.

## Results and Discussion

The glycodendrimers 1 and 2 were prepared by glycosylation of the tetraamino-functionalised cyclam core precursor [4] using the O-acetyl-protected glucosyl isothiocyanates. Deacetylation with MeONa in MeOH gave compounds 1 and 2. Purification was obtained by size exclusion chromatography. Preliminary experiments have been performed in order to achieve information about the kinetics and stability of complex formation of Cu(II) with these glycodendrimers. Kinetics of complex formation of 1 and 2 with Cu(II) was monitored by the change of absorbance at 320 nm (Fig. 2). The maximum of absorbance was obtained at a ratio of 1 between metal to ligand concentration indicating the formation of 1:1 complexes. A slow attainment of complexation equilibrium was observed at room temperature, significantly accelerated at 37 °C. Kinetic

constants were found to be  $185 \pm 8 \text{ M}^{-1}\cdot\text{sec}^{-1}$  (25 °C),  $492 \pm 8 \text{ M}^{-1}\cdot\text{sec}^{-1}$  (37 °C) for **1**Cu(II), and  $340 \pm 30 \text{ M}^{-1}\cdot\text{sec}^{-1}$  (25 °C),  $1580 \pm 20 \text{ M}^{-1}\cdot\text{sec}^{-1}$  (37 °C) for **2**Cu(II).

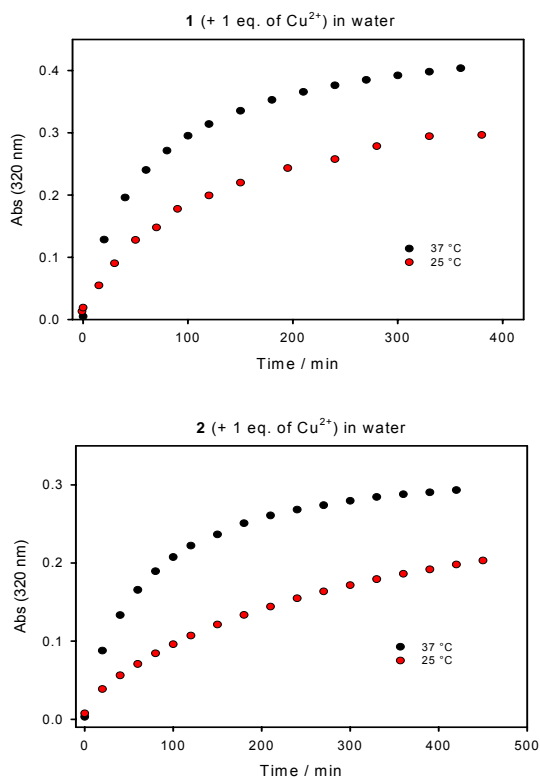


Fig. 2. Absorbance of Cu(II) complexes with 1 and 2 as function of time and temperature.

To estimate the stability of the complexes, TRLFS experiments have been performed [5]. Formal association constants were determined to be  $\log K_{11} = 4.51 \pm 0.51$  (**1**Cu(II)), and  $\log K_{11} = 4.60 \pm 0.50$  (**2**Cu(II)).

## References

- [1] Liang, X. and Sadler, P., Chem. Soc. Rev. 33 (2004) 246-266.
- [2] Izatt, R. M. *et al.*, Chem. Rev. 91 (1991) 1721-2085.
- [3] Vannucci, L. *et al.*, Int. J. Onc. 23 (2003) 285-296.
- [4] Stephan, H. *et al.*, Tetrahedron Lett. 46 (2005) 3209-3212.
- [5] Geipel, G. *et al.*, Spectrochim. Acta A 60 (2004) 417-424.

# Molecular Structure of the Cluster Anion $[\text{TiW}_{11}\text{CoO}_{40}]^{8-}$

H. Stephan, A. Röllich, Z. Matějka<sup>1</sup>, G. Reck<sup>2</sup>, W. Kraus<sup>2</sup>

<sup>1</sup>Institute of Chemical Technology, Prague, <sup>2</sup>Bundesanstalt für Materialforschung und –prüfung, Berlin

Hexapotassium dihydrogen monotitanoundecatungstocobaltate(II) tridecahydrate,  $\text{K}_6\text{H}_2[\text{TiW}_{11}\text{CoO}_{40}] \cdot 13 \text{H}_2\text{O}$ , crystallizes from aqueous solution in the cubic space group  $P43m$ . The  $[\text{TiW}_{11}\text{CoO}_{40}]^{8-}$  anion has a Keggin structure with a central tetrahedral  $\text{CoO}_4$  group and one tungsten site occupied by titanium.

## Introduction

In recent years, interest in the chemistry of metal–oxygen clusters has grown due to their applications in areas including catalysis, materials chemistry and biochemistry. In the latter context, polyoxometallates (POMs) show unique transport behaviour in living cells, and may act as antiviral and antitumoural agents [1]. Specifically, the title compound,  $\text{K}_6\text{H}_2[\text{TiW}_{11}\text{CoO}_{40}]$ , reveals promising antitumour activity when applied as starch and liposome hybrid materials [2, 3]. The structural characterisation of  $\text{K}_6\text{H}_2[\text{TiW}_{11}\text{CoO}_{40}] \cdot 13 \text{H}_2\text{O}$  is reported here.

## Results and Discussion

$\text{K}_6\text{H}_2[\text{TiW}_{11}\text{CoO}_{40}] \cdot 13 \text{H}_2\text{O}$  was prepared according to the method described by Chen *et al.* [4]. X-ray quality crystals were grown by slow evaporation of an aqueous solution at room temperature. As shown in Fig. 1, the cluster ion has a Keggin structure. It can be viewed as a shell of  $\{\text{W}_{11}\text{TiO}_{36}\}$  encapsulating a central tetrahedral  $\{\text{CoO}_4\}$  group. Alternatively, the cluster anion may be described as constructed from  $12\{\text{W}_{0.92}\text{Ti}_{0.08}\text{O}_6\}$  octahedra. According to the coordination environment of oxygen in the anion cluster, the O atoms can be divided into four groups. Two kinds of O atoms in the shell are connected to the tungsten sites. One bridging O atom (O1) has a distance of only 1.819(4) Å to tungsten and the W1-O1-W1 angle is 148.1(9)°. The second bridging O atom (O4) has a distance of 2.034(8) Å to tungsten and a smaller angle of 118.6(7)° (W1-O4-W1). Atom O4 forms hydrogen bonds to water molecules outside the shell [O...O = 2.70(2) Å]. The terminal O3 atoms are connected to only one tungsten atom (O3-W1 = 1.711(11) Å). The O2 atoms from the  $\{\text{CoO}_4\}$  group connected to W1 have a distance of 2.231(7) Å.

In the crystal packing, two symmetry-independent potassium atoms, K1 and K2, have been found, K2 being positionally disordered (Fig. 2). K1 is coordinated by eight cluster O atoms, and K2 by four cluster O atoms and four water molecules. The structure contains 13 water molecules per cluster. The coordination polyhedron formed by K atoms and water molecules stabilises the cluster anions in a three-dimensional network [5].

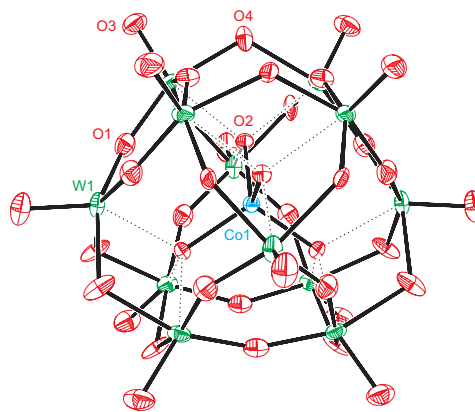


Fig. 1. Crystal structure of  $[\text{TiW}_{11}\text{CoO}_{40}]^{8-}$ .

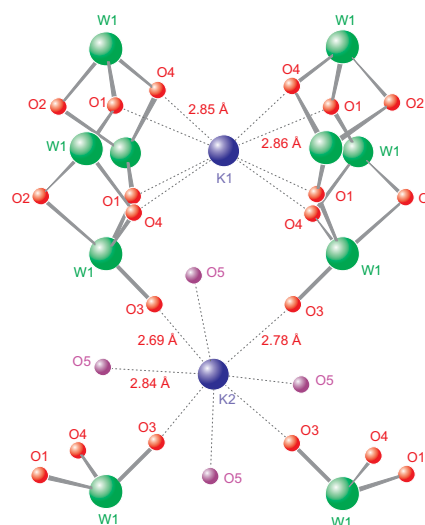


Fig. 2. Coordination spheres of the two K atoms.

Published in [5]: Kraus, W. *et al.*, Acta Cryst. E61 (2005) i35-i37.

## References

- [1] Rhule, J. T. *et al.*, Chem. Rev. 98 (1998) 327-357.
- [2] Wang, X. H. *et al.*, Dalton Trans. (2003) 957-960.
- [3] Yang, Y. *et al.*, Transition Metal Chem. 29 (2004) 96-99.
- [4] Chen, Y. *et al.*, Synth. React. Inorg. Met.-Org. Chem. 27 (1997) 239-250.



# Stability Investigation of Nanoparticles Formed by $[\text{Ti}_2\text{W}_{10}\text{PO}_{40}]^{7-}$ and Chitosan

T. Meißner, H. Stephan, W. Richter<sup>1</sup>, H. Zänker<sup>1</sup>, S. Weiß<sup>1</sup>  
<sup>1</sup>Institut für Radiochemie

Suspensions formed by chitosan and the polyoxotungstate  $[\text{Ti}_2\text{W}_{10}\text{PO}_{40}]^{7-}$  were investigated by zeta potential measurement. The isoelectric point was determined at a  $[\text{Ti}_2\text{W}_{10}\text{PO}_{40}]^{7-}$  to chitosan molar ratio of 5.5. This relation was also found in the isolated associates. These associates show a high hydrolytic stability in aqueous solution.

## Introduction

The modification of antitumorally active polyoxometallates (POMs) with organic molecules enables the development of metallic drugs which have a high biocompatibility, better antitumoral activity and improved stability [1]. Besides the covalent linkage between POM and organic units, organic encapsulation of these anion clusters is increasingly focused on. In this context, promising investigations have been done with POMs encapsulated with starch and liposomes [2, 3]. We deal with associates formed by  $[\text{Ti}_2\text{W}_{10}\text{PO}_{40}]^{7-}$  and the biopolymer chitosan (Fig. 1). The cell uptake of these particles is remarkably enhanced in comparison with the free cluster anion  $[\text{Ti}_2\text{W}_{10}\text{PO}_{40}]^{7-}$  [4]. In this report, we discuss stability studies of the  $[\text{Ti}_2\text{W}_{10}\text{PO}_{40}]$ -chitosan-associates (TCA).

## Results and Discussion

$[\text{Ti}_2\text{W}_{10}\text{PO}_{40}]^{7-}$  rapidly forms associates with chitosan ( $M_r \sim 10.000$  g/mol) in the nanometer size range [5]. Our experiments show that size and suspension stability depend on the concentration and the concentration ratio of the two substances. If the molar quotient chitosan :  $[\text{Ti}_2\text{W}_{10}\text{PO}_{40}]^{7-}$  is 1:5, the particles agglomerate. All suspensions which differ from this ratio form stable solutions. Interestingly, the stoichiometry ratio chitosan :  $[\text{Ti}_2\text{W}_{10}\text{PO}_{40}]^{7-}$  in the isolated associates is also in the range of 1:5 independently of the educt ratio. Zeta potential measurements (Zetasizer Nano NS) of different suspensions have been performed (Fig. 2). The isoelectric point was found at a  $[\text{Ti}_2\text{W}_{10}\text{PO}_{40}]^{7-}$  to chitosan molar ratio of 5.5 indicating the charge neutralisation between protonated chitosan and  $[\text{Ti}_2\text{W}_{10}\text{PO}_{40}]^{7-}$ . Obviously, there is a correlation between the cluster anion to chitosan molar ratio of the associates and the isoelectric point we determined.

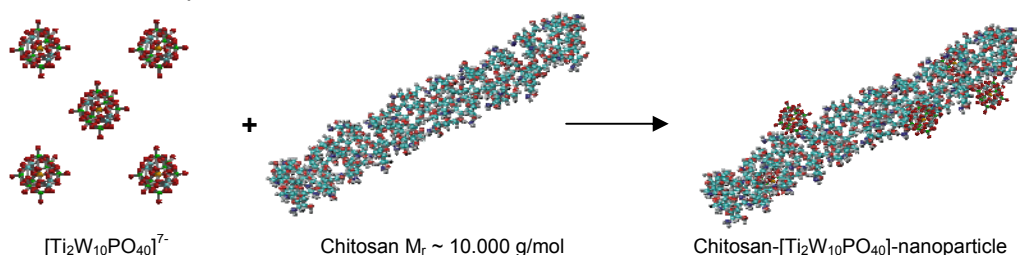


Fig. 1. Schematic image of  $[\text{Ti}_2\text{W}_{10}\text{PO}_{40}]$ -chitosan-nanoparticle forming.

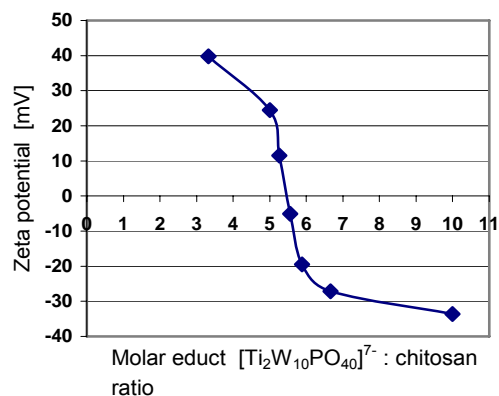


Fig. 2. Zeta potential as function of the concentration ratio  $K_7[\text{Ti}_2\text{W}_{10}\text{PO}_{40}]$  : chitosan ( $C_{\text{Chitosan}} = 4 \cdot 10^{-5}$  M).

To investigate the time-stability behaviour of the TCA, 50 mg were placed in vials with Sørensen buffer solution (pH 7.4) and then kept in an overhead shaker for different times (1 - 48 h). After shaking, the mixture was centrifuged and the W- and Ti-concentrations from the supernatant were detected by ICP-MS which allowed conclusions as to the cluster anions that detached from chitosan. After 48 h less than 1 % of  $[\text{Ti}_2\text{W}_{10}\text{PO}_{40}]^{7-}$  has been released from chitosan.

To be published in: Transit. Metal Chem.

## References

- [1] Rhule, J. T. *et al.*, Chem. Rev. 98 (1998) 327-357.
- [2] Wang, X. H. *et al.*, J. Inorg. Biochem. 99 (2005) 452-457.
- [3] Wang, X. H. *et al.*, J. Nanosci. Nanotechnol. 5 (2005) 905-908.
- [4] Stephan, H. *et al.*, Annual Report 2004, FZR-424, p. 60.
- [5] Richter, W. *et al.*, Annual Report 2004, FZR-424, p. 61.



# New Octahedral Rhenium Cluster Compounds Possessing 3,5-Dimethylpyrazole as Apical Ligands

K. A. Brylev<sup>1</sup>, Y. V. Mironov<sup>1</sup>, V. E. Fedorov<sup>1</sup>, H. Spies, H.-J. Pietzsch, H. Stephan, W. Kraus<sup>2</sup>  
<sup>1</sup>Institute of Inorganic Chemistry, Russian Academy of Science, Novosibirsk, Russia,  
<sup>2</sup>Bundesanstalt für Materialforschung und -prüfung, Berlin

Two new octahedral rhenium cluster complexes,  $[\text{Re}_6\text{S}_7\text{O}(\text{3,5-Me}_2\text{PzH})_6]\text{Br}_2 \cdot \text{3,5-Me}_2\text{PzH}$  (**1**) and  $[\text{Re}_6\text{Se}_7\text{O}(\text{3,5-Me}_2\text{PzH})_6]\text{Br}_2 \cdot \text{3,5-Me}_2\text{PzH}$  (**2**), with the organic ligand 3,5-dimethylpyrazole (3,5-Me<sub>2</sub>PzH), have been synthesised and characterised by single crystal X-ray diffraction.

## Introduction

The chemistry of the rhenium octahedral cluster compounds with the cluster core  $\{\text{Re}_6\text{Q}_8\}^{2+}$  (Q = S, Se) coordinated by organic N- and P-donor ligands is in a stage of rapid development [1, 2]. Such organic-inorganic hybrids show interesting electronic, optical, and structural properties. Furthermore, rhenium clusters may play an important role as agents in photon activation therapy (PAT) [3]. This relatively new treatment paradigm in cancer therapy requires a sufficiently high density of metals in target regions. This could be achieved by organic-inorganic rhenium cluster complexes. Here we report the preparation and crystal structures of two new rhenium octahedral cluster complexes grafted by the organic ligand 3,5-dimethylpyrazole.

## Results and Discussion

Two new octahedral rhenium cluster complexes,  $[\text{Re}_6\text{S}_7\text{O}(\text{3,5-Me}_2\text{PzH})_6]\text{Br}_2 \cdot \text{3,5-Me}_2\text{PzH}$  (**1**) and  $[\text{Re}_6\text{Se}_7\text{O}(\text{3,5-Me}_2\text{PzH})_6]\text{Br}_2 \cdot \text{3,5-Me}_2\text{PzH}$  (**2**), with the organic ligand 3,5-dimethylpyrazole, have been synthesised by reaction of rhenium chalcobromides  $\text{Cs}_3[\text{Re}_6(\mu_3\text{-Q}_7\text{Br})\text{Br}_6]$  (Q = S, Se) with molten dimethylpyrazole. During the reaction, all six apical bromine ligands of the cluster complexes are substituted by the organic ligand, which is coordinated through the aromatic nitrogen atom N2. Additionally, the inner ligand  $\mu_3\text{-Br}$  in the cluster core  $[\text{Re}_6(\mu_3\text{-Q}_7\text{Br})]^{3+}$  is substituted by oxygen, giving cluster cores  $[\text{Re}_6(\mu_3\text{-Q}_7\text{O})]^{2+}$  with mixed chalcogen/oxygen ligands.

Compounds **1** and **2** have been characterised by single crystal X-ray diffraction. The compounds are isostructural. The cluster cations  $[\text{Re}_6\text{Q}_7\text{O}(\text{3,5-Me}_2\text{PzH})_6]^{2+}$  (Q = S, Se) contain the  $\text{Re}_6$  octahedron residing in a  $\text{Q}_7\text{O}$  pseudocube. There is no disorder in the present structures: seven corner positions of the  $\text{Q}_7\text{O}$  cube are occupied exclusively by S (**1**) or Se (**2**) atoms and one by an O atom. Due to the presence of the O atom in the cluster core  $\{\text{Re}_6\text{Q}_8\}$ , the  $\text{Re}_6$  octahedrons in both compounds are slightly irregular. Re-Re distances between Re atoms coordinated by the  $\mu_3\text{-O}$  atom are shorter than those for other Re at-

oms. Each Re atom is coordinated by a 3,5-Me<sub>2</sub>PzH. The structure of the sulfur-containing cluster cation is shown in Fig. 1.

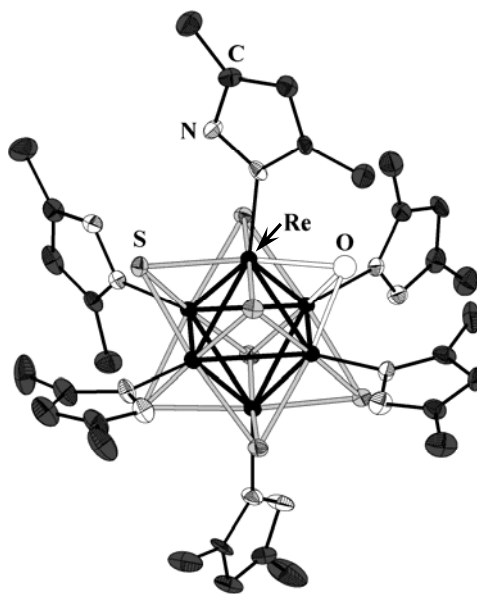


Fig. 1. Crystal structure of the cluster cation  $[\text{Re}_6\text{S}_7\text{O}(\text{3,5-Me}_2\text{PzH})_6]^{2+}$ .

The cluster compounds investigated show promising spectroscopic and photophysical properties [4]. The great variety of organic ligands grafting on the cluster core offers abundant opportunities to modify the spectroscopic and photophysical properties, and the organic shell can make the cluster molecule bioavailable.

Published in [4]: Mironov, Y. V. *et al.*, *Eur. J. Inorg. Chem.* (2005) 657-661.

## References

- [1] Gabriel, J. C. P. *et al.*, *Chem. Rev.* 101 (2001) 2037-2066.
- [2] Selby, H. D. *et al.*, *Acc. Chem. Res.* 36 (2003) 933-944.
- [3] Larsson, B., *Hadrontherapy in Oncology*. In: Amaldi, U. and Larsson, B. (Eds.), Elsevier (1994) p. 33.

# **PET IN DRUG AND FOOD RESEARCH**



## Special Issue: PET in Food Sciences

J. Pietzsch, J. van den Hoff

Recent progresses in food sciences have led to the development of a wide range of excellent analytical methods that enable accurate determination of food composition and to study food ingredients and contaminants at both the micro- and macrostructural level. But this does not necessarily tell enough about the nutritional value or the safety of food of interest, because only a fraction of biologically active compounds present in food can be absorbed into the body, and this fraction strongly depends on the type of food and its preparation. It is therefore important to know how much of a certain substance can be absorbed, what happens to this substance when it enters the body, and, finally, what happens to the body. The interest in these questions steadily increases due to the fact that the design and development of novel foods, genetically modified foods, novel food ingredients and additives, and new methods of food processing is a rapidly evolving field. Furthermore, improved analytical methods and molecular techniques direct our attention to a rapidly growing number of biologically significant substances, including numerous functional food ingredients, 'nutriceuticals', and foodborne toxicants. In this context, experimental approaches *in vitro* offer the advantages of providing rapid results, produced in strictly controlled environments. However, they need to be validated increasingly against *in vivo* studies to make sure that they provide a good prediction of what actually happens in and with the living organism. The latter is a prerequisite to enact new recommendations and regulations, e.g., on novel foods and novel processes. In this line, functional imaging by positron emission tomography (PET) has been proposed as one tool of choice. However, progress in the implementation of PET in food sciences can only be achieved when multidisciplinary PET centers closely cooperate with food scientists and food-producing companies and, furthermore, when industry and regulators are recognizing that the use of functional *in vivo* imaging facilitates decision-making whether food components are riskful or, on the other hand, maintain human health. To instigate a novel discussion forum in this emerging field the 1st Workshop on PET in Food Sciences was held in Rossendorf in May 2004. As major result a *Special Issue* has been published in *Amino Acids* [1]. This issue contains, beside a review article emphasizing new concepts on biomarkers to assess the effects of dietary exposure, a selection of contributions originally presented at this Workshop, under the aus-

pices of the PET Centre at the Research Center Rossendorf and the Institute of Food Chemistry at the University of Technology Dresden [2-11]. In this issue, after a description of the conceptual idea of PET and its multidisciplinary approach, the needs for new experimental tools that allow the *in vivo* assessment of bioavailability, biodistribution, metabolism, and metabolic consequences as well as the safety of food contents are specified. Review articles are essentially concerned with methodological aspects of PET reviewing current developments in PET nuclide production, radiochemistry, radiopharmacology, metabolite analysis, and quantitative data acquisition and analysis. In addition, contributions demonstrating original experimental applications of PET in food sciences have been selected. These articles deal with various classes of dietary compounds under investigation, including isopeptides, and polyphenols. The selected papers cover new methods of radiolabelling of isopeptides, polyphenols, and lipoproteins. Moreover, the use of these novel tracers in dynamic small animal PET studies is demonstrated.

### Acknowledgements

We wish to thank all authors for contributing to the *Special Issue* "PET in Food Sciences". Furthermore, we express our gratitude to Prof. Gert Lubec, Editor-in-Chief, for the opportunity given to prepare this *Special Issue* in *Amino Acids*. We are also grateful to Peter Joehnk, PhD, Administrative Director, and the staff of the administration of the Research Center Rossendorf for their logistic and financial support.

### References

- [1] Pietzsch, J. and van den Hoff, J., *Amino Acids* 29 (2005) 303-305.
- [2] Johannsen, B., *Amino Acids* 29 (2005) 307-311.
- [3] Henle, T., *Amino Acids* 29 (2005) 313-322.
- [4] Wuest F., *Amino Acids* 29 (2005) 323-339.
- [5] van den Hoff, J., *Amino Acids* 29 (2005) 341-353.
- [6] Bergmann, R. and Pietzsch, J., *Amino Acids* 29 (2005) 355-376.
- [7] Pawelke, B., *Amino Acids* 29 (2005) 377-388.
- [8] Pietzsch, J. *et al.*, *Amino Acids* 29 (2005) 389-404.
- [9] Hultsch, C. *et al.*, *Amino Acids* 29 (2005) 405-413.
- [10] Gester, S. *et al.*, *Amino Acids* 29 (2005) 415-428.
- [11] Coolen, S. A. J. *et al.*, *Amino Acids* 29 (2005) 429-436.

## Radiolabelled Flavonoids and Polyphenols

### IV. Biodistribution of an $^{18}\text{F}$ -Labelled Resveratrol Derivative

S. Gester, F. Wüst, B. Pawelke, R. Bergmann, J. Pietzsch

*Radiopharmacological evaluation (biodistribution and PET-studies in vivo) of 5-[(E)-2-(4-[ $^{18}\text{F}$ ]fluoro-phenyl)ethenyl]-1,3-benzenediol (3,5-dihydroxy-4'-[ $^{18}\text{F}$ ]fluoro-trans-stilbene) [ $^{18}\text{F}$ ]-1 in male Wistar rats is described. Compound [ $^{18}\text{F}$ ]-1 shows extensive uptake in the liver and kidneys, respectively.*

#### Introduction

Recently we have reported the radiosynthesis of  $^{18}\text{F}$ -labelled resveratrol derivative 5-[(E)-2-(4-[ $^{18}\text{F}$ ]fluoro-phenyl)ethenyl]-1,3-benzenediol [ $^{18}\text{F}$ ]-1 (Fig. 1). Compound [ $^{18}\text{F}$ ]-1 was obtained in 9 % radiochemical yield (decay-corrected, related to [ $^{18}\text{F}$ ]fluoride) within 120 - 130 min including HPLC separation at a specific radioactivity of up to 90 GBq/ $\mu\text{mol}$ . The radiochemical purity was in the range of 92 - 97 % [1].

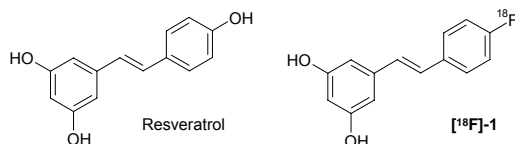


Fig. 1. Structures of resveratrol and [ $^{18}\text{F}$ ]-1.

In this report we performed the radiopharmacological characterisation of  $^{18}\text{F}$ -labelled resveratrol derivative [ $^{18}\text{F}$ ]-1 by means of biodistribution and small animal PET imaging studies.

#### Results and Discussion

First experiments aimed at the biological behaviour of [ $^{18}\text{F}$ ]-1 *in vitro* and *in vivo*. Table 1 shows the distribution of  $^{18}\text{F}$ -radioactivity in male Wistar rats after single intravenous injection of [ $^{18}\text{F}$ ]-1.

Table 1. Radioactivity was expressed as percent injected dose (% ID) and percent injected dose per gram tissue (% ID/g) in different organs. Results are means  $\pm$  SD (n = 4).

Organ	% ID		% ID/g	
	5 min <i>p.i.</i>	60 min <i>p.i.</i>	5 min <i>p.i.</i>	60 min <i>p.i.</i>
Blood	0.92 $\pm$ 0.37	0.31 $\pm$ 0.12	0.53 $\pm$ 0.09	0.15 $\pm$ 0.02
Brain	0.58 $\pm$ 0.20	0.07 $\pm$ 0.02	0.33 $\pm$ 0.12	0.05 $\pm$ 0.01
Pancreas	0.30 $\pm$ 0.07	0.06 $\pm$ 0.01	0.52 $\pm$ 0.11	0.09 $\pm$ 0.01
Spleen	0.44 $\pm$ 0.12	0.32 $\pm$ 0.10	0.72 $\pm$ 0.15	0.48 $\pm$ 0.19
Adrenals	0.06 $\pm$ 0.01	0.02 $\pm$ 0.00	0.86 $\pm$ 0.23	0.22 $\pm$ 0.02
Kidneys	9.50 $\pm$ 0.35	5.59 $\pm$ 1.23	4.86 $\pm$ 1.09	2.71 $\pm$ 0.54
White fat	0.05 $\pm$ 0.01	0.02 $\pm$ 0.01	0.16 $\pm$ 0.06	0.06 $\pm$ 0.01
Muscle	0.11 $\pm$ 0.02	0.03 $\pm$ 0.01	0.20 $\pm$ 0.01	0.04 $\pm$ 0.01
Heart	0.29 $\pm$ 0.03	0.08 $\pm$ 0.01	0.37 $\pm$ 0.10	0.10 $\pm$ 0.02
Lungs	2.27 $\pm$ 0.32	0.49 $\pm$ 0.03	1.67 $\pm$ 0.37	0.34 $\pm$ 0.04
Liver	25.26 $\pm$ 3.29	12.59 $\pm$ 1.11	2.18 $\pm$ 0.55	1.03 $\pm$ 0.24
Femur	0.19 $\pm$ 0.02	0.05 $\pm$ 0.01	0.18 $\pm$ 0.04	0.05 $\pm$ 0.00
Intestine	4.79 $\pm$ 0.84	31.05 $\pm$ 3.00	-	-
Urine	28.81 $\pm$ 5.13	37.87 $\pm$ 5.15	-	-

The biodistribution studies showed a very rapid clearance of  $^{18}\text{F}$ -radioactivity from the blood.

The radioactivity concentration at 5 min was nearly on the final level. This process was accompanied by a rapid uptake both in the liver and the kidneys. The fast systemic clearance was similarly accompanied by hepatobiliary and renal elimination. The observed  $^{18}\text{F}$ -radioactivity concentration in various tissues after intravenous administration of [ $^{18}\text{F}$ ]-1 reflects the predominant nonspecific distribution presumably according to the high lipophilicity of the compound. This observation is consistent with data from the literature.

Small animal PET imaging studies further confirmed this observation. From these studies, time-activity curves were obtained for heart, liver, kidneys, and intestine (Fig. 2).

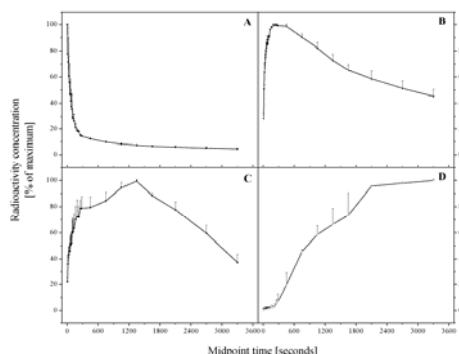


Fig. 2. Kinetics of the  $^{18}\text{F}$ -radioactivity calculated by PET measurements from ROIs over heart (A), liver (B), kidneys (C), and intestine (D). Results are means  $\pm$  SD (n = 3).

The results from ROI analysis of these organs show fast blood clearance, rapid uptake in liver and kidneys, and substantial excretion of  $^{18}\text{F}$ -radioactivity into the intestine. These data are in agreement with the corresponding results obtained from biodistribution experiments. The tissue localisation of  $^{18}\text{F}$ -radioactivity reflects both, intact [ $^{18}\text{F}$ ]-1 and its  $^{18}\text{F}$ -labelled metabolites. The very fast excretion of  $^{18}\text{F}$ -radioactivity into bile/intestine and urine found is consistent with findings from rapid formation of hydrophilic metabolites from resveratrol and analogues in the literature.

Published in: Gester, S. *et al.*, Amino Acids 29 (2005) 415-428.

#### References

- [1] Gester, S. *et al.*, Annual Report 2004, FZR-424, p. 67.

# **CYCLOTRON OPERATION**



# Operation of the Rossendorf PET Cyclotron "CYCLONE 18/9" in 2005

St. Preusche, F. Wüst

## Routine operation

The radionuclides produced in routine operation in 2005 were F-18 and C-11, available as  $[^{18}\text{F}]\text{F}^-$ ,  $[^{18}\text{F}]\text{F}_2$  and  $[^{11}\text{C}]\text{CO}_2$ . The improved version of the Rossendorf solid target system [1] was used for the routine production of  $^{86}\text{Y}$ . Table 1 gives an overview of the 2005 radionuclide production.

Due to an increasing demand of C-11 based radiopharmaceuticals and radiotracers the daily operating time of the CYCLONE 18/9 increased by 15 % with regard to the maximum value of 2004 and varied now between three and six hours.

Table 1. Radionuclide production in 2005

RN	Radionuclide production	
	Number of irradiations	Sum $A_{\text{EOB}}$ [GBq]
$[^{18}\text{F}]\text{F}^-$	307	11145
$[^{18}\text{F}]\text{F}_2$ *)	326	1282
$^{11}\text{C}$	278	12101
$^{86}\text{Y}$	19	24.6

\*) including pre-irradiations

Fig. 1 shows the number of target irradiations and Fig. 2 the total amount of activity produced over the last seven years (1999 to 2005).

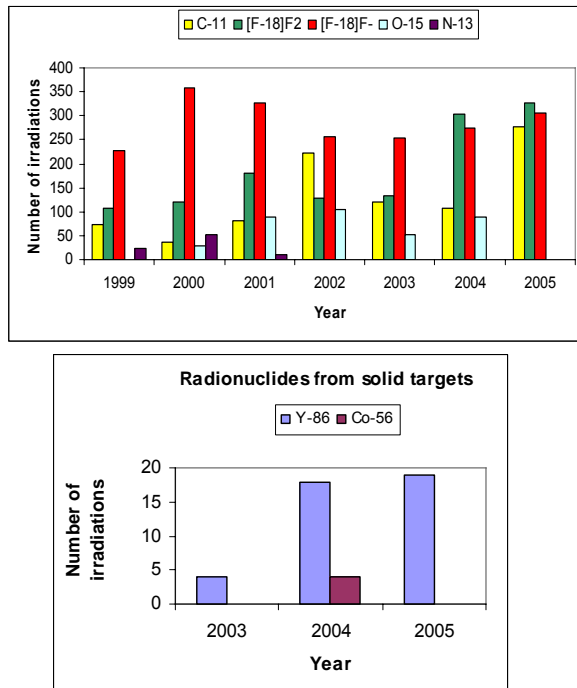


Fig. 1a, b. Number of irradiations of radionuclides produced.

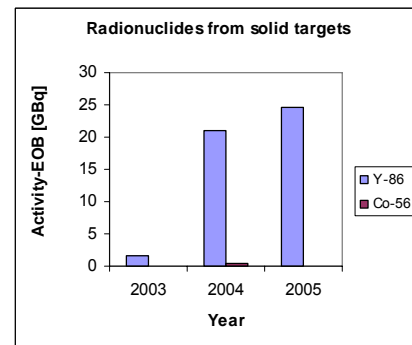
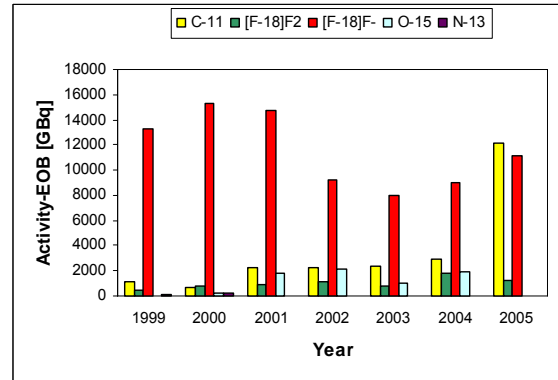


Fig. 2a, b. Total amount of activity produced.

## Maintenance and service

### - Stripper foils

The serious problems with the carbon stripper foils occurred in 2004 [2] were overcome. We now use pyrolytic graphite foils of  $1000 \mu\text{g}/\text{cm}^2$  areal density (Minteq International Inc./USA). These foils are more resistant against possible RF currents and neutral beam effects inside the vacuum chamber.

### - Annual check of the cyclotron

The annual check of the CYCLONE 18/9 facility by the TÜV Sachsen organisation (TÜV = Association for Technical Inspection) under § 66 (2) of the Radiation Protection Regulation was carried out in the second half of September 2005. There were no objections to the further operation of the cyclotron.

## Status of the CYCLONE 18/9

Though the number of beam hours (ion beam on the targets) has increased over the last years (see Fig. 3) and we are still able to fulfil all demands until now it is worth to mention that many of the CYCLONE 18/9 subsystems are of 'state of the art' of the beginning of the 1990<sup>th</sup>. The same is true for our 500 m in length Radionuclide transport system (RATS) between the cyclotron building and the radio-



chemistry building including the control systems of the cyclotron and RATS.

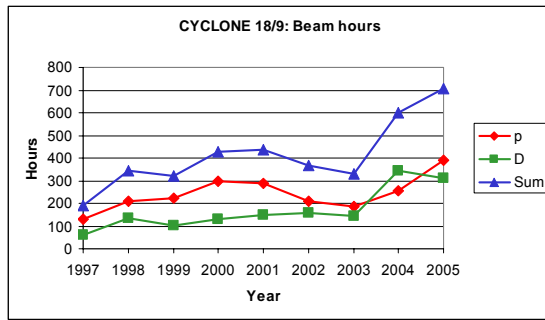


Fig. 3. Beam hours over the years (p = protons, D = deuterons)

Our cyclotron is the second one of the IBA CYCLONE 18/9 series and has some disadvantages (dees fixed on the top, targets outside the yoke) that have been overcome with the following ones. Especially the old PLC system (SIMATC S5) could lead to problems in the future.

### Radiation protection

- *Emission of radionuclides with the exhaust air*  
The emission of radionuclides with the exhaust air is routinely monitored. As shown in Table 2, it is well below the limit of  $2.0 \times 10^{11}$  Bq.

Table 2. Emission of radionuclides with the exhaust air in 2005 as a result of cyclotron operation

Radionuclide	Emission [Bq/a]
$^{41}\text{Ar}$	1.9E10
$^{18}\text{F}$	4.6E09
Sum	2.3E10
Percentage of the annual limit	11.7

- *Exposure to radiation of the cyclotron staff*  
The cyclotron staff belongs to category A of occupational exposed persons. The average exposure to radiation of the cyclotron staff over the years of cyclotron operation is shown in Table 3.

Table 3. Average exposure to radiation of the cyclotron staff

Year	Exposure [mSv]
1997	1.8
1998	2.9
1999	3.5
2000	6.2
2001	4.6
2002	1.7
2003	2.6
2004	5.2
2005	3.1

### References

- [1] Preusche, St. *et al.*, *Annual Report 2004*, FZR-424, p. 73.
- [2] Preusche, St. *et al.*, *Annual Report 2004*, FZR-424, p. 71.

## **II. PUBLICATIONS, LECTURES, PATENTS AND AWARDS OF THE INSTITUTE AND THE PET- CENTRE ROSSENDORF**



## PUBLICATIONS

Anchisi, D.; Borroni, B.; Franceschi, M.; Kerrouche, N.; Kalbe, E.; Beuthien-Baumann, B.; Cappa, S.; Lenz, O.; Ludecke, S.; Marconi, A.; Mielke, R.; Ortelli, P.; Padovani, A.; Pelati, O.; Pupi, A.; Scarpini, E.; Weisenback, S.; Herholz, K.; Salmon, E.; Holthoff, V.; Sorbi, S.; Fazio, F.; Perani, D.

Heterogeneity of brain glucose metabolism in mild cognitive impairment and clinical progression to Alzheimer disease.

Arch. Neurol. 62 (2005) 1728-1733.

Bauer, R.; Walter, B.; Vorwieger, G.; Fritz, A.; Füchtner, F.; Zwiener, U.; Brust, P.

Effect of moderate hypercapnic hypoxia on cerebral dopaminergic activity and brain O<sub>2</sub> uptake in intrauterine growth-restricted newborn piglets.

Pediatric Research 57 (2005) 363-370.

Bergmann, R.; Pietzsch, J.

Small animal positron emission tomography in food sciences.

Amino Acids, 29 (2005) 355-376.

Beuthien-Baumann, B.; Holthoff, V. A.; Rudolf, J.

Functional imaging of vegetative state applying Single Photon Emission Tomography and Positron Emission Tomography.

Neuropsychological Rehabilitation 15 (2005) 276-282.

Fernandes, C.; Correia, D. G.; Gano, L.; Santos, I.; Seifert, S.; Syhre, R.; Bergmann, R.; Spies, H.

Dramatic effect of the tridentate ligand on the stability of Tc-99m "3+1" oxo complexes bearing arylpiperazine derivatives.

Bioconjugate Chem. 16 (2005) 660-668.

Garcia, R.; Paulo, A.; Domingos, A.; Santos, I.; Pietzsch, H.-J.

Disruption of unprecedented B-H...M agostic interactions: an alternative approach for labeling bioactive molecules.

Synthesis and Reactivity in Inorganic Metal-Organic and Nano-Metal Chemistry 35 (2005) 35-42.

Garcia, R.; Xavier, C.; Paulo, A.; Santos, I.; Knieß, T.; Bergmann, R.; Wüst, F.

Synthesis and biological evaluation of S-[<sup>11</sup>C]methylated mercaptoimidazole piperazinyl derivatives as potential radioligands for imaging 5-HT<sub>1A</sub> receptors by positron emission tomography (PET).

J. Labelled Compd. Radiopharm. 48 (2005) 301-315.

Gester, S.; Wüst, F.; Pawelke, B.; Bergmann, R.; Pietzsch, J.

Synthesis and biodistribution of an <sup>18</sup>F-labelled resveratrol derivative for small animal positron emission tomography (PET).

Amino Acids 29 (2005) 415-428.

Gloe, K.; Antonioli, B.; Gloe, K.; Stephan, H.

Dendrimers for separation processes.

In: C. A. M. Afonso, J. G. Crespo (Eds.): Green Separation Processes, Weinheim: Wiley-VCH (2005) pp. 304-322.

Grote, M.; Noll, B.; Noll, S.

Synthesis of <sup>18</sup>F-labeled acyclic purine and pyrimidine nucleosides intended for monitoring gene expression.

Radiochim. Acta 93 (2005) 585-588.

Heinrich, T.; Kraus, W.; Pietzsch, H.-J.; Smuda, C.; Spies, H.

A novel rhenium chelate system derived from dimercaptosuccinic acid for the selective labeling of biomolecules.

Inorg. Chem. 44 (2005) 9930-9937.

Herting, B.; Beuthien-Baumann, B.; Reichmann, H.

Kortikobasale Degeneration, asymmetrisch mit Dystonie, Myoklonus und Apraxie.

Der Neurologe und Psychiater 1-2 (2005) 41-44.

Holthoff, V.; Beuthien-Baumann, B.; Kalbe, E.; Lüdecke, S.; Lenz, O.; Zündorf, G.; Spirling, S.; Schierz, K.; Winiacki, P.; Herholz, K.  
Regional cerebral metabolism in early Alzheimer's disease with clinically significant apathy or depression.

Biological Psychiatry 57 (2005) 412-421.

Hultsch, C.; Bergmann, R.; Pawelke, B.; Pietzsch, J.; Wüst, F.; Johannsen, B.; Henle, T.  
Biodistribution and catabolism of <sup>18</sup>F-labelled isopeptide N (varepsilon)-(gamma-glutamyl)-L-lysine.  
Amino Acids 29 (2005) 405-413.

Julius, U.; Pietzsch, J.

Glucose-induced enhancement of hemin-catalyzed LDL oxidation in vitro and in vivo.  
Antioxid. Redox Signal. 7 (2005) 1507-1512.

Kopprasch, S.; Grässler, J.; Pietzsch, J.

Pathological consequences of systemic oxidative stress and dyslipidemia in impaired glucose tolerance and diabetes mellitus.

London: Trends in Cell & Molecular Biology, Vol. 1, Elsevier Science (2005) pp. 1-14.

Kraus, W.; Stephan, H.; Röllich, A.; Matějka, Z.; Reck, G.

K<sub>6</sub>H<sub>2</sub>[TiW<sub>11</sub>CoO<sub>40</sub>]·13H<sub>2</sub>O, with a monotitanoundecatungstocobaltate(II) anion.  
Acta Crystallographica Section E61 (2005) i35-i37.

Mäding, P.; Füchtner, F.; Wüst, F.

Module-assisted synthesis of the bifunctional labelling agent N-succinimidyl 4-[<sup>18</sup>F]fluorobenzoate ([<sup>18</sup>F]SFB).

Appl. Radiat. Isot. 63 (2005) 329-332.

Mironov, Y. V.; Shestopalov, M. A.; Brylev, K. A.; Yarovoi, A. S.; Romanenko, G. V.; Fedorov, V. E.; Spies, H.; Pietzsch, H.-J.; Stephan, H.; Geipel, G.; Bernhard, G.; Kraus, W.

[Re<sub>6</sub>Q<sub>7</sub>O(3,5-Me<sub>2</sub>PzH)<sub>6</sub>]Br<sub>2</sub>·3,5-Me<sub>2</sub>PzH (Q = S, Se) – new octahedral rhenium cluster complexes with organic ligands: original synthetic approach and unexpected ligand exchange in cluster core.  
Eur. J. Inorg. Chem. (2005) 657-661.

Pawelke, B.

Metabolite analysis in positron emission tomography studies: examples from food sciences.  
Amino Acids 29 (2005) 377-388.

Pietzsch, J.; Bergmann, R.; Wüst, F.; van den Hoff, J.

In vivo metabolism of oxidized low density lipoproteins: insights from small animal positron emission tomography (PET) studies.

Kerala/India: Research Signpost/Recent Res. Devel. Mol. Cell. Biochem. 2 (2005) pp. 153-177.

Pietzsch, J.; Bergmann, R.; Wüst, F.; Pawelke, B.; Hultsch, C.; van den Hoff, J.

Catabolism of native and oxidized low density lipoproteins (LDL): in vivo insights from small animal positron emission tomography studies.

Amino Acids 29 (2005) 389-404.

Pietzsch, J.; van den Hoff, J.

Positron emission tomography in food sciences.

Amino Acids 29 (2005) 303-305.

Schiller, E.; Kraus, W.; Reck, G.; Spies, H.; Pietzsch, H.-J.

{2-Carboxy-2-{bis[(2-thiolato\_<sub>S</sub>)ethyl]amino\_<sub>N</sub>}ethanthiolato\_<sub>S</sub>} (triphenylphosphin\_<sub>P</sub>)rhenium(III).  
Acta Crystallogr. Sect. E - Structure reports online 61(2005) M1373-M1375.

Schiller, E.; Seifert, S.; Tisato, F.; Refosco, F.; Bolzati, C. Kraus, W.; Spies, H.; Pietzsch, H.-J.

Mixed-ligand rhenium-188 complexes with tetradentate/monodentate NS<sub>3</sub>/P ('4+1') coordination: relation of structure with antioxidation stability.

Bioconjugate Chem. 16 (2005) 634-643.

- Stephan, H.; Geipel, G.; Bernhard, G.; Appelhans, D.; Tabuani, D.; Komber, H.; Voit, B.  
Pegylation of 1,4,8,11-tetraazacyclotetradecane (cyclam) and its copper(II) complexation.  
*Tetrahedron Lett.* (2005) 3209-3212.
- Stephan, H.; Geipel, G.; Bernhard, G.; Comba, P.; Rajaraman, G.; Hahn, U.; Vögtle, F.  
Synthesis and binding properties of dendritic oxybathophenanthroline ligands towards copper(II).  
*Eur. J. Inorg. Chem.* 22 (2005) 4501-4508.
- van den Hoff, J.  
Principles of quantitative positron emission tomography.  
*Amino Acids* 29 (2005) 341-353.
- Wermann, K.; Walther, M.; Günther, W.; Görls, H.; Anders, E.  
Novel triazinium-imidothioate zwitterions: intermediates in the reaction of [1,3,4]thiadiazolo[2,3-d][1,2,4]triazolo[1,5-a][1,3,5]-triazinium cations with amines.  
*Tetrahedron* 61 (2005) 673-685.
- Wüst, F.  
Aspects of positron emission tomography (PET) radiochemistry as relevant for food chemistry.  
*Amino Acids* 29 (2005) 323-339.
- Wüst, F.  
Radiopharmakaforschung: Trends und neue Konzepte.  
*Der Nuklearmediziner* 28 (2005) 206-213.
- Wüst, F.; Höhne, A.; Metz, P.  
Synthesis of  $^{18}\text{F}$ -labelled COX-2 inhibitors via Stille Reaction with 4- $^{18}\text{F}$ fluoro-iodobenzene.  
*Org. Biomol. Chem.* (2005) 503-507.
- Wüst, F.; Knieß, T.  
*N*-Arylation of indoles with 4- $^{18}\text{F}$ fluoroiodobenzene: synthesis of  $^{18}\text{F}$ -labelled  $\sigma_2$  receptor ligands for positron emission tomography (PET).  
*J. Labelled Compd. Radiopharm.* 48 (2005) 31-43.
- Wüst, F.; Berndt, M.  
 $^{11}\text{C}$ -C bond formation by palladium-mediated cross-coupling of alkenylzirconocenes with  $^{11}\text{C}$ methyl iodide.  
*J. Labelled Compd. Radiopharm.* 49 (2005) 91-100.
- Wüst, F.; Knieß, T.; Kretschmar, M.; Bergmann, R.  
Synthesis and radiopharmacological evaluation of 2'-(4-fluorophenyl)-21- $^{18}\text{F}$ fluoro-20-oxo-11 $\beta$ ,17 $\alpha$ -dihydroxy-pregn-4-eno[3,2-c]pyrazole as potential glucocorticoid receptor ligand for positron emission tomography (PET).  
*Bioorganic & Medicinal Chemistry Letters* 15 (2005) 1303-1306.
- Zippe, C.; Hoppe, D.; Fietz, J.; Hampel, U.; Hensel, F.; Mäding, P.; Prasser, H.-M.; Zippe, W.  
Messung von Phasen- und Konzentrationsverteilungen in Blasensäulen mit Positronen-Emissions-Tomographie.  
*Chemie Ingenieur Technik* 77 (2005) 1581-1587.

## PROCEEDINGS

Heinrich, T.; Kraus, W.; Pietzsch, H.-J.; Seifert, S.; Spies, H.; Johannsen, B.  
Entwicklung von Rhenium-188-Komplexen basierend auf neuartigen, sich von Dimercaptobernsteinsäure (DMSA) ableitenden Chelatoren, geeignet zur Bindung an Biomoleküle.  
*In: Kurzreferate GDCh-Jahrestagung 2005: Chemie schafft neue Strukturen, Gesellschaft Deutscher Chemiker, Düsseldorf, p. 504.*

Heinrich, T.; Kraus, W.; Pietzsch, H.-J.; Seifert, S.; Jentschel, C.; Faltin, I.; Pawelke, B.; Bergmann, R.; Spies, H.; Johannsen, B.  
Rhenium-188-Komplexe verbrückter DMSA-Derivate: Stabilitätsbetrachtungen in vitro und in vivo.  
*In: Programm und Abstract 13. Arbeitstreffen AG Radiochemie/Radiopharmazie, Seefeld, Österreich (2005), p. 24.*

Hoppmann, S.; Steiniger, B.; Pietzsch, J.  
Catabolism of hypochlorite-modified low density lipoprotein (LDL) in vivo: insights from small animal positron emission tomography studies.  
*In: Proceedings of the 5<sup>th</sup> European Life Science Organisation (ELSO), Dresden (2005), p. 230.*

Hultsch, C.; Hellwig, M.; Bergmann, R.; Henle, T.  
Bioverteilung und Metabolisierung des <sup>18</sup>F-markierten Amadori-Produktes Fructoselysin.  
*In: Programm und Abstract 13. Arbeitstreffen AG Radiochemie/Radiopharmazie, Seefeld, Österreich (2005), p. 30.*

Juran, S.; Schubert, R.; Steinbach, J.; Stephan, H.; Kraus, W.  
Synthese und Charakterisierung neuer sechszähliger 3,7-Diazabicyclo-[3.3.1]nonan-Derivate und ihrer Kupfer(II)-Komplexe.  
*In: Programm und Abstract 13. Arbeitstreffen AG Radiochemie/Radiopharmazie, Seefeld, Österreich (2005), p. 13.*

Juran, S.; Stephan, H.; Schubert, R.; Geipel, G.; Kraus, W.; Jakob, M.; Kerscher, M.; Comba, P.  
Synthese und Komplexbildungseigenschaften neuer sechszähliger Bispindinderivate mit Pyridin- und Imidazolgruppen.  
*In: Kurzreferate GDCh-Jahrestagung 2005: Chemie schafft neue Strukturen, Gesellschaft Deutscher Chemiker, Düsseldorf, p. 535.*

Rode, K.; Knieß, T.; Wüst, F.  
Erfahrungen zur Herstellung von [<sup>11</sup>C]CH<sub>3</sub>I unter Berücksichtigung langer Transportleitungen zwischen Zyklotron und Synthesemodul.  
*In: Programm und Abstract 13. Arbeitstreffen AG Radiochemie/Radiopharmazie, Seefeld, Österreich (2005), p. 16.*

Stephan, H.; Meißner, T.; Bergmann, R.; Rode, K.; Kraus, W.; Emmerling, F.  
Darstellung und Charakterisierung von Nanopartikeln auf der Basis von [Ti<sub>2</sub>W<sub>10</sub>PO<sub>40</sub>]<sup>7-</sup> und Chitosan.  
*In: Book of Abstracts, BioNanoMaT "Bioinspired Nanomaterials for Medicine and Technologies, DECHEMA, Marl (2005), p. 67.*

Stephan, H.; Röhrich, A.; Steinbach, J.; Geipel, G.; Bernhard, G.  
Dendritic encapsulation of radiometals by glycodendrimers having a cyclam-core.  
*In: Book of Abstracts, BioNanoMaT "Bioinspired Nanomaterials for Medicine and Technologies, DECHEMA, Marl (2005), p. 57.*

Stephan, H.; Steinbach, J.; Buske, N.  
Radioaktiv markierte Magnetit-Nanoteilchen mit einer DMSA-Hülle.  
*In: Proceedings 2. Workshop über Molekulare Bildgebung und magnetische Nanopartikel, Institut für Diagnostische und Interventionelle Radiologie, Friedrich-Schiller-Universität Jena (2005), pp. 103-104.*

Yoshizuka, K.; Pietzsch, H.-J.; Seifert, S.; Stephan, H.  
Novel computational chemistry for molecular design of radioactive metal complexes.  
*In: Proceedings of the International Solvent Extraction Conference, Beijing, China (2005), pp. 424-428.*

## ABSTRACTS

Bergmann, R.; Hultsch, C.; Bergmann, S.; Pietzsch, J.; Gunawan, J.; Burchert, W.; van den Hoff, J.  
Evaluation of F-18 labelled annexin V: apoptosis imaging in mice.  
Nuklearmedizin 44 (2005) A13.

Bergmann, R.; Pietzsch, J.; Bergmann, S.; van den Hoff, J.  
Dynamic 2-deoxy-2-[<sup>18</sup>F]fluoro-D-glucose (<sup>18</sup>F-FDG) positron emission tomography imaging of small laboratory animals: effect of simultaneous glucose infusion on <sup>18</sup>F-FDG uptake in rats.  
Eur. J. Nucl. Med. Mol. Imaging 32 (2005) S267.

Berndt, M.; Wüst, F.  
<sup>11</sup>C-C bond formation by palladium-mediated cross-coupling of alkenylzirconocenes with [<sup>11</sup>C]methyl iodide.  
J. Labelled Compd. Radiopharm. 48 (2005) S24.

Beuthien-Baumann, B.; Heinke, M.; van den Hoff, J.; Oehme, L.; Will, E.; Kotzerke, J.; Hummel, T.  
Untersuchung der zentralen Verarbeitung trigeminaler Reize.  
Nuklearmedizin 44 (2005) A13.

Friebe, M.; Hecht, M.; Graham, K.; Stephens, A. W.; Hilger, C. S.; Johannsen, B.; Dinkelborg, L. M.  
S-trityl protected mercaptoacetyl-glycyl-glycine - a useful purification handle for oligonucleotide-chelator conjugates as precursors for radiolabeling of aptamers with Tc(V) and Re(V).  
J. Labelled Compd. Radiopharm. 48 (2005) S242.

Füchtner, F.; Zessin, J.; Wüst, F.  
Aspects of 6-[<sup>18</sup>F]fluoro-L-dopa preparation: experiences with chloroform as a substitute solvent for Freon 11.  
J. Labelled Compd. Radiopharm. 48 (2005) S211.

Graessler, J.; Westendorf, T.; Kopprasch, S.; Pietzsch, J.  
LDL isolated from subjects with impaired glucose tolerance increases the expression of CD36 and PPAR-gamma in macrophages.  
Diabetes und Stoffwechsel (2005) 31-32.

Haase, C.; Oswald, J.; Pietzsch, J.; Bergmann, R.  
Characterization of L amino acid transporter 1 (LAT1) for 3-O-methyl-6-<sup>18</sup>F-fluoro-L-DOPA (OMFD) in tumor cells and tumor tissues.  
Molecular Imaging 4 (2005) 285.

Heinrich, T.; Kraus, W.; Pietzsch, H.-J.; Smuda, C.; Seifert, S.; Spies, H.  
Development of rhenium-188 complexes based on novel chelators derived from dimercaptosuccinic acid (DMSA) suitable for easy linking of biomolecules.  
J. Labelled Compd. Radiopharm. 48 (2005) S234.

Hofheinz, F.; Pöttsch, C.; van den Hoff, J.  
Automatisierte Koregistrierung von PET-Ganzkörperaufnahmen mit stückweise starren Transformationen.  
Nuklearmedizin 44 (2005) A162.

Hofheinz, F.; Pöttsch, C.; van den Hoff, J.  
Automatic coregistration of whole-body positron emission tomography images using piece-wise rigid body transformations.  
Molec. Imag. Biol. 7 (2005) 134.

Holthoff, V.; Beuthien-Baumann, B.; Meyer, S.; Pöttrisch, K.; Kalbe, E.; Sorbi, S.; Herholz, K.  
Messung der regionalen Hirnfunktion bei spezifischen neuropsychiatrischen Symptomen der frühen Demenz vom Alzheimerstyp.  
Nuklearmedizin 44 (2005) A30.



- Langner, J.; Pöttsch, C.; Bühler, P.; van den Hoff, J.  
Entwicklung von Methoden zum beschleunigten Zugriff auf Akquisitionsdaten ACS2-basierter PET-Scanner.  
Nuklearmedizin 44 (2005) A161.
- Liepe, K. F.; Geidel, H.; Bergmann, R.; Barth, M.; Runge, R.; Kotzerke, J.  
Autoradiographic studies with rhenium-188-HEDP of bone metastases and skeleton.  
Eur. J. Nucl. Med. Mol. Imaging 32 (2005) S111.
- Meißner, T.; Richter, W.; Stephan, H.; Zänker, H.; Kraus, W.  
Darstellung und Charakterisierung von Nanopartikeln auf der Basis von  $[\text{Ti}_2\text{W}_{10}\text{PO}_{40}]^{7-}$  und Chitosan.  
Chemie Ingenieur Technik 77 (2005) 227.
- Oswald, J.; Haase, C.; Wüst, F.; Bergmann, R.  
Experimental hypoxia as potent stimulus for radiotracer uptake in vitro: comparison of different primary endothelial cells.  
Molecular Imaging 4 (2005) 301.
- Oswald, J.; Haase, C.; Wüst, F.; Bergmann, R.  
Human primary endothelial cells incorporate increased levels of  $[\text{}^{18}\text{F}]\text{FDG}$  under hypoxic conditions.  
Eur. J. Nucl. Med. 32 (2005) S44.
- Paulo, A.; Garcia, R.; Maria, L.; Xavier, C.; Santos, I.; Knieß, T.; Wüst, F.; Bergmann, R.  
Mercaptoimidazole derivatives labelled with  $^{11}\text{C}/^{99\text{m}}\text{Tc}$  for the targeting of 5-HT<sub>1A</sub> receptors.  
Molecular Imaging 4 (2005) 337.
- Pietzsch, J.; Berndt, M.; Wüst, F.; van den Hoff, J.  
Radiolabeling of human apolipoproteins using SH-reactive  $^{18}\text{F}$ -labeling agents: a potential approach for characterization and differentiation of metabolism of native and modified lipoproteins by small animal positron emission tomography (PET) in vivo.  
Amino Acids 29 (2005) 18-19.
- Pietzsch, J.; Hoppmann, S.; Bergmann, R.; Steiniger, B.; van den Hoff, J.  
Assessment of catabolism of glycosylated and glycosylated LDL in vivo: insights of small animal positron emission tomography (PET) studies.  
Diabetologia 48 (2005) A416.
- Pöttsch, C.; Hofheinz, F.; van den Hoff, J.  
Fast user guided segmentation and quantification of volumes in 3-d datasets.  
Molec. Imag. Biol. 7 (2005) 152.
- Pöttsch, C.; Hofheinz, F.; van den Hoff, J.  
Minimierung der Inter-Observer-Variabilität bei volumetrischen Auswertungen von onkologischen Ganzkörperstudien in der PET.  
Nuklearmedizin 44 (2005) A16.
- Pöttsch, C.; Hofheinz, F.; van den Hoff, J.  
Integration von erweiterten Visualisierungsoptionen in ein System zur quantitativen Auswertung von 3D PET-Datensätzen bei onkologischen Fragestellungen.  
Nuklearmedizin 44 (2005) A162.
- Schiller, E.; Seifert, S.; Tisato, F.; Refosco, F.; Kraus, W.; Spies, H.; Heinrich, T.; Pietzsch, H.-J.  
 $^{188}\text{Re}(\text{III})\text{-}^4+1\text{-mixed-ligand complexes: stability studies and labeling of biomolecules.}$   
J. Labelled Compd. Radiopharm. 48 (2005) S232.
- Schlesinger, J.; Wüst, F.; Bergmann, R.  
Yttrium-86 labelling of oligonucleotide derivatives.  
Eur. J. Nucl. Med. Mol. Imaging 32 (2005) S279.

Seo, J. W.; Chi, D. Y.; Luyt, L. G.; Wüst, F.; Dence, C. S.; Sharp, T. L.; Mach, R. H.; Welch, M. J.; Katzenellenbogen, J. A.

Sigma-2 selective fluorinated ligands: synthetic method and optimization of decarbonylation for radio-labeling.

J. Labelled Compd. Radiopharm. 48 (2005) S170.

Wüst, F.; Neumeyer, J.; Bergmann, R.; Kretzmar, M.; van den Hoff, J.

Synthesis and characterization of [ $^{18}\text{F}$ ]MCL-322 as a potential PET radiotracer for imaging the dopamine transporter.

J. Labelled Compd. Radiopharm. 48 (2005) S204.

## LECTURES AND POSTERS

### Lectures

Bergmann, R.; Hultsch, C.; Bergmann, S.; Pietzsch, J.; Gunawan, J.; Burchert, W.; van den Hoff, J.

Evaluation of F-18 labelled annexin V: apoptosis imaging in mice.

Gemeinsame Jahrestagung der Deutschen, Österreichischen und Schweizerischen Gesellschaft für Nuklearmedizin, Basel, Schweiz, 27.-30.04.2005.

Berndt, M.; Wüst, F.

$^{11}\text{C}$ -C bond formation by palladium-mediated cross-coupling of alkenylzirconocenes with [ $^{11}\text{C}$ ]methyl iodide.

International Symposium on Radiopharmaceutical Chemistry (IRSC 2005), Iowa City, Iowa, USA, 24.-28.06.2005.

Beuthien-Baumann, B.; Heinke, M.; van den Hoff, J.; Oehme, L.; Will, E.; Kotzerke, J.; Hummel, T.

Untersuchung der zentralen Verarbeitung trigeminaler Reize.

Gemeinsame Jahrestagung der Deutschen, Österreichischen und Schweizerischen Gesellschaft für Nuklearmedizin, Basel, Schweiz, 27.-30.04.2005.

Graessler, J.; Westendorf, T.; Kopprasch, S.; Pietzsch, J.

LDL isolated from subjects with impaired glucose tolerance increases the expression of CD36 and PPAR-gamma in macrophages.

The Metabolic Syndrome - a postprandial disease. Satellite Symposium of the 1st International Congress on "Prediabetes and the Metabolic Syndrome", Dresden, 16.-18.04.2005.

Heinrich, T.; Kraus, W.; Pietzsch, H.-J.; Seifert, S.; Jentschel, C.; Faltin, I.; Pawelke, B.; Bergmann, R.; Spies, H.; Johannsen, B.

Rhenium-188-Komplexe verbrückter DMSA-Derivate: Stabilitätsbetrachtungen in vitro und in vivo.

13. Arbeitstreffen der AG Radiochemie/Radiopharmazie, Seefeld, Österreich, 06.-08.10.2005.

Heinrich, T.; Kraus, W.; Pietzsch, H.-J.; Seifert, S.; Spies, H.; Johannsen, B.

Entwicklung von Rhenium-188-Komplexen basierend auf neuartigen, sich von Dimercaptobernsteinsäure (DMSA) ableitenden Chelatoren, geeignet zur Bindung an Biomoleküle.

GDCh-Jahrestagung, Düsseldorf, 11.-14.09.2005.

Holthoff, V.; Beuthien-Baumann, B.; Meyer, S.; Pöttrisch, K.; Kalbe, E.; Sorbi, S.; Herholz, K.

Messung der regionalen Hirnfunktion bei spezifischen neuropsychiatrischen Symptomen der frühen Demenz vom Alzheimerstyp.

Gemeinsame Jahrestagung der Deutschen, Österreichischen und Schweizerischen Gesellschaft für Nuklearmedizin, Basel, Schweiz, 27.-30.04.2005.

Hultsch, C.; Hellwig, M.; Bergmann, R.; Henle, T.

Bioverteilung und Metabolisierung des  $^{18}\text{F}$ -markierten Amadori-Produktes Fructoselysin.

13. Arbeitstreffen AG Radiochemie/Radiopharmazie, Seefeld, Österreich, 06.-08.10.2005.

Juran, S.

Synthesis and characterization of novel bispidine derivatives and their copper(II) complexes.  
2<sup>nd</sup> SUPRAPHONE Meeting, Dresden, 05.-07.05.2005.

Juran, S.; Schubert, R.; Steinbach, J.; Stephan, H.; Kraus, W.

Synthese und Charakterisierung neuer sechszähliger 3,7-Diazabicyclo-[3.3.1]nonan-Derivate und ihrer Kupfer(II)-Komplexe.

13. Arbeitstreffen der AG-Radiochemie/Radiopharmazie Seefeld, Österreich, 06.-08.10.2005.

Juran, S.; Schubert, R.; Stephan, H.; Kraus, W.

Synthese und Charakterisierung neuer sechszähliger 3,7-Diazabicyclo-[3.3.1]nonan-Derivate und ihrer Kupfer(II)-Komplexe.

Wissenschaftstage Fachhochschule Lausitz, Senftenberg, 23.-25.11.2005 (invited).

Liepe, K. F.; Geidel, H.; Bergmann, R.; Barth, M.; Runge, R.; Kotzerke, J.

Autoradiographic studies with rhenium-188-HEDP of bone metastases and skeleton.

Annual Congress of the European Association of Nuclear Medicine, Istanbul, Turkey, 15.-19.10.2005.

Oswald, J.; Haase, C.; Wüst, F.; Bergmann, R.

Human primary endothelial cells incorporate increased levels of [<sup>18</sup>F]FDG under hypoxic conditions.

Annual Congress of the European Association of Nuclear Medicine, Istanbul, Turkey, 15.-19.10.2005.

Pietzsch, H.-J.; Heinrich, T.; Kraus, W.; Seifert, S.; Spies, H.

<sup>188</sup>Re complexes based on novel chelators derived from dimercaptosuccinic acid.

"Radiotracers for In vivo Assessment of Biological Function New Directions", COST Action B12 - Final Conference, Warsaw, Poland, 22.-23.04.2005.

Pietzsch, J.

Dyslipidämien beim metabolischem Syndrom: Glykierte LDL und Atherogenese.

Symposium Metabolisches Syndrom 2005, Radebeul, 19.11.2005 (invited).

Pietzsch, J.

Pathophysiologie der Fettstoffwechselstörungen.

40. Jahrestagung der Deutschen Diabetes Gesellschaft, Berlin, 04.-07.05.2005 (invited).

Pietzsch, J.; Berndt, M.; Wüst, F.; van den Hoff, J.

Radiolabeling of human apolipoproteins using SH-reactive <sup>18</sup>F-labeling agents: a potential approach for characterization and differentiation of metabolism of native and modified lipoproteins by small animal positron emission tomography (PET) in vivo.

9<sup>th</sup> International Congress on Proteins and Amino Acids, Vienna, Austria, 08.-12.08.2005 (invited).

Pietzsch, J.; Hoppmann, S.; Bergmann, R.; Steiniger, B.; van den Hoff, J.

Assessment of catabolism of glycated and glycoxidized LDL in vivo: insights of small animal positron emission tomography (PET) studies.

41<sup>st</sup> Annual Meeting of the European Association for the Study of Diabetes (EASD), Athens, Greece, 10.-15.09.2005.

Pöttsch, C.; Hofheinz, F.; van den Hoff, J.

Minimierung der Inter-Observer-Variabilität bei volumetrischen Auswertungen von onkologischen Ganzkörperstudien in der PET.

Gemeinsame Jahrestagung der Deutschen, Österreichischen und Schweizerischen Gesellschaft für Nuklearmedizin, Basel, Schweiz, 27.-30.04.2005.

Preusche, S.; Roß, H.; Dohn, N.; Wüst, F.; Steinbach, J.

The Rossendorf Solid Target System CYCLONE 18/9 & 10/5 User Community, 5. Workshop, Montreal, Canada, 01.-04.05.2005.

Rode, K.; Knieß, T.; Wüst, F.

Erfahrungen zur Herstellung von [<sup>11</sup>C]CH<sub>3</sub>I unter Berücksichtigung langer Transportleitungen zwischen Zyklotron und Synthesemodul.

13. Arbeitstreffen der AG Radiochemie/Radiopharmazie, Seefeld, Österreich, 06.-08.10.2005.

Röhrich, A.  
Cyclam-core PAMAM dendrimers having sugar moieties as terminal groups.  
2<sup>nd</sup> SUPRAPHONE Meeting, Dresden, 05.-07.05.2005.

Stephan, H.  
Highly stable metal complexes with tuneable transport properties.  
2<sup>nd</sup> SUPRAPHONE Meeting, Dresden, 05.-07.05.2005.

Stephan, H.; Juran, S.  
Entwicklung von Radiometallverbindungen für die nuklearmedizinische Diagnostik und Therapie.  
Institutskolloquium, Universität Heidelberg, Institut für Anorganische Chemie, Heidelberg, 24.10.2005  
(invited).

Wüst, F.  
Fluorine-18 labelling of small molecules.  
Ernst Schering Research Foundation Workshop 62, PET chemistry: The driving force in molecular  
imaging, Berlin, 05.-07.12.2005 (invited).

Wüst, F.; Knieß, T.; Pietzsch, J.; Bergmann, R.  
Synthesis and evaluation of [<sup>11</sup>C]Al-438 as a nonsteroidal glucocorticoid receptor ligand for imaging of  
brain glucocorticoid receptors.  
X. Turku PET Symposium, Turku, Finland, 28.-31.05.2005.

Yoshizuka, K.; Pietzsch, H.-J.; Seifert, S.; Stephan, H.  
Novel computational chemistry for molecular design of radioactive metal complexes.  
International Solvent Extraction Conference, Beijing, P. R. China, 19.-23.09.2005.

## Posters

Bergmann, R.; Pietzsch, J.; Bergmann, S.; van den Hoff, J.  
Dynamic 2-deoxy-2-[<sup>18</sup>F]fluoro-D-glucose (<sup>18</sup>F-FDG) positron emission tomography imaging of small  
laboratory animals: effect of simultaneous glucose infusion on <sup>18</sup>F-FDG uptake in rats.  
Annual Congress of the European Association of Nuclear Medicine, Istanbul, Turkey, 15.-19.10.2005.

Bomkamp, M.; Stephan, H.; Waldvogel, S.  
Determination of association constants by distribution studies.  
2<sup>nd</sup> SUPRAPHONE Meeting, Dresden, 05.-07.05.2005.

Friebe, M.; Hecht, M.; Graham, K.; Stephens, A. W.; Hilger, C. S.; Johannsen, B.; Dinkelborg, L. M.  
S-trityl protected mercaptoacetyl-glycyl-glycine - a useful purification handle for oligonucleotide-  
chelator conjugates as precursors for radiolabeling of aptamers with Tc(V) and Re(V).  
International Symposium on Radiopharmaceutical Chemistry (IRSC 2005) Iowa City, Iowa, USA, 24.-  
28.06.2005.

Füchtner, F.; Zessin, J.; Wüst, F.  
Aspects of 6-[<sup>18</sup>F]fluoro-L-dopa preparation: experiences with chloroform as a substitute solvent for  
Freon 11.  
International Symposium on Radiopharmaceutical Chemistry (IRSC 2005) Iowa City, Iowa, USA, 24.-  
28.06.2005.

Gniazdowska, E.; Stephan, H.; Pietzsch, H.-J.  
The synthesis of novel „4+1” Tc(III)/Re(III) mixed-ligand complexes with a dendritic modified monodentate  
ligand.  
4<sup>th</sup> National Conference on Radiochemistry and Nuclear Chemistry, Kraków-Przegorzały, 09.-  
11.05.2005.

Haase, C.; Oswald, J.; Pietzsch, J.; Bergmann, R.  
Characterization of L amino acid transporter 1 (LAT1) for 3-O-methyl-6-<sup>18</sup>F-fluoro-L-DOPA (OMFD) in  
tumor cells and tumor tissues.  
Fourth Annual Meeting of Molecular Imaging, Köln, 07.-10.09.2005.

Heinrich, T.; Kraus, W.; Pietzsch, H.-J.; Smuda, C.; Seifert, S.; Spies, H.  
Development of rhenium-188 complexes based on novel chelators derived from dimercaptosuccinic acid (DMSA) suitable for easy linking of biomolecules.  
International Symposium on Radiopharmaceutical Chemistry (ISRC 2005), Iowa City, Iowa, USA; 24.-28.06.2005.

Hofheinz, F.; Pöttsch, C.; van den Hoff, J.  
Automatisierte Koregistrierung von PET-Ganzkörperaufnahmen mit stückweise starren Transformationen.  
Gemeinsame Jahrestagung der Deutschen, Österreichischen und Schweizerischen Gesellschaft für Nuklearmedizin, Basel, Schweiz, 27.-30.04.2005.

Hofheinz, F.; Pöttsch, C.; van den Hoff, J.  
Automatic coregistration of whole-body positron emission tomography images using piece-wise rigid body transformations.  
Annual Conference of the Academy of Molecular Imaging, Orlando, Florida, USA, 18.-23.03.2005.

Hoppmann, S.; Steiniger, B.; Pietzsch, J.  
Catabolism of hypochlorite-modified low density lipoprotein (LDL) in vivo: insights from small animal positron emission tomography studies.  
5<sup>th</sup> European Life Science Organisation (ELSO), Dresden, 03.-06.09.2005.

Juran, S.; Stephan, H.; Schubert, R.; Geipel, G.; Kraus, W.; Jakob, M.; Kerscher, M.; Comba, P.  
Synthese und Komplexbildungseigenschaften neuer sechszähliger Bispindinderivate mit Pyridin- und Imidazolgruppen.  
GDCh-Jahrestagung 2005, Düsseldorf, 11.-14.09.2005.

Langner, J.; Pöttsch, C.; Bühler, P.; van den Hoff, J.  
Entwicklung von Methoden zum beschleunigten Zugriff auf Akquisitionsdaten ACS2-basierter PET-Scanner.  
Gemeinsame Jahrestagung der Deutschen, Österreichischen und Schweizerischen Gesellschaft für Nuklearmedizin, Basel, Schweiz, 27.-30.04.2005.

Meißner, T.; Richter, W.; Stephan, H.; Zänker, H.; Kraus, W.  
Darstellung und Charakterisierung von Nanopartikeln auf der Basis von  $[\text{Ti}_2\text{W}_{10}\text{PO}_{40}]^{7-}$  und Chitosan.  
GVC/DECHEMA-Jahrestagung 2005, Wiesbaden, 06.-08.09.2005.

Oswald, J.; Haase, C.; Wüst, F.; Bergmann, R.  
Experimental hypoxia as potent stimulus for radiotracer uptake in vitro: comparison of different primary endothelial cells.  
Fourth Annual Meeting of Molecular Imaging, Köln, 07.-10.09.2005.

Oswald, J.; Steudel, C.; Joergensen, B.; Salchert, K.; Ehninger, G.; Thiede, C.; Bornhäuser, M.; Werner, C.  
Gene expression analysis of CD34+ hematopoietic stem cells cultivated on bioartificial materials.  
2<sup>nd</sup> Max Bergmann Symposium, Institut für Polymerforschung Dresden, 17.-18.02.2005.

Paulo, A.; Garcia, R.; Maria, L.; Xavier, C.; Santos, I.; Knieß, T.; Wüst, F.; Bergmann, R.  
Mercaptoimidazole derivatives labelled with  $^{111}\text{C}/^{99\text{m}}\text{Tc}$  for the targeting of 5-HT<sub>1A</sub> receptors.  
Fourth Annual Meeting of the Society for Molecular Imaging, Köln, 07.-10.09.2005.

Pöttsch, C.; Hofheinz, F.; van den Hoff, J.  
Fast user guided segmentation and quantification of volumes in 3-d datasets.  
Annual Conference of the Academy of Molecular Imaging, Orlando, Florida, USA, 18.-23.03.2005.

Pöttsch, C.; Hofheinz, F.; van den Hoff, J.  
Integration von erweiterten Visualisierungsoptionen in ein System zur quantitativen Auswertung von 3D PET-Datensätzen bei onkologischen Fragestellungen.  
Gemeinsame Jahrestagung der Deutschen, Österreichischen und Schweizerischen Gesellschaft für Nuklearmedizin, Basel, Schweiz, 27.-30.04.2005.

- Preusche, S.; Wüst, F.; Schilling, K.-D.; Roß, H.; Dohn, N.  
Production of  $^{86}\text{Y}$  and  $^{56}\text{Co}$  at the Rossendorf CYCLOTRON 18/9.  
CYCLONE 18/9 & 10/5 User Community, 5. Workshop, Montreal, Canada, 01.-04.05.2005.
- Röhrich, A.; Bernhard, G.; Geipel, G.; Stephan, H.  
Synthesis and copper(II) complexation of glycodendrimers having a cyclam-core.  
XXX. International Symposium on Macrocyclic Chemistry (ISMC), Dresden, 17.-21.07.2005.
- Schiller, E.; Seifert, S.; Tisato, F.; Refosco, F.; Kraus, W.; Spies, H.; Pietzsch, H.-J.  
 $^{188}\text{Re(III)}$  mixed-ligand complexes: stability studies and labeling of biomolecules.  
„Radiotracers for In vivo Assessment of Biological Function New Directions“, COST Action B12 - Final Conference, Warsaw, Poland, 22.-23.04.2005.
- Schiller, E.; Seifert, S.; Tisato, F.; Refosco, F.; Kraus, W.; Spies, H.; Heinrich, T.; Pietzsch, H.-J.  
 $^{188}\text{Re(III)-,4+1-}$ -mixed-ligand complexes: stability studies and labeling of biomolecules.  
International Symposium on Radiopharmaceutical Chemistry (ISRC 2005), Iowa City, Iowa, USA; 24.-28.06.2005.
- Schlesinger, J.; Wüst, F.; Bergmann, R.  
Yttrium-86 labelling of oligonucleotide derivatives.  
Annual Congress of the European Association of Nuclear Medicine, Istanbul, Turkey, 15.-19.10.2005.
- Schubert, R.; Juran, St.; Stephan, H.; Geipel, G.; Comba, P.; Kerscher, M.; Kraus, W.  
Hexadentate bispidine ligands with pyridine and imidazole groups.  
2<sup>nd</sup> SUPRAPHONE Meeting, Dresden, 05.-07.05.2005.
- Seo, J. W.; Chi, D. Y.; Luyt, L. G.; Wüst, F.; Dence, C. S.; Sharp, T. L.; Mach, R. H.; Welch, M. J.; Katzenellenbogen, J. A.  
Sigma-2 selective fluorinated ligands: synthetic method and optimization of decarbonylation for radio-labeling.  
International Symposium on Radiopharmaceutical Chemistry (IRSC 2005), Iowa City, Iowa, USA, 24.-28.06.2005.
- Stephan, H.; Meißner, T.; Bergmann, R.; Rode, K.; Kraus, W.; Emmerling, F.  
Darstellung und Charakterisierung von Nanopartikeln auf der Basis von  $[\text{Ti}_2\text{W}_{10}\text{PO}_{40}]^{7-}$  und Chitosan.  
BioNanoMaT "Bioinspired Nanomaterials for Medicine and Technologies", Marl, 23.-24.11.2005.
- Stephan, H.; Röhrich, A.; Steinbach, J.; Geipel, G.; Bernhard, G.  
Dendritic encapsulation of radiometals by glycodendrimers having a cyclam-core.  
BioNanoMaT "Bioinspired Nanomaterials for Medicine and Technologies", Marl, 23.-24.11.2005.
- Stephan, H.; Steinbach, J.; Buske, N.  
Radioaktiv markierte Magnetit-Nanoteilchen mit einer DMSA-Hülle.  
2. Workshop über molekulare Bildgebung und magnetische Nanopartikel, Jena, 17./18.06.2005.
- Wüst, F.; Neumeyer, J.; Bergmann, R.; Kretzschmar, M.; van den Hoff, J.  
Synthesis and characterization of  $^{18}\text{F}$ MCI-322 as a potential PET radiotracer for imaging the dopamine transporter.  
International Symposium on Radiopharmaceutical Chemistry (IRSC 2005), Iowa City, Iowa, USA, 24.-28.06.2005.

## PATENTS

- Heinrich, T.; Johannsen, B.; Pietzsch, H.; Seifert, S.; Spies, H.  
Metallkomplexe auf der Basis von Tetrathiol-Liganden und deren Anwendung in der nuklearmedizinischen Diagnostik und Endoradionuklidtherapie sowie Verfahren zur Herstellung der Metallkomplexe.  
DE 10 2004 022 461 A1.

## AWARDS

S. Juran

Bester Kurzvortrag anlässlich des 13. Arbeitstreffens der AG Radiochemie/Radiopharmazie, Seefeld, Österreich, 06.-08.10.2005.

## DIPLOMA

H. Mölle

Implementation von Methoden zur iterativen Bildrekonstruktion für einen Kleintier-PET.  
Hochschule für Technik und Wirtschaft Dresden, 05.07.2005.

A. Müller

Optimierung der Synthese der Radiotracer [<sup>11</sup>C]Methionin, [<sup>18</sup>F]MISO und [<sup>18</sup>F]FLT.  
Technische Universität Dresden, 30.08.2005.

S. Hoppmann

Untersuchungen zum in vivo-Metabolismus oxidierter und nativer Lipoproteine geringer Dichte am Tiermodell mittels Positronen-Emissions-Tomographie.  
Universität Würzburg, 30.09.2005.

A. Röhrich

Darstellung und Charakterisierung von Glycoclustern auf der Basis von PAMAM-Dendrimern mit einem Cyclam-Core.  
Technische Universität Dresden, 06.07.2005.

D. Herrmann

Aufnahme der Parameter eines neuartigen Detektors zur Messung von Positronen in kleinen Blutproben.  
Berufsakademie Bautzen, 10/2005.

C. Jentschel

Präparation und in-vitro-Charakterisierung von Re-188-Komplexen mit verbrückten DMSA-Liganden.  
Fachhochschule Zittau – Görlitz, 01.12.2005.

A. Pietzschmann

Synthese und Charakterisierung modifizierter Nuklein-Säurebausteine zur Kopplung von Radiometallen.  
Fachhochschule Zittau – Görlitz, 01.12.2005.

C. Smuda

Untersuchungen zur Markierung von Biomolekülen mit Ga-68.  
Technische Universität Bergakademie Freiberg, 27.9.2005.

T. Meißner

Synthese und Charakterisierung von Nanopartikeln auf der Basis von Chitosen und Polyoxowolframat.  
Hochschule für Technik und Wirtschaft Dresden, 10.11.2005.

## PhD THESIS

E. Schiller

Re(III)-Gemischtligandkomplexe mit tetradentater/monodentater NS3/P-Koordination ("4+1"): ein Beitrag zur Entwicklung von Re-188-Radiotherapeutika.  
Technische Universität Dresden, 29.06.2005.

### **III. COLLABORATIONS, FUNDED PROJECTS AND FINANCIAL SUPPORT**





## COLLABORATIONS

The Institute sustains a number of valuable collaborations with other research institutions and is engaged in joint projects funded by federal and trans-national authorities and research initiatives as well as by the industry.

Naturally, the Technical University of Dresden continues to be an important partner in our cooperative relations. Cooperations exist with various groups in the Department of Chemistry and the Faculty of Medicine. Common objects of radiopharmacological and medical research link the Institute with the University Hospital in Dresden, above all with its Department of Nuclear Medicine (Prof. Kotzerke) which contributes to the staff of the jointly operated PET Centre Rossendorf. Application of the positron emission tomography technique has been successfully extended to new questions in collaboration with the Institute of Food Chemistry (Prof. Henle). Fruitful collaborations on the development of novel PET radiotracers have been established with the Institute of Organic Chemistry (Prof. Metz) and the Institute of Biochemistry (Prof. van Peè). Bioinorganic research activities are closely linked with the Department of Coordination Chemistry (Prof. Gloe).

On the national and international level, there exist a number of collaborations.

In 2005, the new interdisciplinary research centre "OncoRay" for radiation research in oncology has been established in Dresden. OncoRay's vision is to improve the treatment of cancer by means of biologically individualised, technically optimised radiotherapy. Our institute is one of the main collaborators of OncoRay, the focus of the collaboration currently being on small animal investigations with PET and MRI.

The identification of common objects in PET radiopharmacy has led to collaborative research with the Institute of Interdisciplinary Isotope Research at the University of Leipzig (Prof. Steinbach). Both institutes constitute an alliance of research in radiopharmaceutical sciences.

Cooperation in PET tracer chemistry and radiopharmacology has been established with the Turku Medical PET Center (Prof. Solin), Washington University, School of Medicine in St. Louis (Prof. Welch and Prof. Anderson), Harvard School of Medicine in Boston (Dr. Neumeyer), Northeastern University Boston (Prof. Hanson), University of Illinois in Champaign-Urbana (Prof. Katzenellenbogen) and the Instituto Tecnológico e Nuclear in Sacavém (Dr. Santos).

Cooperation in the field of peptide chemistry and receptor research exists with the University of Leipzig (Prof. Beck-Sickinger) and the Free University of Brussels (Prof. Tourwe).

Investigations on the field of metabolic research (lipoprotein metabolism, atherogenesis and inflammation) are closely performed in collaboration with the Medical Clinic and Outpatient Department III, University Hospital Dresden (Prof. Julius; Dr. Koppasch).

Strong collaboration exists in the field of development and characterisation of new metalloradiopharmaceuticals with the University of Ferrara (Prof. Duatti), Research Centre ICIS CNR Padova (Dr. Tisato), Institute of Nuclear Chemistry and Technology Warsaw (Prof. Narbutt), Russian Academy of Sciences, Institute of Inorganic Chemistry Novosibirsk (Prof. Fedorov), University of Heidelberg (Prof. Comba).

Structural modelling and structure-property correlations of new radiometal complexes are performed together with groups of the University of Heidelberg (Prof. Comba) and the University of Kitakyushu (Prof. Yoshizuka).

Very effective cooperation exists with the Federal Material Research Institute in Berlin (Dr. Emmerling, Mr. Kraus), whose staff members carried out X-ray crystal structure analysis of new technetium and rhenium complexes.

In the field of supramolecular chemistry, successful cooperation exists with the University of Bonn (Prof. Vögtle), Free University of Berlin (Prof. Schalley), University of Münster (Prof. De Cola), University of Duisburg-Essen (Prof. Klärner), University of Bologna (Prof. Balzani), University of Fribourg (Prof. Belser), University of Lisbon (Prof. Pina) and the Institute of Chemical Technology Prague (Dr. Urbanova).

## PUBLIC FUNDED PROJECTS

The Institute is part of the Research Center Rossendorf, which is financed by the Federal Republic of Germany and the Free State of Saxony on a fifty-fifty basis.

The Institute participated in the following networks supported by Commission of the European Communities:

Radiotracers for *in vivo* assessment of biological function  
COST B12  
in collaboration with Sweden, Italy and Switzerland.  
02/1999 – 04/2005

Since 2004, the Institute is engaged in the SIXTH FRAMEWORK PROGRAMME PRIORITY 1 FP6-2002 LIFESCIHEALTH, in the project BioCare, Molecular Imaging for Biologically Optimized Cancer Therapy, Contract no.: 505785. The Institute contributes to the work packages: WP 3 - Molecular imaging of radiation therapy induced alteration of tumour cell proliferation and functional receptor expression, WP 4 - Aptamer based PET and SPECT tracers for molecular tumour imaging, together with partners from the Technical University of Dresden, Universitair Ziekenhuis Gasthuisberg, Université Catholique de Louvain, and University of Hamburg.  
04/2004-10/2008

The Institute further contributes to POL-RAD-PHARM (MARIE CURIE TRANSFER OF KNOWLEDGE FELLOWSHIP). Project full title: Chemical Studies for Design and Production of New Radiopharmaceuticals. The project aims at commencing and intensifying research in radiopharmaceutical chemistry – a new discipline for the host institution. For this purpose the host institution, located in Poland, has established partnership with other seven European laboratories.

The research part of the project includes:

- (1) learning and/or mastering methods for obtaining novel potential radiopharmaceuticals labelled with  $^{99m}\text{Tc}$  (diagnostic) and with  $^{188}\text{Re}$  (therapeutic);
- (2) developing a method for labelling biomolecules with  $^{211}\text{At}$  by formation of stable heteroleptic complexes between astatide ( $\text{At}^-$ ) and chelates of soft metal cations;
- (3) developing methods for obtaining selected radionuclides of potential use in manufacturing radiopharmaceuticals, including metallic PET nuclides and alpha-emitters;
- (4) developing analytical methods for purity control and stability studies of the novel radiopharmaceuticals.

07/2004-06/2008

The Institute participates in the following networks supported by Commission of the European Communities (1) and International Atomic Energy Agency (2):

(1) Toward Bio-Inspired Photoaddressable Supramolecular Systems. Synthesis, Light-emission, Dynamics, Biomedical Application (COST D31)  
in collaboration with Italy, Switzerland, Portugal and Czech Republic.  
04/2005-02/2009

(2) IAEA Co-ordinated Research Programme on “Development of  $^{99m}\text{Tc}$  based Small Bio Molecules Using Novel  $^{99m}\text{Tc}$  Cores”  
in collaboration with Italy, Hungary, Uruguay, USA, Austria, Greece and Portugal.  
05/2003-05/2006

On the national level, two research projects concerning tracer design, biochemistry and PET radiochemistry were supported by the Deutsche Forschungsgemeinschaft (DFG):

Molecular encapsulated  $^{188}\text{Re}$  complexes: development of robust and tunable radioactive rhenium complexes on the basis of novel chelators derived from dimercaptosuccinic acid (DMSA).

PI 255/5-2 (H.-J. Pietzsch) 04/2005 – 03/2007

F-18-labelled corticosteroides as ligands for imaging brain glucocorticoid-receptors by means of PET.

WU 340/1-2 (F. Wüst) 11/2004 – 10/2006

The Sächsisches Staatsministerium für Wissenschaft und Kunst provided support for the following project:

MeDDrive 2002

01/2004 – 12/2006

The Sächsisches Staatsministerium für Wirtschaft und Arbeit provided support for the following projects:

Radioimmunodiagnosics of inflammation

05/2004 - 06/2007

Radioactively labelled human serum albumin microspheres for tumour therapy

03/2005 – 06/2007

Analytics of  $\text{MAG}_3$  (GWT)

10/2005 – 08/2007

The Bundesministerium für Bildung und Forschung supported cooperation with

Czech Republic: Polyoxometallo compounds

WTZ, 08/2002 – 07/2005

Russia: Polynuclear metallo drugs

WTZ, 07/2003 – 06/2006

The Bundesministerium für Wirtschaft und Arbeit supported research projects on:

Preparation of  $^{86}\text{Y}$

08/2003 - 01/2005

Several laboratory visits were supported by the “Deutscher Akademischer Austauschdienst” (DAAD).

VIGONI-Project with Padova (Italy):

Labelling Dithiol Ligands with a TcN-Synthon

01/2005 – 12/2005

## FINANCIAL SUPPORT BY THE INDUSTRY

The following projects were supported by cooperations with the industry:

ABX advanced biomedical compounds GmbH Dresden  
GSK/5-HT<sub>6</sub> tracer and ligand characterisation  
04/2005 – 12/2006

ABX advanced biomedical compounds GmbH Dresden  
PET surrogate parameters  
10/2003 - 06/2006

Apogepha Arzneimittel GmbH  
Cooperation in pharmacokinetics and metabolism of propiverin  
07/2003 – 04/2005

A.R.T. Hersching  
Cooperation in movement tracking for PET  
09/2002 – 12/2006

Bayer AG Leverkusen  
Cooperation in drug development  
05/2002 – 09/2005

Bruker BioSpin MRI GmbH  
MPI/PET-Coupling  
11/2003 – 12/2006

Nihon-Medi-Physics (Japan/USA)  
Development and evaluation of technetium-99m-labelled fatty acids  
01/2003 – 12/2005

ROTOP Pharmaka GmbH  
Agent syntheses  
06/2004 – 12/2006

Schering AG Berlin  
Pharmaceutical research  
07/1996 - 12/2006

Schering AG Berlin  
Metal chelates  
05/2003 - 12/2006

Schering AG Berlin  
Dialysis  
09/2005 – 09/2006

AEA Technology, QSA GmbH, Braunschweig  
Preparation of <sup>86</sup>Y  
10/2003 – 03/2007

## LABORATORY VISITS

Dr. J.-U. Künstler  
Medizinische Universität Innsbruck, Nuklearmedizin, Austria  
06.-13.11.2005

Dr. M. Walther  
Forschungszentrum Jülich GmbH, Institut für Nuklearchemie  
05.-09.12.2005

## GUESTS

Dr. E. Gniazdowska  
Institute of Nuclear Chemistry, Warsaw, Poland  
17.01.-13.03.2005

Dr. M. Urbanová  
Institute of Chemical Technology, Prague, Czech Republic  
21.-22.02.2005

D. Janković  
Vinča Institute of Nuclear Sciences, Belgrade, Serbia and Montenegro  
03.-07.04.2005

M. Bomkamp  
Universität Duisburg-Essen  
04.04.-05.05.2005

J. Nový  
Institute of Chemical Technology, Prague, Czech Republic  
04.-08.05.2005

Dr. V. Setnička  
Institute of Chemical Technology, Prague, Czech Republic  
04.-08.05.2005

Dr. M. Urbanová  
Institute of Chemical Technology, Prague, Czech Republic  
04.-08.05.2005

Prof. M. T. Gandolfi  
University of Bologna, Italy  
05.-08.05.2005

G. Bergamini  
University of Bologna, Italy  
05.-08.05.2005

Dr. E. Gniazdowska  
Institute of Nuclear Chemistry, Warsaw, Poland  
15.09.-12.11.2005

O. Efremova  
Nikolaev Institute of Inorganic Chemistry, Novosibirsk, Russia  
02.10.-25.12.2005

## MEETINGS ORGANISED

2<sup>nd</sup> SUPRAPHONE Meeting  
Supramolecularphotonicsnetwork in Europe, Dresden  
05.-07.05.2005

## TEACHING ACTIVITIES

Summer term 2005

H.-J. Pietzsch  
One term course on Metals in Biosystems (Introduction into Bioinorganic Chemistry)

J. Pietzsch  
Lipoproteins and Atherogenesis

Winter term 2005

F. Wüst  
One term course on Radiopharmaceutical Chemistry

J. Oswald  
Molecular Biology/Genetic Engineering

## OTHER ACTIVITIES

H. Stephan  
Coordinator of Working Group 0011/04 "Toward Bio-Inspired Photoaddressable Supramolecular Systems. Synthesis, Light-emission, Dynamics, Biomedical Applications" within the COST Action D31 "Organising Non-Covalent Chemical Systems with Selected Functions".

## **IV. SEMINARS**





## TALKS OF VISITORS

Dr. M. Urbanová, Institute of Chemical Technology Prague  
Circular dichroism spectroscopy of biomolecules  
21.02.2005

Dr. N. Budisa, Max-Planck-Institut für Biochemie, Martinsried  
Expanding the genetic code for expression of novel protein derivatives and conjugates  
08.06.2005

M. Eiblmaier, Washington University, School of Medicine  
Nuclear localization of two Cu-64 labeled somatostatin analogs in a cell line stably transfected with SSTR2  
06.07.2005

Prof. O. Solin, Turku PET Centre  
High specific radioactivity  $^{18}\text{F}$ -tracers for positron emission tomography  
16.09.2005

Prof. Dr. K. Takeshita, Tokyo Institute of Technology  
Extraction separation of Am(III) and Eu(III) with TPEN (N,N,N',N'-tetrakis(2-pyridylmethyl)ethylenediamine) and its derivatives  
29.09.2005

Prof. Dr. F.-G. Klärner, Institut für Organische Chemie der Universität Duisburg-Essen  
Neues aus der Chemie der molekularen Pinzetten und Klammern  
11.10.2005

Prof. Dr. K. Lützenkirchen, Institute for Transuranium Elements Karlsruhe, Joint Research Center – European Commission  
Aktiniden für die Radio-Immuntherapie  
11.11.2005

## INTERNAL SEMINARS

K. Strobel

Grundlagen der Magnet-Resonanz-Tomographie (MRT) und –Spektroskopie (MRS)  
07.03.2005

H. Stephan

Dendritische Komplexe als potentielle Radiotherapeutika  
21.03.2005

R. Bergmann

EU-Projekt „BIOCARE“ (WP4): Entwicklung von Aptameren zur Tumordarstellung  
05.04.2005

R. Bergmann/C. Pötzsch

Bericht vom Jahreskongress der Academy of Molecular Imaging: Aktuelle Entwicklungen  
18.04.2005

B. Beuthien-Baumann

EU-Projekt: „BIOCARE“ (WP3): Etablierte und neue PET-Tracer in der Strahlentherapie – Evaluierung mittels MicroPET, Autoradiographie und „Funktioneller“ Histologie am Tiermodell.  
02.05.2005

St. Preusche/F. Wüst

Radionuklidherstellung am Zyklotron  
23.05.2005

F. Füchtner

GMP-gerechte Herstellung von Radiopharmaka  
06.06.2005

S. Juran

Synthese und Charakterisierung neuer sechszähliger 3,7-Diazabicyclo[3.3.1]nonan-Derivate und ihrer radioaktiven Kupferkomplexe  
21.06.2005

## **V. PERSONNEL**



## Director

Prof. Dr. Steinbach, J.

## Administrative Staff

Kersten, M.

Neubert, G.

## Scientific Staff

Dr. Berndt, M.\*

Dr. Bergmann, R.

Dr. Füchtner, F.

Dr. Haase, C.\*

Dr. Knieß, T.

Künstler, J.-U.\*

Mädig, P.

Dr. Noll, B.

Dr. Noll, S.

Dr. Oswald, J.\*

Dr. Pietzsch, H.-J.

Dr. Pietzsch, J.

Preusche, S.

Dr. Rother, A.\*

Dr. Schiller, E.\*\*\*

Dr. Seifert, S.

Dr. Spies, H.\*

Dr. Stephan, H.

Dr. Strobel, K.\*

Prof. Dr. van den Hoff, J.

Dr. Walther, M.\*

Dr. Will, E.

Dr. Wüst, F.

Dr. Zessin, J.

## Technical Staff

Barth, M.\*

Dohn, N.

Gläser, H.

Görner, H.

Große, B.

Hentges, A.

Herrlich, R.

Herzog, W.

Jährig, P.\*\*

Kasper, H.

Kolbe, U.

Krauß, E.

Krauß, T.\*

Kreisl, B.

Landrock, K.

Lehnert, S.

Lenkeit, U.

Lipps, B.

Lücke, R.\*

Rode, K.\*

Scheibke, J.\*

Sterzing, R.

Suhr, A.

Wenzel, R.

## PhD Students

Gester, S.

Hecht, M.

Heinrich, T.

Hoppmann, S.

Hultsch, C.

Juran, S.

Just, U.

Langner, J.

Mölle, H.

Pöttsch, C.

Röhrich, A.

Schiller, E.

Schlesinger, J.

Steiniger, B.

## Former Personnel

(who left during the period covered by the report)

**Administrative Staff:**

Forker, S.

**Scientific Staff:**

Dr. Grote, M.\*

Dr. Pawelke, B.\*

**Technical Staff:**

Roß, H.

\* term contract

\*\* on maternity leave

\*\*\* guest scientist